

SESSION 10

FILTERS AND FILTER PERFORMANCE

Wednesday: August 26, 1992  
Co-Chairmen: W. Bergman  
W. L. Anderson

OPENING COMMENTS OF SESSION CO-CHAIRMAN BERGMAN

CHALLENGES WITHIN VENTILATION SYSTEMS DURING ACCIDENT SITUATIONS

M. Fronhöfer, M. Neuberger, J.G. Wilhelm

RADIAL FLOW SYSTEMS FOR THE NUCLEAR INDUSTRY

M.L. Davis

BEHAVIOR OF THE LOADED POLYGONAL HEPA FILTER EXPOSED TO WATER DROPLETS CARRIED BY THE OFF-GAS FLOW

K. Jannakos, H. Mock, G. Potgeter, J. Furrer

THE APPLICATION OF HEPA FILTER UNITS IN GAS STREAMS OF HIGH DUST CONCENTRATIONS

H. Leibold, I. Döffert, T. Leiber, M. Fronhöfer, J.G. Wilhelm

PREDICTING MASS LOADING AS A FUNCTION OF PRESSURE DIFFERENCE ACROSS PREFILTER/HEPA FILTER SYSTEMS

V.J. Novick, J.F. Klassen, P.R. Monson, T.A. Long

APPLICATION OF HIGH-EFFICIENCY METAL FIBER FILTERS IN VENTILATION SYSTEMS OF NON-REACTOR NUCLEAR FACILITIES

G. Grewal, Z. Milatović, F.L. Landon, W.M. Harty

DEVELOPMENT AND EVALUATION OF A CLEANABLE HIGH EFFICIENCY STEEL FILTER

W. Bergman, G. Larsen, F. Weber, P. Wilson, R. Lopez, G. Valha, J. Conner, J. Garr, K. Williams, A. Biermann, K. Wilson, P. Moore, C. Gellner, D. Rapchun, K. Simon, J. Turley, L. Frye, D. Monroe

DEVELOPMENT AND EVALUATION OF A HEPA FILTER FOR INCREASED STRENGTH AND RESISTANCE TO ELEVATED TEMPERATURE

H. Gilbert, W. Bergman, J.K. Fretthold

CLOSING COMMENTS OF SESSION CO-CHAIRMAN ANDERSON



OPENING COMMENTS OF SESSION CO-CHAIRMAN BERGMAN

Welcome to the session on Filters and Filter Performance. We will have a series of presentations dealing with filter performance under various test conditions, high-strength HEPA filters, and steel high-efficiency filters. The latter two technologies were pioneered in the laboratories of Mr. Wilhelm at KfK, and I would like to acknowledge this pioneering work in my introduction of Mr. Wilhelm.

During the past decade, Mr. Wilhelm and his colleagues have investigated the effect of accident conditions on the performance of HEPA filters. His studies with Dr. Ruedinger and Dr. Ricketts on the effect of moisture and high flow conditions on HEPA filter failures led to an understanding of the failure mechanisms and to the development of a high strength HEPA filter that is presently used in German nuclear power plants. An important finding in their studies is that high moisture exposure on slightly used HEPA filters can result in structural damage, even if a demister is used to protect the HEPA filter. The common U.S. practice of protecting HEPA filters from fires with a water deluge-demister system should be evaluated in light of the German studies.

The paper by Mr. Gilbert on high-strength HEPA filters represents the first study of this topic in the U.S. since the initial German studies reported by Mr. Wilhelm and his colleagues. The high-strength HEPA filter offers a solution to many of the failure modes that occur with standard HEPA filters under off-normal environmental conditions.

CHALLENGES WITHIN VENTILATION SYSTEMS  
DURING ACCIDENT SITUATIONS

M. Fronhöfer, M. Neuberger, J. G. Wilhelm

Kernforschungszentrum Karlsruhe GmbH  
Laboratorium für Aerosolphysik und Filtertechnik II  
Postfach 3640, W - 7500 Karlsruhe 1  
Federal Republic of Germany

Abstract

A numerical code (LAFIS) is developed which allows accurate modelling of flow transient in air cleaning systems under accident situations. With the support of this code the mechanical loadings on the filter units can be calculated. In addition a new type of High-Strength HEPA filter for accident stresses recently developed at Karlsruhe Nuclear Research Center is tested.

Clean and particle loaded High-Strength HEPA filters in the standard size of 610x610x292 mm were exposed to shock waves producing a peak differential pressure up to 170 kPa (24.6 psi), to evaluate their structural limit. For differential pressures between 80 and 170 kPa the residual particle removal efficiencies were greater than 99,8%. For preloaded filters (TiO<sub>2</sub>) no sign of particle release was evident in high-speed video films (400 frames/s) taken during transient conditions.

The results show High-Strength HEPA filters should be employed in air cleaning systems with high risk due to shock waves. Such filters have been implemented as an additional Engineered Safety Feature (ESF) in the air cleaning systems of German nuclear power plants.

I. Introduction and Problem Outline

During the last years there have been cases in which conventional HEPA filters were damaged even in normal operation and the reliable retention of activities was no longer ensured /1, 2/. A number of observations years ago had shown that conventional HEPA filters will tolerate only low mechanical loads without being damaged and suffering a drastic decline in removal efficiency /3/.

For better assessment of the failure risk of HEPA filters and, consequently, the risk of hazardous substances being released into the environment in increased amounts under off-normal operating conditions of a nuclear power plant, the loads arising within ventilation systems due to flow dynamics and thermodynamics must

## 22nd DOE/NRC NUCLEAR AIR CLEANING AND TREATMENT CONFERENCE

be known. A number of computer codes have been developed in nuclear technology over the past few years which allow the loads acting on the containment and on the surrounding auxiliary buildings to be modeled /4/.

The structural loads to which HEPA filters may be subjected at their places of installation within ventilation systems are determined by the accident under consideration and by the sequences of accident steps. This situation so far has been covered only by very rough estimates which, in nuclear power plants, indicate the occurrence of high specific radioactivity of the atmosphere, high air humidities, including periods in which the dew point is under-run, elevated temperatures, and high pressure drops /5/. More precise data can be generated only by means of special computer codes which allow the flow dynamics and thermodynamics to be modeled in the complex nuclear ventilation systems, some of which have several hundreds of components.

The importance of the annulus exhaust air filter systems, and their reliable functioning in environmental protection in the vicinity of nuclear power plants, asks to quantify in more detail and enhance, respectively, the existing safety margins of filter plenum at the end of the ventilation systems. For practical purposes, this is tantamount to an improvement in the mechanical stability of HEPA filters and to the development of a computer code LAFIS (LAF Iteration Solver) for transient flow dynamics conditions to model the very complex ventilation systems in nuclear facilities, including the condensation of water vapor.

### II. Numerical Code LAFIS for Modelling Accident Loads in Ventilation Systems

A ventilation network is considered a complex combination of a large number of components including straight duct sections, ducts changing direction (elbows), throttles, ducts changing cross section (nozzles and diffusers), "active" components (blower), and duct branches. In addition, randomly defined components may be added which can be described by their flow resistance characteristics and are called "discrete losses" (filters, dampers, heat exchangers, etc.).

In calculating the fluid dynamic and thermodynamic state variables, Kirchhoff's rules known from electrical engineering are employed for the steady-state case. In determining flow variables and state variables, the laws of conservation of mass, momentum and energy are used, thus allowing compressible non-steady state flow processes to be described. A detailed description of the code LAFIS will be published /6/.

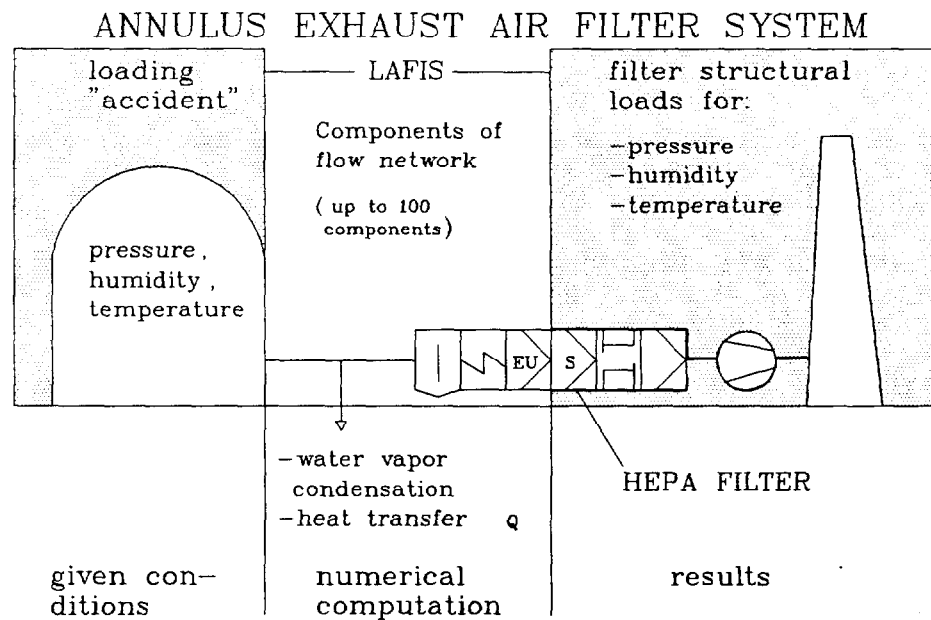


**Fig.1:** Numerical code LAFIS for modelling pressure and flow transients at filter service locations in ventilation systems.

In the laws of conservation some aspects are mentioned taking into consideration the special characteristics of steady- and non-steady-state flow in ventilation systems. Conservation of Mass: For non-steady state flows, inertia must be taken into account while, in compressible flows, it is the capacitance of large volumes that must be considered. Conservation of Momentum: The law of conservation of momentum describes the pressure loss and the pressure change, respectively, in each component (elbows, cross sectional changes, heaters, coolers, filters, ducts, etc.) as a function of the mass flow through these components /7/. Law of Energy Conservation: If the assumption of constant temperature is dropped, and if condensation phenomena in the ventilation duct is to be included, the energy equation must be used for each individual component. For nonsteady state flows, again the capacitance of large volumes must be taken into account.

The LAFIS (LAF Iteration Solver) ventilation code enables users, for given levels of pressure, temperature, mass flow or humidity as a function of time in a complex ventilation network, to calculate these same quantities at any other position in the ventilation system. There is also a possibility in the LAFIS code to calculate the changes in relative humidity and condensation of water vapor, if any, for each individual component. In this case, the humidity at the ambient nodes is given and its change determined as a function of pressure and temperature in the components.

### Code Description

The input part has the function of indicating all geometric data and flow data for each component of the ventilation system and their interconnection at the nodes. All ambient nodes and connecting nodes must be defined. Ambient nodes are connections between the ventilation system and its environment, e.g., the exhaust air stack or the pressure vessel and containment, respectively, etc. The ACRITH program package, based on an improved Newtonian procedure with interval arithmetics, was developed at Karlsruhe University in cooperation with IBM. The output part is used as post-processor for graphic data representation. In this way, the tabulated state variables and flow parameters can be output in a clearcut way both on the screen and by means of a plotter. To represent the results for nonsteady state flows, the pressure, density, temperature, and humidity for a certain node, and the mass flow, volume flow, velocity and Mach number, respectively, for a specific component, are plotted as a function of time.

### Shock Propagation in Ventilation Systems

In accidents in nuclear facilities or process installations, explosions or deflagrations may give rise to pressure disturbances (compression waves) which, under certain conditions, may be amplified into shock waves in ventilation ducts. In order to estimate the resultant hazard potential to the ventilation system and the downstream filter sections, shock propagation in ventilation system was studied.

Implementing empirical pressure coefficients, which can be taken either from steady-state flow studies or from handbooks /7/ on ventilation technology, allows wave propagation to be computed in any plant component. The occurrence of secondary shocks as a result of the flow being accelerated to the velocity of sound can also be taken into account. Even more complex ventilation networks can be modeled by combining the components of the plant. In this way, it is possible to extrapolate from familiar relations associated with steady-state flows to nonsteady-state shock wave propagation /8/.

### III. High-Strength HEPA Filters under Accident Conditions

The LAFIS program package described above allows, for a given accident at the inlet end of a ventilation system, to describe the loads (temperature, humidity, pressure) expected to arise in the filter at the outlet end of the ventilation system. To protect the environment from the effects of a potential accident, two possibilities are available which, in combination, can result in technically optimum environmental protection. On the one hand, protective devices should be provided for in the design of the ventilation system at specific points in order, e.g., to attenuate pres-

sure waves. On the other hand, the filters installed at the exhaust of the ventilation system should have higher mechanical strength without generating higher pressure drops during normal operation, in order to achieve maximum safety.

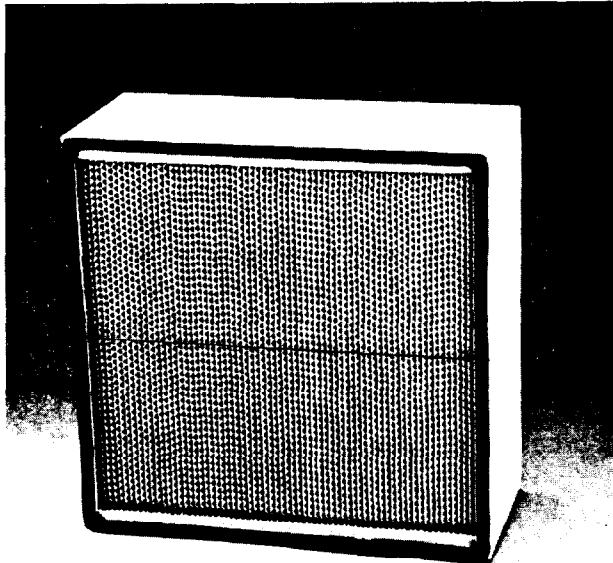


**Fig. 2:** High-Strength HEPA filter (610x610x292 mm) developed at Karlsruhe Nuclear Research Center (KfK).

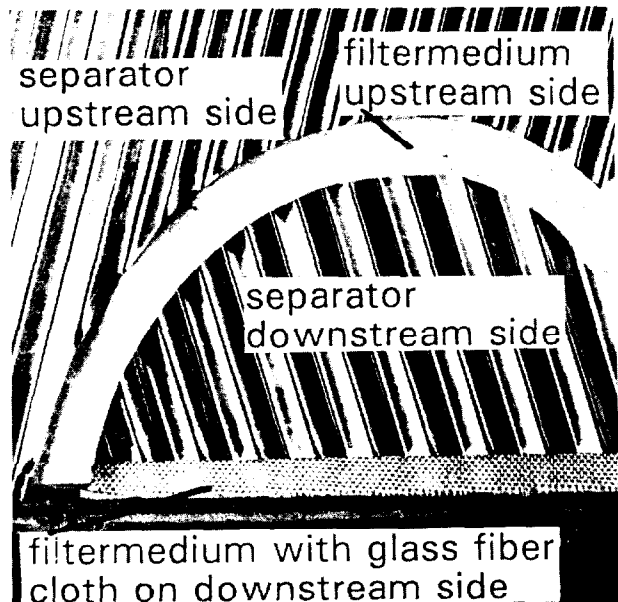


**Fig. 3:** Construction of High-Strength HEPA filter: aluminium separators with inclined corrugations; filtermedium reinforced with a fiberglass cloth on downstream side.

For almost three decades, commercial HEPA filters have been studied for application in the ventilation systems of nuclear plants. To this day, the mechanic load-bearing capacity of conventional commercial deep pleat and mini-pleat filters has not improved significantly over the initial levels /9, 10/. In the period between 1984 and 1987, High-Strength HEPA filter units have been developed at the Laboratorium für Aerosolphysik und Filtertechnik II, which withstand extreme pressure drops and volume flows. To this day, they have worked satisfactorily in many exhaust filter systems of German nuclear power plants and in critical experimental facilities with high potentials for releases of radioactive and toxic dusts. The filters are available commercially under \*license from two German companies and one English company. The operating experience accumulated, and the test results generated, with the newly developed High-Strength HEPA filters will be compared below with conventional HEPA filters.

\* Atex Filter GmbH, Camfil Luftfilter GmbH, Vokes Ltd.

## HIGH STRENGTH HEPA FILTER

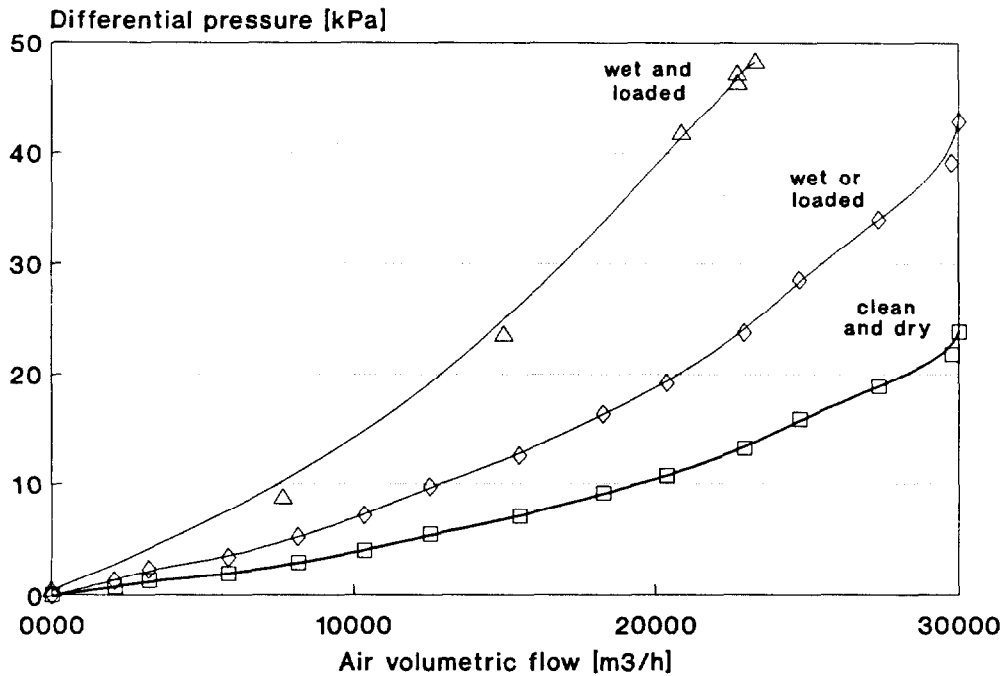


**Fig. 4:** Flow-resistance curves for High-Strength HEPA filter: 1. clean and dry, 2. wet or loaded, 3. wet and loaded.

Characteristics of High-strength HEPA Filters at High Pressures, High Temperatures, and High Air Relative Humidities

The failure mechanisms of conventional deep pleat and mini-pleat filters were studied in detail in a test facility built 1984, BORA /5, 11, 12/. The conventional deep pleat filter was used as a model for a High-Strength filter (610x610x292 mm). The external characteristics of the High-Strength filter are an increased number of pleats and ribs installed in the middle of the upstream and downstream sides to prevent the frame from ballooning (Fig. 2). The high mechanical strength of the filter is achieved by crossed separators on the upstream and downstream sides (Fig. 3) and a fiberglass cloth reinforced on the downstream side /13/.

High-Strength filters can be subjected to a steady-state flow in the BORA test facility; in this way filters may be tested also under prolonged accident conditions. Figure 4 shows the characteristic curves (pressure versus volume flow) for various filter loads. A new, unloaded, High-Strength HEPA filter can be exposed to a volumetric flow of 30,000 m<sup>3</sup>/h (at 30 °C) of air, which gives rise to a pressure drop of 25 kPa across the filter. If the filter unit is loaded or moist, or if a filter is exposed to combined loads and stresses, the pressure drop will rise to more than 50 kPa at a lower volumetric flow. The characteristics of the

blowers in the BORA test facility do not allow higher pressures to be generated at the flows mentioned above. Tests conducted in the BORA facility were raised up to pressure drops of 56 kPa, and none of the High-Strength filters showed any visible damage. After the tests, all filters had removal efficiencies 99.97% for particle sizes of 0.3  $\mu\text{m}$ , which is required for HEPA filters, and were leakfree as measured with the oil plume test according to DIN 24184.

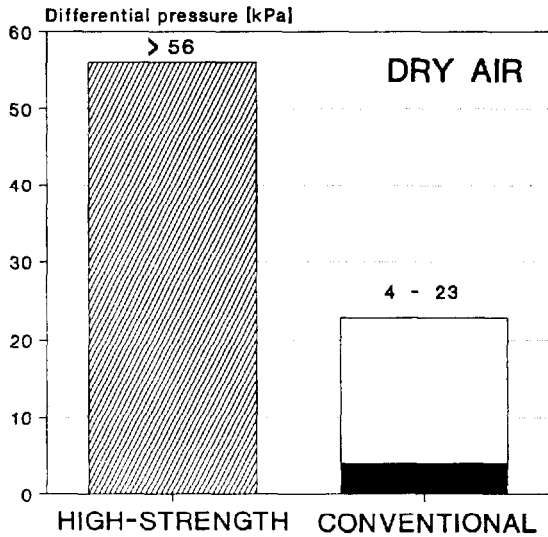


**Fig. 5:** Comparison of structural limits for conventional HEPA filters in dry air (differential pressure at failure) to those of High-Strength HEPA filters (differential pressure without failure at test rig maximum).

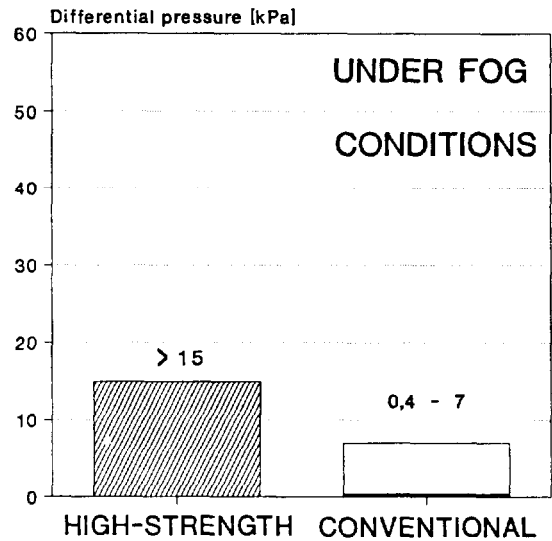


**Fig. 6:** Comparison of structural limits for conventional HEPA filters under fog conditions (differential pressure at failure) to those of High-Strength HEPA filters (differential pressure without failure at test rig maximum).

The pressure drops achieved without the High-Strength HEPA filters showing any structural failure are compared in Fig. 5 and, for moist air, in Fig. 6 with the structural limits of conventional commercial HEPA filters. The actual failure limit of the new High-Strength HEPA filters was not determined. In conventional filters, the range of failure is indicated, with some filters showing failure already at a pressure drop of 4 kPa in dry air and only 0.4 kPa in moist air.

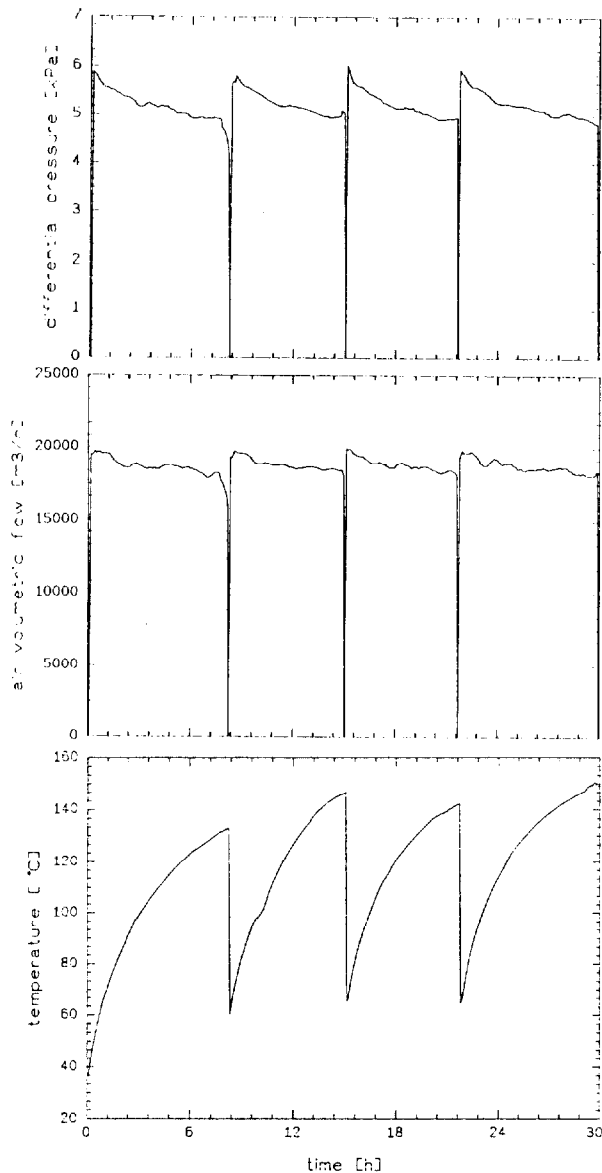


**Fig. 7:** Test of 30 h duration with High-Strength HEPA filters.

The facility cooled down to 60 °C over night. The filter was again challenged by an air flow in three additional cycles of 7 hours each, until a temperature limit of 140 °C, which is above the design temperature, had been reached. The High-Strength HEPA filter was not removed from testsection in between and, consequently, was subjected also to thermal cycling. After the end of the test, the filter was free from oil plumes and had a removal efficiency of  $\eta = 99.97\%$  required for a HEPA filter (DIN 24184 or equivalent).

Normal glass fiber paper loses some 85% of its tensile strength (about 50 N/5 cm), if it is moist and pleated at the same time, this is reduced to a tear strength of about 7 N/5 cm specimen width. The glass fiber filter medium reinforced with a glass fiber cloth on the downstream side has a 16 times higher tensile strength of about 800 N/5 cm in the dry state. Even in the wet, pleated state, the tear strength of the reinforced filter medium is about 620 N/5 cm, which is approximately 12 times higher than that of normal filter paper in a dry condition.

In a prolonged experiment, High-Strength HEPA filters were subjected to a volumetric flow of approx. 20,000 m<sup>3</sup>/h of air for 30 hours, with the mean pressure drop being 5 kPa (Fig. 7). The High-Strength HEPA filters have been designed to a max. service temperature of 120 °C. After 8 hours of continuous operation without cooling, the air recirculated in the BORA experimental facility was heated to 130 °C. The volumetric flow and the pressure drop prevailing across the filter decreased to lower levels.

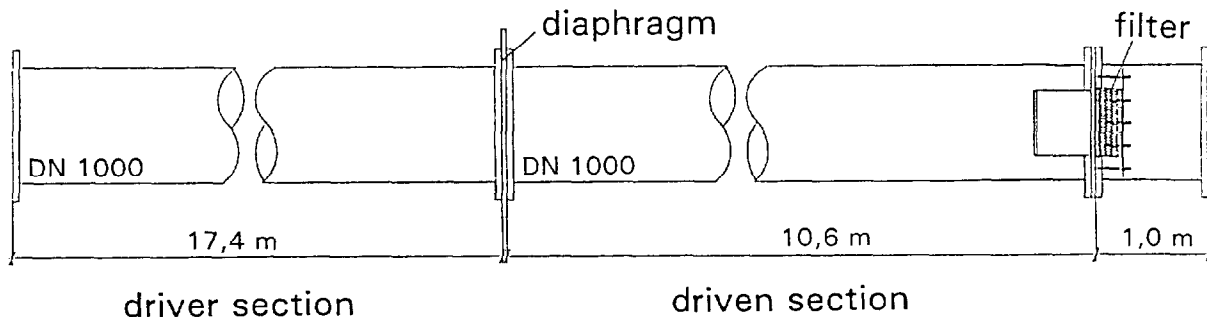


Fig. 8: Schematic of shock tube.

High-Strength HEPA Filters Exposed to Shock Waves up to  $\Delta p=170$  kPa

In many test facilities, the structural limits of HEPA filters are determined by transient loads. In conventional deep pleated HEPA filters (610x610x292 mm) the structural limit corresponds to the pressure drops of 4-20 kPa as determined in a steady state flow /9, 10/.

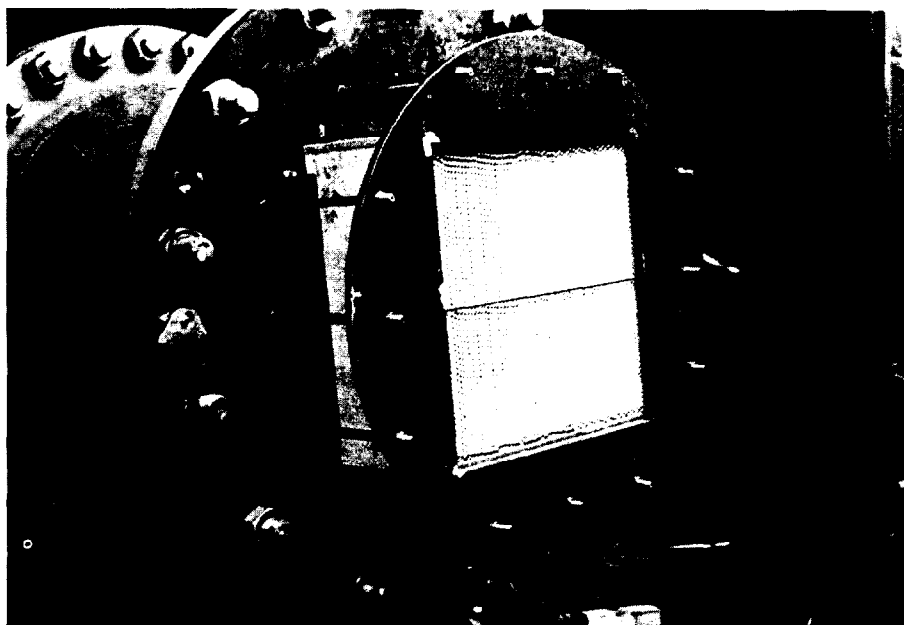


Fig. 9: High-Strength HEPA filter at the end wall of the shock tube.

At the Ernst Mach Institute of the Fraunhofer Society in Germany, a shock tube (Fig. 8) of 1 m diameter and 28 m length was

available for testing High-Strength HEPA filters up to the occurrence of the first visible structural damage. The High-Strength HEPA filters were tested relative to the ambient pressure (Fig. 9); consequently, the maximum possible pressure drop prevailed across the filter. The filters were subjected to shock waves generating maximum peak pressure drops of 30-170 kPa (4.3 psi - 24.2 psi).

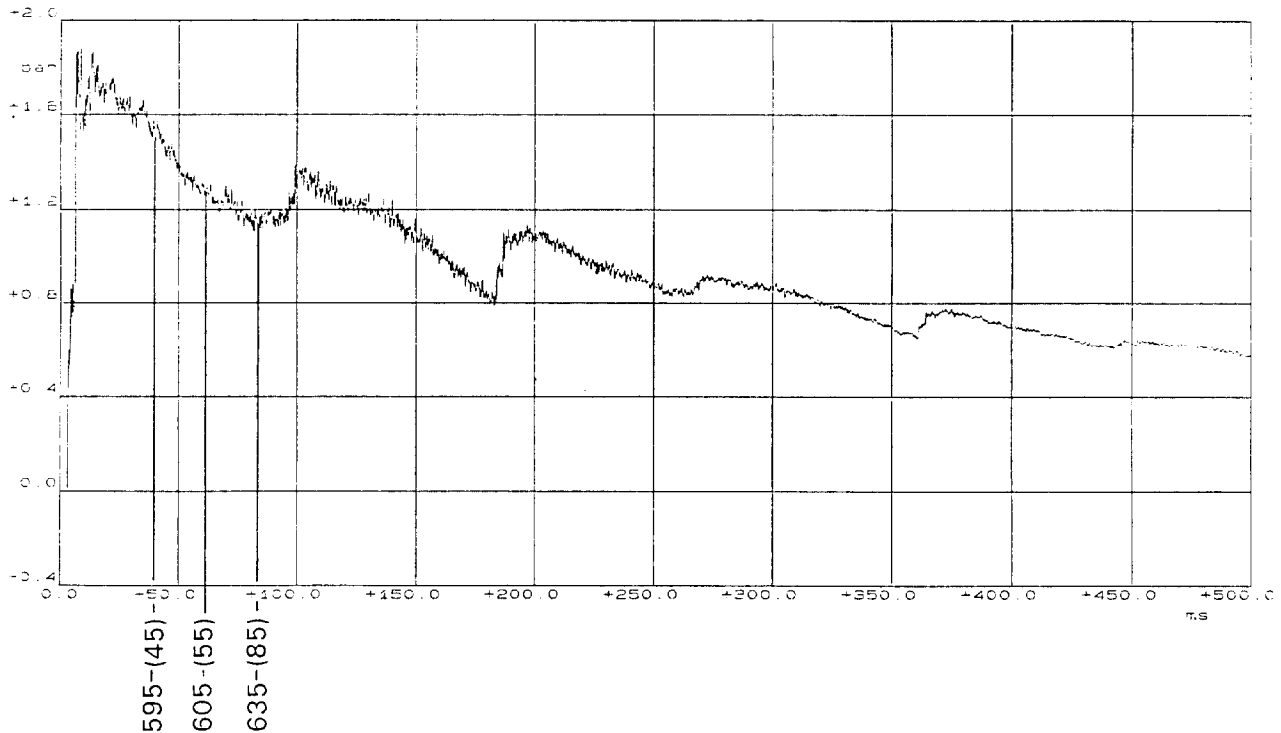


Fig. 10: Pressure transients from HEPA filter test ( $P_{21} = 1.8$ ,  $\Delta p = 170$  kPa).

The most spectacular experiment with a maximum pressure drop of 170 kPa (24.2 psi) will be described below. The development of pressure versus time in the experiment as measured directly at the filter is shown in Fig. 10.

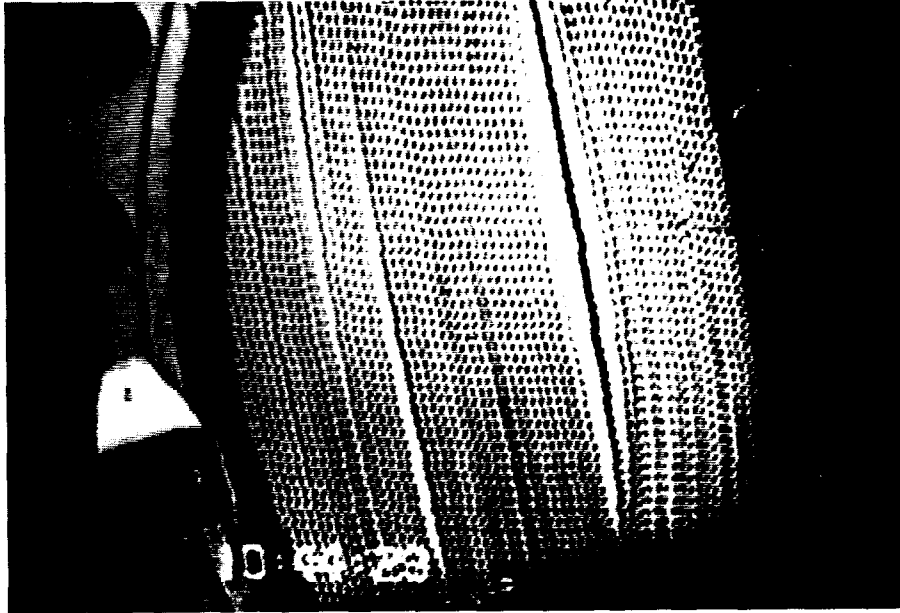


Fig. 11: Behavior of High-Strength HEPA filter under shock wave ( $P_{21} = 1.8$ ,  $\Delta p = 170$  kPa)

Figure 11 show the decisive picture taken during the test at a pressure drop of 170 kPa (24.2 psi). The time at which the pictures was taken is shown in the diagram in Fig. 10 (635 - (85)). The pictures were recorded by means of a high-speed video camera operating at 400 frames per second. The shock wave starts, hits the filter after some 2.5 ms and is reflected (Fig. 10), thus causing a pressure drop rise across the filter of 170 kPa. After some delay, the filter unit begins to be passed through which, after 40-45 ms, leads to the first ballooning of the filter pleats. Another 12 ms later, the flow continues to increase. The wooden frame expands despite the powerful clamping device. The threaded rod installed in the middle, to prevent the frame from buckling, is ruptured. The filter pack is exposed to pronounced dynamic forces until the weakest spot in the filter pack has been found, at which it can show maximum buckling. The inflated pleats migrate through the filter pack until, after 85 ms, a state has been reached in which the highest flow occurs and the filter thus is subjected to the highest load. After about one second, the approx.  $14 \text{ m}^3$  of compressed air in the driver section under a pressure of 240 kPa (35.5 psi), have been discharged through the filter.

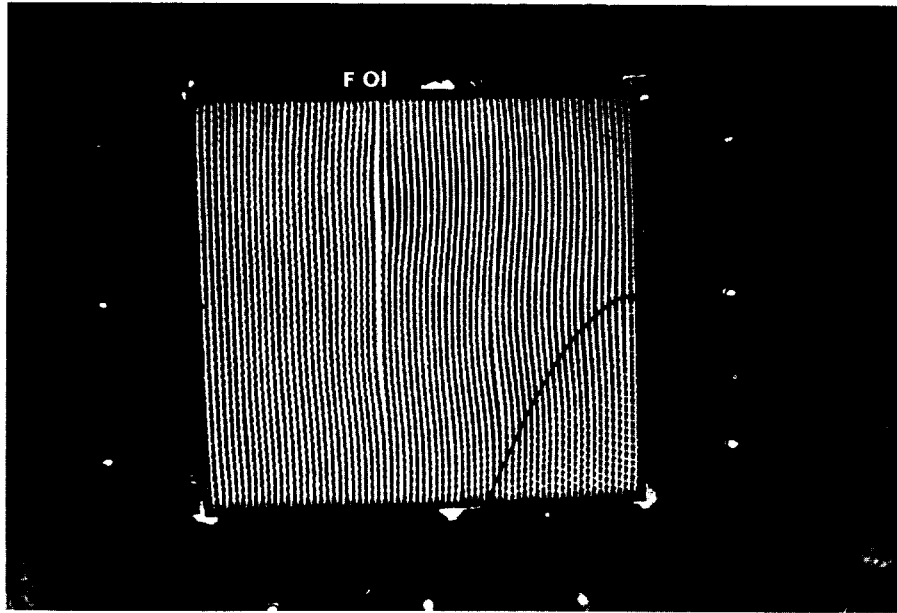


Fig. 12: High-Strength HEPA filter after shock wave exposure ( $P_{21} = 1.8$ ,  $\Delta p = 170$  kPa).

The High-Strength HEPA filter was inspected for visible damage while still installed in the test facility (Fig. 12). The recognizable defects were dented separators and the ruptured connecting rod. No cracks in the filter paper and in the elastomeric sealant were seen. The fiber glass on the downstream side prevents the filter pleats from breaking up. Where the pleats had expanded, the glass fibers of the glass fiber filtermedium were partly fractured. The filters subsequently were taken through a removal efficiency test with DEHS\*\* at a nominal volume flow of  $1700 \text{ m}^3/\text{h}$ . In line with their loading in the tests, their removal efficiency declined (Fig.13). High-Strength HEPA filters are required to have a removal efficiency at least of  $\eta = 99.97\%$ . The filters, which were subjected to a pressure drop of 30 and 40 kPa during the test, did not indicate any decreasing removal efficiency. After a pressure drop load of 75 and 80 kPa, the removal efficiency dropped to  $\eta = 99.96\%$ , which barely misses the criteria applied to HEPA filters. But even after a load of 120 kPa, the removal efficiency drops only to  $\eta = 99.9\%$  and, at 170 kPa, to  $\eta = 99.8\%$ . The oil plume test indicated leakages of individual oil filaments (40 kPa) up to an oil mist covering a larger area (120 kPa and 170 kPa). This is indicative of broken fibers in the fiberglass mat, whose further rupturing is prevented by the supporting structure.

---

\*\* DEHS: Di- (2-ethylhexyl)-sebacat (DES), particle distribution like DOP

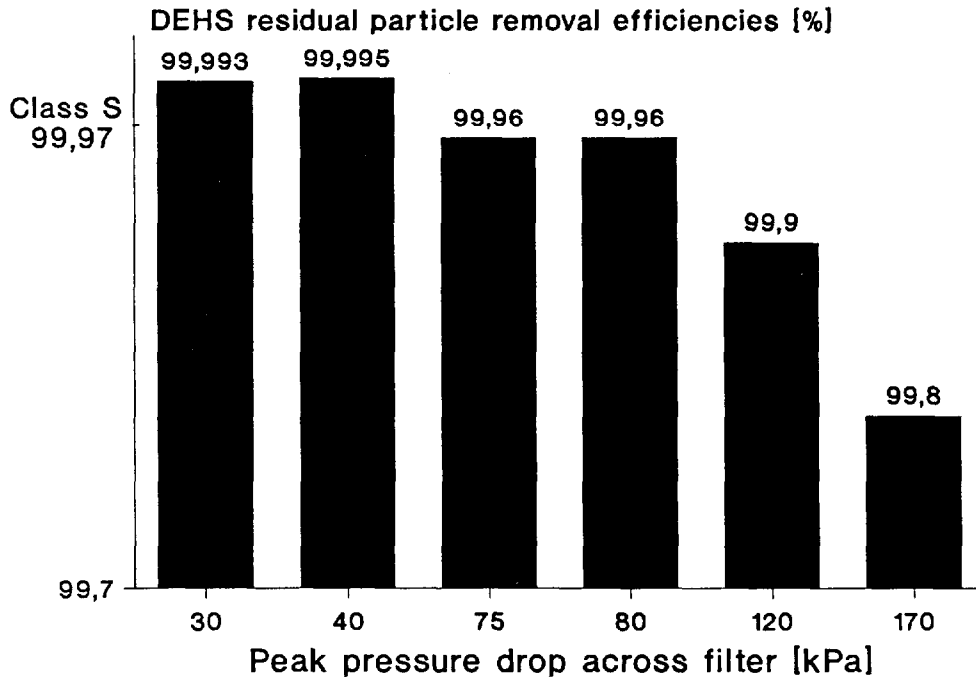


Fig. 13: Comparison of residual DEHS particle collection efficiencies of High-Strength HEPA filters after shock wave pressures across the filter.

The results are significant, as no High-Strength HEPA filter showed total failure even under extreme pressure drops (no cracks in the filter medium or in the elastomeric sealant), and all filters had removal efficiencies afterwards at least of Class R ( $\eta > 98\%$ ).

Two HEPA filters were exposed to  $\text{TiO}_2$  particles ( $x_{50} = 0.3 \mu\text{m}$ ) applied by a brush dosing unit up to a pressure drop of 1000 Pa. Both filters then were exposed to shock waves, which generated pressure drops of 48 kPa and 90 kPa across the filter. No sizeable dust discharge was observed, but dust migrated into deeper layers of the filter medium. After the test the filters, at nominal volume flow ( $1700 \text{ m}^3/\text{h}$ ), had pressure drops of 760 Pa (after a load of 48 kPa) and 600 Pa (after 90 kPa) instead of the 1000 Pa they had before the test. Under the more pronounced shock wave impact there was also a more pronounced migration of  $\text{TiO}_2$  particles into deeper layers (Fig. 14). Evaluation of the high-speed video film shows a peak-like penetration of dust for a few milliseconds, as has also been determined with DOP droplets /8/. The downstream side of the filter (Fig. 15) was examined under the scanning electron microscope (SEM), but no  $\text{TiO}_2$  particles were found to adhere. The removal efficiencies after the tests corresponded to those shown in Fig. 13 for new filters:  $\eta = 99.97\%$  at a pressure drop load of 48 kPa (still class S) and  $\eta = 99.93\%$  at 90 kPa (Class R).

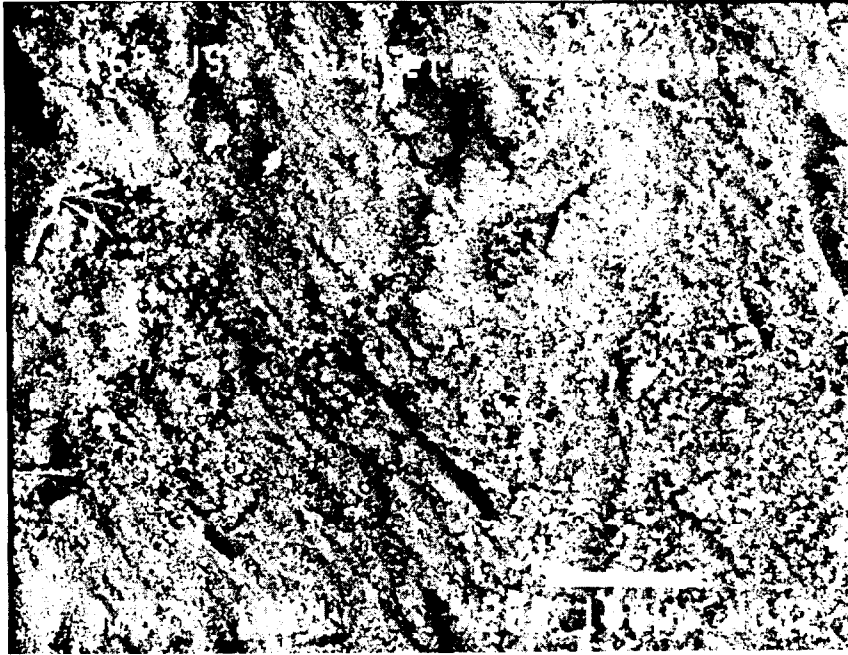


Fig. 14: SEM - photograph of filter medium on the upstream side from  $\text{TiO}_2$  loaded High-Strength HEPA filter after shock exposure ( $P_{21} = 1.42$ ,  $\Delta p = 90$  kPa).

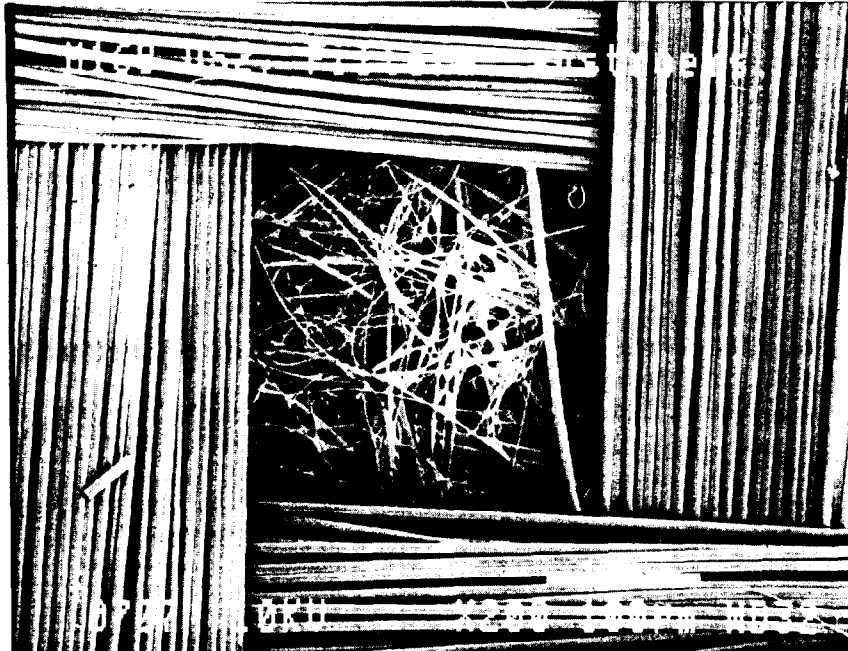


Fig. 15: SEM - photograph of reinforced filtermedium on the downstream side from  $\text{TiO}_2$  loaded High-Strength HEPA filter after shock exposure ( $P_{21} = 1.42$ ,  $\Delta p = 90$  kPa).

IV. Conclusion

With the numerical code LAFIS it is possible to calculate the mechanical loading on filter units at the discharge of exhaust air filter systems with more than one hundred components (e.g. ducts, elbows, duct branches, nozzels and diffusors, blowers and compressors, filters, dampers, heat exchangers, described by their  $\Delta p$ -V characteristic) for a given accident at the inlet end (e.g. containment) of a ventilation system.

All test results obtained with the high-strength HEPA filters, newly developed at the Laboratorium für Aerosolphysik und Filtertechnik II, indicate that it is possible to protect critical test installations with a high hazard potential by the appropriate HEPA filters. In dry air, pressure drops at the filter should not exceed 50 kPa, a level which still leaves a wide safety margin. Under high relative humidity conditions, pressure drops up to 15 kPa have been found to cause no damage and still leave a safety margin. A detailed description of all experiments and results will be given in a report /14/.

The High-Strength HEPA filters have been designed specifically for accident filter systems in German nuclear power plants and can be built in various sizes with the same levels of mechanical strength. This has greatly reduced the hazard of releases of radioactive and toxic dusts, respectively, through exhaust air filter systems. Other areas of application for these filters are ventilation systems in the chemical industry and processing industry with high hazard potentials, and facilities for the extraction of explosible dusts.

V. References

- /1/ Carbaugh, E. H.  
Survey of HEPA Filter Applications and Experiments at  
Department of Energy Sites;  
PNL - 4020 (Pacific Northwest Laboratory), 1981.
- /2/ Czarnecki, J.  
Some Experiences with Measurements of Stack Releases and  
their Correlations with Environmental Measurements;  
IRPA - Tagung, Sydney, 10. - 17. April 1988, S. 689 - 692.
- /3/ Ricketts, C. I.; Rüdinger, V.; Wilhelm J. G.  
HEPA - Filter Response to High Differential Pressures and  
High Air Velocities;  
Proc. 5th International Meeting on Thermal Nuclear Reactor  
Safety, Karlsruhe 1984, KfK 3880 (1984), Bd. 2, S. 1572.

## 22nd DOE/NRC NUCLEAR AIR CLEANING AND TREATMENT CONFERENCE

- /4/ Fischer, M. et al.  
The Multi Compartment Code WAVCO to Analyse the Behavior of Non-Condensibles During Hypothetical Accidents;  
Second Int. Meeting on Nuclear Thermohydraulic, Santa Barbara, Cal., Jan. 1983.
- /5/ OECD/NEA - Report  
Air Cleaning in Accident Situations,  
Paris, OECD 1984, S.26
- /6/ Neuberger, M.  
LAFIS - Ein Rechenprogramm zur Bestimmung der strömungs- und thermodynamischen Belastungen in Lüftungssystemen;  
LAF II, PSF - Bericht, Kernforschungszentrum Karlsruhe GmbH, to be published, (1992)
- /7/ Idelchik, I. E.  
Handbook of Hydraulic Resistance;  
Second Edition, Springer Verlag 1986.
- /8/ Neuberger, M.  
Zur Ausbreitung schwacher Stoßwellen in Lüftungssystemen;  
KfK 4920 (1991).
- /9/ Billings, C. E. et al.  
Blast Effects on Air Cleaning Equipment - Results of Filter Test;  
Proc. 4th AEC Air Cleaning Conference, TID Report 7513,  
p. 279, (1956).
- /10/ Cuccuru, A. et al.  
Effects of shock Waves on High - Efficiency Filter Units,  
EUR 10580 (1986), S. 877
- /11/ Rüdinger, V., Arnitz, Th., Ricketts, C. I., Wilhelm J. G.  
BORA - A facility for experimental investigations of air cleaning during accident situations;  
CONF 840806, p. 1441 (1985).
- /12/ Rüdinger, V., Ricketts, C. I., Wilhelm J. G., Alken, W.  
Development of Glass-Fiber HEPA Filters of High Structural Strength on the Basis of the establishment of the Failure Mechanisms;  
CONF 860830 (1987).
- /13/ Rüdinger, V., Ricketts, C. I., Wilhelm J. G.  
High Strength High Efficiency Particulate Air Filters for Nuclear Applications;  
Nuclear Technology, Vol. 92. Oct. 1990.
- /14/ Fronhöfer, M. et al.  
Hochfeste Schwebstofffilter - Typ KfK;  
KfK - Bericht, Kernforschungszentrum Karlsruhe GmbH, to be published, (1992).

## 22nd DOE/NRC NUCLEAR AIR CLEANING AND TREATMENT CONFERENCE

### DISCUSSION

**TSAL:** Does your LAFIS computer program for non-steady state transient flow analysis include simulations of the control system as well as the HVAC systems? Is the program commercially available or is it a proprietary code of your company.

**WILHELM:** LAFIS is assigned for simulation of HVAC and control systems. It will be available by KfK as LAF II next year. It is based on the algorithm of the Fortran-ACRITH program package by IBM.

**JANNAKOS:** Could you tell me what was the size of the filter exposed to the wave shocks, and whether efficiency depends on the size of filters and differential pressure?

**WILHELM:** The size of the high-strength HEPA filters is that of the standard 610 x 610 x 292 mm HEPA filter. They are also built in larger sizes for some of the reactors. But there is neither an effect on efficiency nor on strength. Filters larger than standard size were not tested. The effect of pressure differential is given in the paper.

**BERGMAN:** Can you tell us the cost of this filter?

**WILHELM:** The cost of one of those filters is 650 marks at the moment which in Germany is 2.5 times more than that of the standard HEPA filter. KfK originally didn't want to buy these HEPA filters because they had a higher price but they have extended life and one can put more dust on them. In addition, one saves money for the exchange of the HEPA filters, which is very important. So, a few years ago KfK changed completely to high strength HEPA filters expecting that the total price would be lower for air cleaning. I should like to add one thing. Mr. Leibold will also speak about these HEPA filters being used in conventional plants and recleaned. Some of them have been in service for 18 months up to now.

RADIAL FLOW SYSTEMS FOR THE NUCLEAR INDUSTRY

Michael L. Davis  
Flanders Filters Inc.  
Washington, N.C.

Abstract

Handling and disposing of HEPA filters in the nuclear industry is often difficult, dangerous and inefficient. This paper presents containment filtration systems designed to address these problems using round, radial flow filters.

Most filtration systems in use presently use rectangular shaped axial flow filters. The most commonly use size (size 5) is 24" X 24" X 12", delivering 1000 CFM at 1" Water Gage of pressure drop. These filters are made using one of two basic frame materials, wood and metal. Most wood framed models weigh approximately 35 pounds. Most metal models weigh approximately 50 pounds. Changing these filters, especially when they are above floor grade, can be hazardous and difficult simply because of their weight. When bag-in bag-out systems are required, the corners on rectangular filters present a potential for damaging the bags. An equivalent 1000 CFM radial flow filter, with stainless steel end caps and faceguards, weighs approximately 28 pounds, and has no corners to threaten bag integrity. This paper includes a description of a system which uses a waste storage drum as the filter housing, which eliminates entirely the handling of filter inserts and the attendant hazards.

Long term hazardous waste storage is a major problem for the nuclear industry. We believe that radial flow systems present a potential for reducing the volume of this waste. Spent filters which contain radioactive filtrates are often placed in 55 gallon drums for long term storage. In order to get it into a drum, the size 5 filter must first be dismantled or crushed. Either method releases filtrate into the air, necessitating the use of specially designed (and costly) facilities and equipment. We have designed radial flow filters so that they fit into drums with no dismantling or crushing needed. One size is rated at 1500 CFM, and still easily fits into a DOT 55 gallon drum. Usually, one drum holds one size F filter, which means 1000 CFM of spent capacity per drum. The radial flow system allows 1500 CFM per drum with no filter crushing or dismantling. The paper presents designs, configurations, and performance characteristics of filtration systems utilizing radial flow filters. It includes descriptions of methods for performing in-place efficiency testing for multiple filter housings.

---

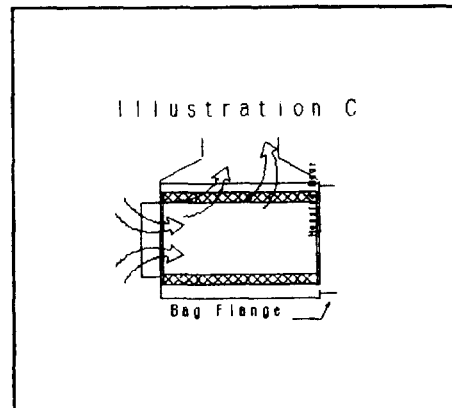
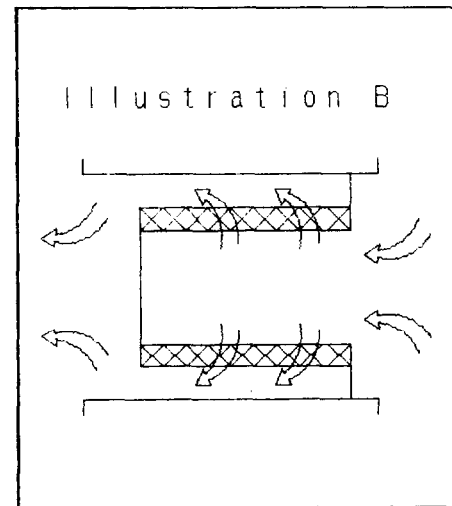
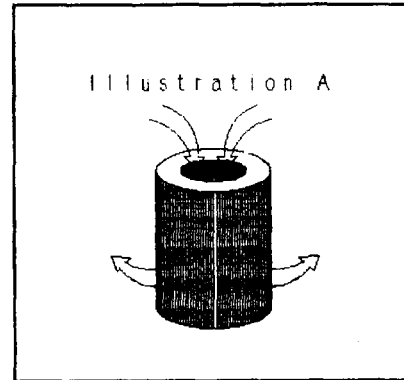
A radial flow filter directs air flow through the filtration medium in a direction which is radial relative to the filter's center axis (Illustration A). Radial flow systems work with the airflow direction either in toward the axis or out away from it. If air flow is directed into the center of the filter and then out through the medium, the filter acts like a canister, helping to maintain control of the filtrate during handling of spent filters. If the housing is designed so that it's inlet is also the filter's

22nd DOE/NRC NUCLEAR AIR CLEANING AND TREATMENT CONFERENCE

inlet (Illustrations B & C), this keeps the entire housing free from particulate contamination. All of the designs we have been working on utilize this intrinsic safety feature.

The physical size we have concentrated our development on is a 20" outside diameter 32" long cylinder. The obvious rationale for this is that it fits into a DOT 55 gallon drum, with enough room left over for a containment bag. With a 2" deep pack, yielding a 16" inside diameter, this filter has about 346 square feet of available medium. The traditional size 5 aluminum separator design has about 215 square feet. Illustration D shows flow versus pressure drop curves for both of these filters, plus a radial filter of 15" outside diameter and a 20" O.D. filter with a 4" deep pack. This last filter has about 486 square feet of medium. However, the smaller inside diameter (12") which this presents creates a pressure drop penalty. All the air which passes through a radial filter must pass through the orifice created by its inside diameter. Pushing 2000 CFM through a 12" orifice takes about a .85" pressure drop. For a 16" orifice, the pressure drop is about .32" at 2000 CFM. For this reason the 16" ID filter has a better flow versus pressure drop performance, even though it has less medium surface.

The 15" OD filter contains about 230 square feet of medium. It can fit inside the 20" OD 16" ID filter, thus enabling the storage of about 675 square feet of medium in one drum with no filter deformation required. A relatively simple hydraulic ram compactor could double that. With waste handling and storage costs running as high as \$8,000 per drum, this presents a potential for a five-fold reduction in spent filter storage volume and cost, with little or no added handling complication. We believe that this is a compelling reason for considering radial flow designs.



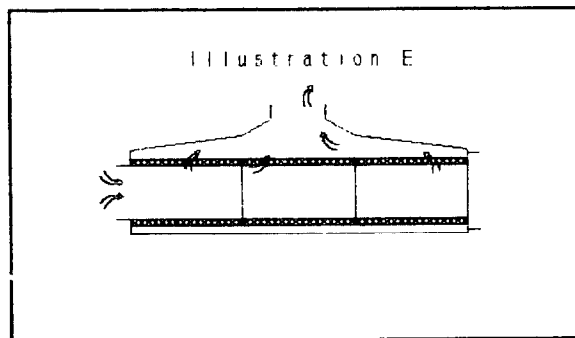
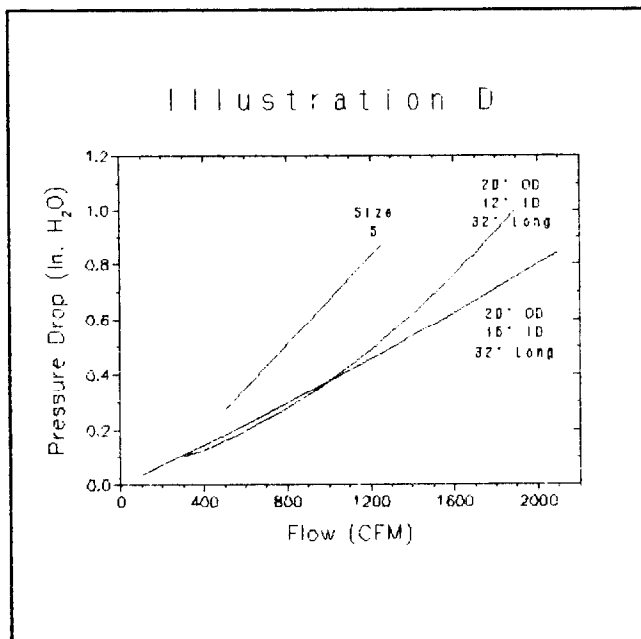
Filter Size	Square Feet of Medium
Size 5	215
20" OD 16" ID 32" Long	346
20" OD 12" ID 32" Long	486
15" OD 11" ID 31" Long	230

There are two basic housing design schemes suitable for radial filters. One is the traditional side load (Illustration B), with filters inserted into the housing normal to the entering air flow direction. The other is end load (Illustration C), with filters inserted parallel to the entering air flow direction.

Side load designs have the advantage of allowing vertical stacking of housings. A large bank of filters would present a design very similar to what is used for axial flow systems. In effect, even though the filter itself is radial flow, the housing remains axial flow. Testing has shown that each filter needs a minimum of 2" of clearance in a radial direction to allow enough plenum space for leaving air without imposing a noticeable pressure drop penalty. This means that a housing for a 20" OD filter would have the same 24" inside cross section as a size 5 housing. For a 32" long filter, however, the housing would have to be longer than a size 5 housing. This difference is offset by the increased medium area, which means that a radial design can be smaller in filter count than an axial system of equivalent air handling capacity. If we use a conservative 1500 CFM capacity for the radial filter, and the standard 1000 CFM for the size 5, two radial filters replace 3 axial filters.

An end load design is especially appropriate where leaving air direction turns 90 degrees from entering direction (Illustration C). Housings can be closely packed in one direction, but a 2 dimensional matrix of them would not be possible. Filters can be mounted end to end, like shells in a shotgun magazine (Illustration E). There is a limit to how many can be strung together in this manner. The filter's inside diameter presents a pressure drop penalty at high velocities, much like a section of duct. More than 3 filters in a line would probably not be practical.

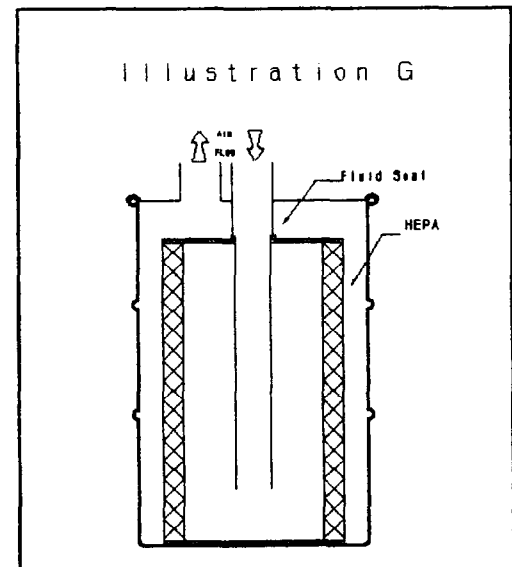
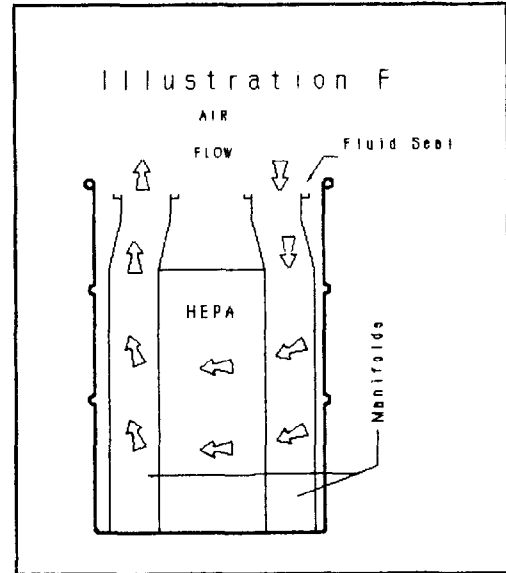
Locking mechanisms for side load housings would be similar to current axial system designs. For end load systems, however, the design can be very uncomplicated. Replaceability is easy to design, and field replacement is simplified. This results in decreased expense and greater reliability. In critical systems, the simplicity and reliability can be high priority considerations.



In-place testing would be accomplished in much the same way as with axial flow filters. In side load systems, in-place test designs can be virtually identical to traditional axial systems. End load systems which have only one filter per housing can be very similar. End load systems with more than one filter per housing, however, present a complication. Since in essence, these filters act like one very long filter, all the filters in a housing dump leaving air into a common plenum. This makes the problem of isolating a leak to an individual filter or filter-to-filter seal very difficult. We have some ideas as to how this could be done, but none have been developed fully as of now.

There are reasons other than waste storage efficiency for considering radial flow filter design. For instance, a radial filter of equivalent capacity weighs less than an axial flow filter. A size 5 filter with a wood frame and face guards on both faces weighs about 35 pounds. With a stainless steel frame and face guards, it weighs about 50 pounds. A radial filter with the same amount of media as a size 5 filter, with stainless steel end caps and stainless steel mesh on both upstream and downstream faces, weighs 28 pounds. The 20" OD 16" ID 32" long radial filter, which delivers over 2000 CFM at 1" pressure drop, weighs about 32 pounds. This weight advantage is important to whomever is loading or changing filters. In bag-in/bag-out systems, the lack of corners on radial filters, along with the lighter weight, is a distinct safety advantage. The lighter, rounded design decreases the likelihood of bag puncture. Also, since the filtrate is trapped in the inside of the cylindrical filter, the probability of filtrate escaping, even if a bag does get damaged, is decreased.

There are some other applications which uniquely lend themselves to radial design. One is the "filter-in-a-drum" idea. We were recently asked to quote on the design shown in illustration F. This is a design incorporating a DOT 55 gallon drum as the filter housing. Note, however, that it still requires a substantial amount of stainless steel fabrication to make the inlet and outlet plenum systems. The filter, a size 4, presents 100 square feet of medium. Compare this with the design in illustration G. This utilizes a radial filter element with 275

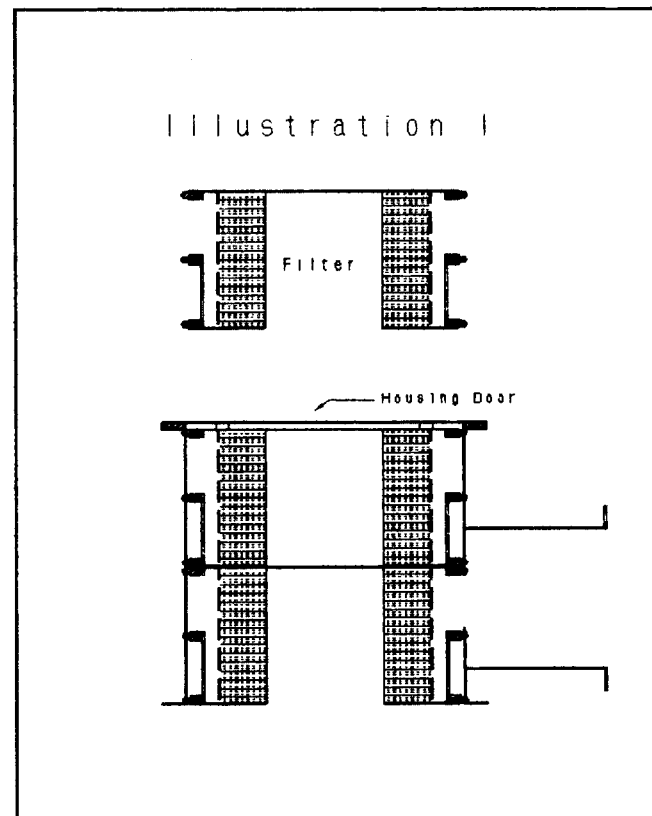
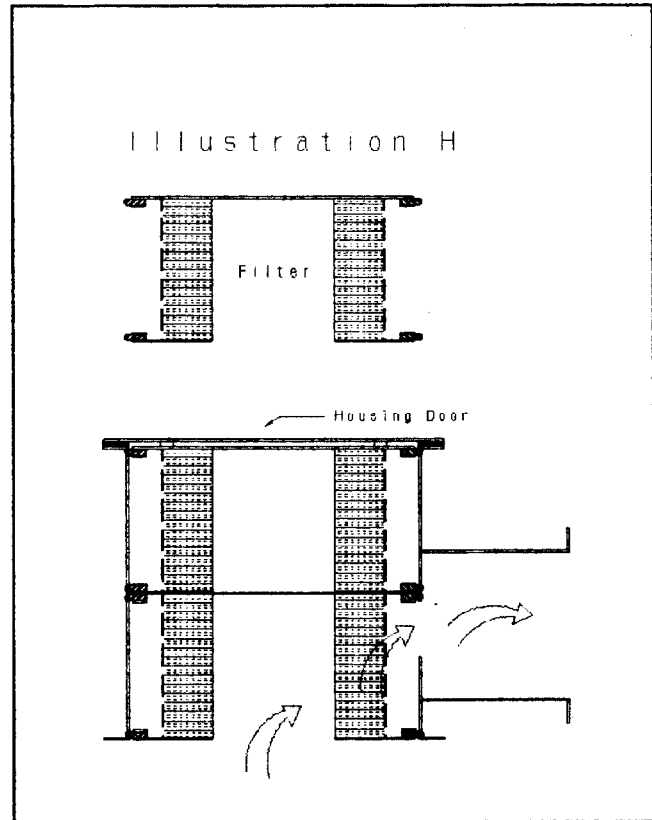


square feet of medium. It also eliminates the costly stainless plenum fabrication. When the element is spent, the drum top with the inlet and outlet ducting is removed, and a standard drum top is mounted. The filter is then enclosed in a drum, ready for handling or storage.

Another application which works well with the radial design is what we call the push-through housing. It is a design which is often seen on glove box applications. Illustration H depicts the concept. The spent filter is displaced by pushing a new filter into the housing. The displaced filter is pushed into the glove box, where it is then removed through a bag-out port or otherwise processed.

Illustration I shows a modification of the design which prevents bypass from the glove box to the outlet during filter change. This is accomplished by the addition of a third gasket (gasket C). As the filter moves out of the housing, gasket C prevents unfiltered air from entering the outlet after gasket A loses contact with the housing wall. Without gasket C, air could bypass the filter as soon as gasket A loses contact. This feature eliminates the need to provide shutoff dampers or other means of preventing bypass during filter changeout.

We believe that there are some very sound reasons to consider using radial flow filters in the nuclear industry. There is another issue to consider besides mechanical design, however. That issue is the need to comply with regulations. Test specifications to insure quality, safety, and suitability have been in place for axial flow rectangular filters for a long time. Issues like



## 22nd DOE/NRC NUCLEAR AIR CLEANING AND TREATMENT CONFERENCE

dimensions, efficiency, pressure drop, resistance to rough handling, heat, flame, and wet overpressure are thoroughly covered by current specifications. Equivalent specifications and test procedures are not now in place for round radial filters. There is also no current provision (no specifications or test equipment) for placing radial filters on the U.S. Qualified Products List. Therefore, there are no radial filters on the list. There may be some cases where radial systems can be used despite this lack, but we believe that for the industry to safely incorporate radial filter designs, appropriate specifications and procedures must be developed. The U.S. Army CRDEC has said that they see no barrier to developing test equipment with which to qualify radial filters for inclusion on the QPL. But for that to happen, they must be directed to do that. This means that you, as users of filtration system, must let it be known through proper channels that there is a need. We are confident that a cooperative effort between manufacturers and potential users will result in the rapid development of standards, thereby assuring the safe application of this exciting new technology.

### DISCUSSION

**DYMENT:** Is the speaker aware of the situation regarding the use of radial flow filters in the U.K.? I can outline it as follows: I must agree with your sentiments that this type of filter has great potential within the nuclear industry. I say that as a user. I can give you a very quick rundown to illustrate what I mean. The position in U.K. on radial flow filters is that our development phase was reported to this Conference by Ron Pratt of UK AEA some few meetings back. Over the last 8 years, we have prepared and improved standards for two main types of radial flow filters in housings. The push-through type, we use for smaller applications, 50 or 100 cfm, and my own establishment has some hundreds of these installed in glove-boxes as the first-line filter. For the larger size applications, e.g., ventilation applications, there is a plug-in type which can be changed by a bagout or a remote manipulation system depending on the application. These units have all received full approvals for regular use in the most critical nuclear applications. At MoD, they are first line filters in the 400 glove box Pu facility and, I believe, they are used exclusively in BNF's THORP reprocessing facility. In the construction of new facilities, they have largely displaced the square format filters. There are at least two manufacturers in U.K. currently producing these units. As you pointed out, there have been advantages in the types which are produced in U.K. They have a lip-seal which gives a virtually hermetic seal without the need for compression, there is no clamping required, they contain minimal material other than the media and end plates and, as you say, they are readily crushable. The largest units of 2,000 cfm capacity fit readily into the European 200 liter waste drum. If you crush them, of course, you can get a number of them into one drum.

**DAVIS:** Have you done crushing studies? How many of them are you able to put into a drum?

**BERGMAN:** Could we just hold that discussions until later.

## 22nd DOE/NRC NUCLEAR AIR CLEANING AND TREATMENT CONFERENCE

**PORCO:** The radial filter is very similar to the M56 filters supplied to the military which are tested at Edgewood Arsenal. Are you using Mil Spec. F-51079 media?

**DAVIS:** Yes.

**PORCO:** Have you done any qualification testing, such as heated air, moisture, over-pressure, rough handling?

**DAVIS:** No. As far as I know, there are no test facilities available for doing these tests on filters of this size and shape. There are no specifications in place for testing radial filters. The M56 military filters are not subjected to heated air or wet over-pressure testing at Edgewood. Only pressure drop and efficiency testing have been done.

## 22nd DOE/NRC NUCLEAR AIR CLEANING AND TREATMENT CONFERENCE

### BEHAVIOR OF THE LOADED POLYGONAL HEPA FILTER EXPOSED TO WATER DROPLETS CARRIED BY THE OFFGAS FLOW

K. Jannakos, H. Mock, G. Potgeter, HIT  
J. Furrer, LAF II

Kernforschungszentrum Karlsruhe GmbH  
Postfach 3640, D-7500 Karlsruhe 1  
Federal Republic of Germany

#### Abstract

For cleaning of the dissolver offgas from reprocessing plants a HEPA polygonal filter was developed and tested which can be used to filter also exhausts from processes in other facilities. The following tests were carried out in order to obtain information about the behavior of the loaded filter element exposed to water droplets in the offgas stream:

The filter elements were loaded up to 1300 Pa differential pressure with a) alumina powder particulates  $< 3 \mu\text{m}$  in size, b) a sorted fine dust fraction taken from dust bags of household vacuum cleaners, and c) salt aerosols and then exposed to water aerosols supplied to the offgas flow upstream of the filter.

Throughout the tests with filter element loading according to a) and b) the filter elements were not damaged. Whereas in the test series with type a) loading the differential pressure remained almost unchanged, it increased at different degrees in the tests with loading according to b), depending on the amount of water aerosols supplied. In the tests involving type c) loading the differential pressure steeply rose at the filter and the filter element was damaged after about 25 minutes at a final differential pressure of approx. 14.5 kPa. With the results from the last test campaign on hand, mechanical testing of the HEPA polygonal filter element was terminated.

A special device was developed, built and put into operation for manufacturing the HEPA polygonal filter element. This device will be briefly described here.

#### Introduction

The polygonal filter is a pentagonal chamber filter; the filter element is cylinder shaped. The offgas flows from the bottom through a circular cross-section in axial direction into the inner space and then radially to the outside passing through the filter media of the five chambers. The circular cross-section of face flow is much smaller than the face flow surface of the filter medium and dimensioned such that at nominal volume flow rate in the non-loaded state the total pressure drop of the filter element is approximately 300 Pa. The maximum admissible service temperature is 160° C. With the test results available, the mechanical structure of the filter element has been optimized so that the axial strain of the stainless steel filter frame does not exert an influence on the filter medium at service temperatures up to 180° C.

In a first test series the behavior of non-loaded or little loaded filter elements exposed to water droplets was investigated and reported at the 21st DOE/NRC Nuclear Air Cleaning Conference (1). Mechanical testing of the polygonal filter was continued and has been terminated meanwhile, and the results of a

## 22nd DOE/NRC NUCLEAR AIR CLEANING AND TREATMENT CONFERENCE

second test series dealing with the behavior of loaded polygonal filter elements during exposure to water droplets will be reported here.

The second series of tests were carried out in the same test facility as the first test series. The water droplets were generated by means of a two-fluid nozzle. The mean droplet diameter was about 18  $\mu\text{m}$  at 150 mm distance from the nozzle. The diameter of the droplets immediately before they hit the filter paper was not measured.

Filter elements were examined which had been loaded with the following materials:

- alumina powder: grain size  $\leq 3 \mu\text{m}$ ,
- sorted fine dust fraction from dust bags of household vacuum cleaners,
- salt aerosols.

The solids and the salt solution ( $\text{NaNO}_3$  solution) used to generate the salt aerosols were supplied to the intake line of the filter element by means of two-fluid nozzles.

Testing under condition of loading with salt aerosols was the primary goal and necessary because the polygonal filter elements had been developed in the first line for purification of the dissolver offgas arising in fuel element reprocessing plants and as it is envisaged to actually use them in such plants (e.g. JNFS plant). Due to the nitric acid solution present in the dissolver, the dissolver offgas is loaded with salt aerosols.

### Experimental

The new filter elements were installed at the test facility in conformity with conditions of operation and loaded up to about 1300 Pa differential pressure at the filter, with solid particulates or salt aerosols supplied at constant volume flow rate. The differential pressure of 1300 Pa was chosen because the filters have to be replaced upon attainment of that value at the latest. After loading the filter elements were dried, if necessary, and exposed to water droplets in the same test facility without any modifications being made. In all experiments with salt aerosols the water was injected at a flow rate of about 5.5 l/h and about 9.2 g/m<sup>3</sup> gas respectively. For the operating condition under consideration of the dissolver offgas this water volume corresponds to approx. 5°C underrating of the dew point which in case of failure of the heater of a dissolver offgas purification system would be quite possible. In the experiments involving alumina powder, and dust also smaller amounts of water were injected. It has been outlined in (1) that the differential pressure establishing across the filter during exposure to water droplets is dependent on the amount of water injected. If the amounts of water differ from those chosen for the test, the differential pressure establishing across the filter will be lower (smaller water volume) or higher (larger water volume).

## 22nd DOE/NRC NUCLEAR AIR CLEANING AND TREATMENT CONFERENCE

### Test Data:

volume flow rate: 600 m<sup>3</sup>/h ambient air  
face flow surface of the filter: 0.13 m<sup>2</sup> corresponding to 1/5 (one chamber) of the polygonal filter  
filter medium surface: 5.4 m<sup>2</sup>  
intake condition: room conditions  
filter condition: the tests were performed with new filter elements each

The measurements related to:

- test duration,
- amounts of dust and water,
- residual water downstream of the filter,
- differential pressure across the filter.

It was possible to observe the filter condition at any moment because part of the filter housing was made of Plexiglas.

### Results Obtained

In order to be able to attain 1300 Pa differential pressure across the filter, approx. 518 g of powder were needed for loading with alumina powder. The loaded filters were exposed to water droplets supplied at a rate of 2.5 l/h (4.2 g/m<sup>3</sup>) for about five hours. The differential pressure across the filter did not rise. At the end of testing no damage had occurred to the filter elements.

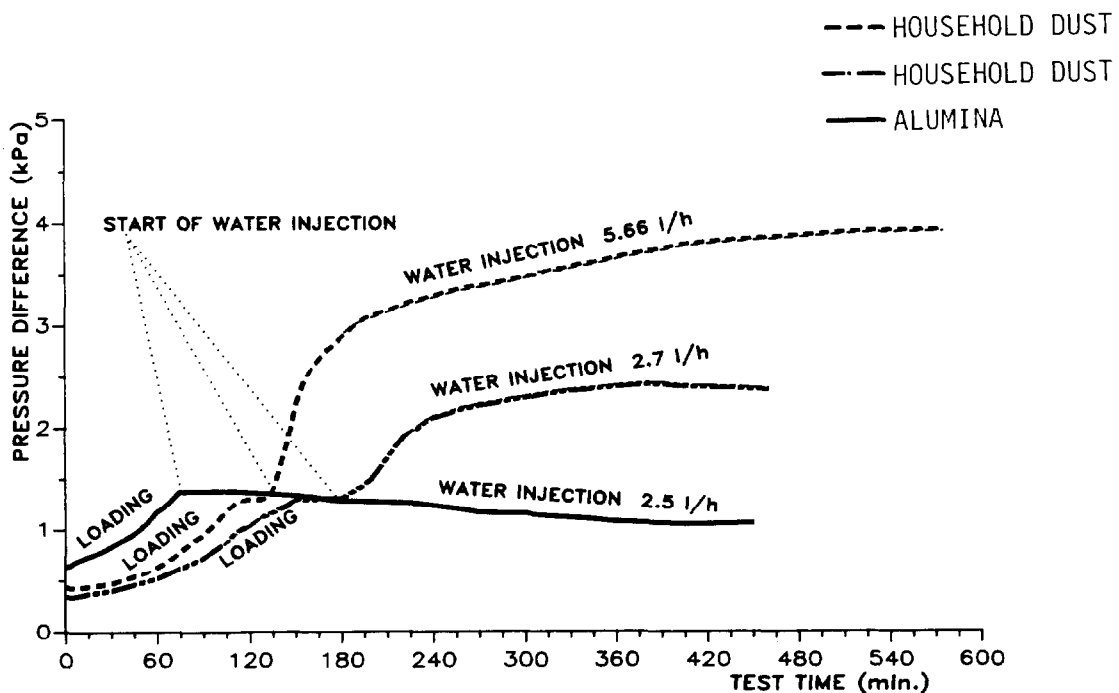


Fig. 1 Pressure differences across polygonal filter during the tests

## 22nd DOE/NRC NUCLEAR AIR CLEANING AND TREATMENT CONFERENCE

For loading with the fine dust fraction from household vacuum cleaners 1482 g of dust were needed in order to attain a differential pressure of 1300 Pa across the filter. The subsequent exposures to water droplets supplied at the rates of 9.5 (4.5) g/m<sup>3</sup>, were interrupted after about eight (five) hours. During that interval the differential pressure across the filter increased continuously to about 3930 (2450) Pa. At the end of testing the filter elements had not suffered any damage. Figure 1 is a plot of the differential pressure establishing across the filter element during loading and the subsequent exposure to water droplets.

When loading the filters with salt aerosols, NaNO<sub>3</sub> was dissolved in water and the solution fed into the intake line of the test facility by means of a two-fluid nozzle. The flow rate of the solution was set at 1.3 l/h so that the water evaporated before it reached the filter surface and only the salt aerosols together with air reached the filter medium. Approx. 980 g of salt (NaNO<sub>3</sub>) were needed to attain a differential pressure across the filter of 1300 Pa.

During the subsequent exposure to water droplets supplied at a rate of approx. 5.7 l/h (9.5 g/m<sup>3</sup>) the differential pressure rose to approx. 14.5 kPa within about 25 min. With this differential pressure tears developed in the filter paper and the differential pressure dropped. As during the last seconds the rise in differential pressure was very steep, it is supposed that the peak value was higher but that it could not be recorded due to attenuation of the plotter. It was observed that at the chosen rate of flow of the salt feed the salt aerosols deposit on the face flow surface of the filter so that the gaps between the spacer and the filter paper close.

With larger aggregate amounts of salt supplied, the filter face flow surface during loading became gradually covered almost completely with salt particulates, which attached to it. Under that condition the air was capable of passing only through a few paper pleats, which expanded. Then the differential pressure across the filter rose steeply until tears developed in the filter paper at the edge of pleating. This happened for approx. 1300 g of salt supply and a differential pressure of approx. 15 kPa in our tests. At this differential pressure the rate of flow dropped from 600 m<sup>3</sup>/h to approx. 450 m<sup>3</sup>/h (controlling no longer possible) (tests 24 and 25). Figure 2 is a plot of the differential pressure across the filter element during loading and exposure to water droplets. Figure 3 shows tears in the filter paper on the downstream face of the filter element occurring in a test after exposure to water droplets (test 27).

The tests have shown that measures have to be taken in dissolver offgas purification to the effect that the exhaust air temperature upstream of HEPA filters is higher than its dew point temperature and that in case the dew point is underrated (e. g. by failure of the gas heater) the system must be switched over to the non-loaded standby filter system within the following 15 minutes.

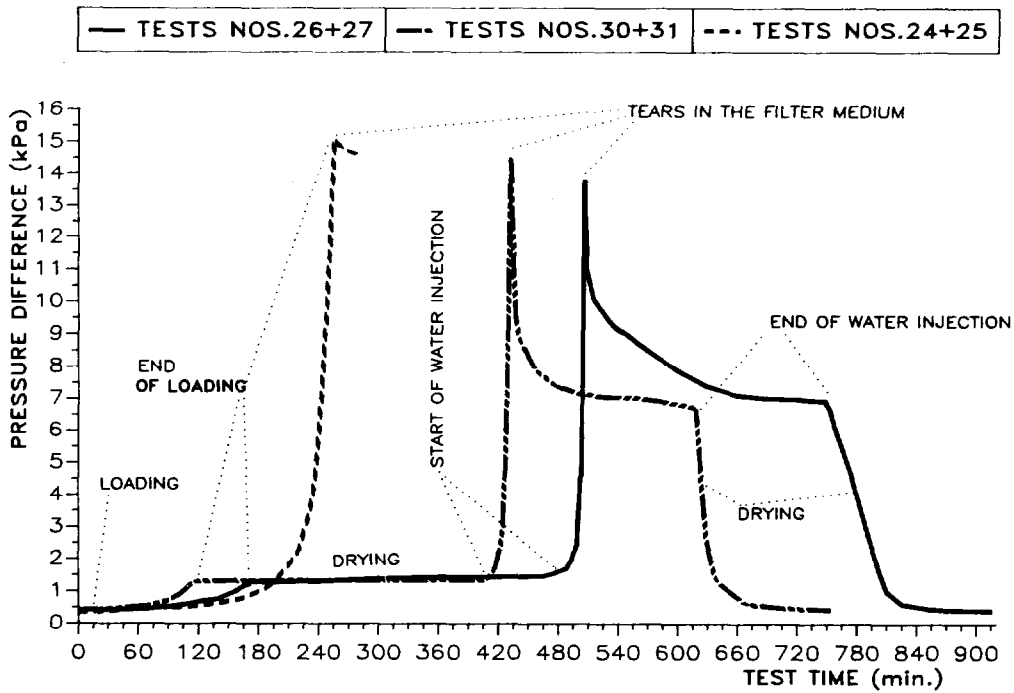


Fig. 2 Pressure differences across  $\text{NaNO}_3$  loaded polygonal filter during the tests

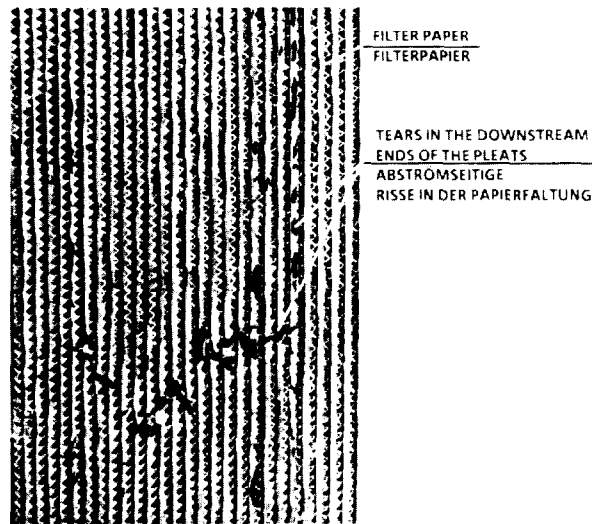


Fig. 3 With  $\text{NaNO}_3$  loaded polygonal filter element after exposure to water droplets

## 22nd DOE/NRC NUCLEAR AIR CLEANING AND TREATMENT CONFERENCE

### Manufacture of the Polygonal Filter Element

To manufacture the filter element a device was developed which allows the pleated filter paper equipped with spacers to be arranged as a polygon. This gives in the ready for use version a cylindrical (circular) filter element. Figure 4 shows the filter mounting device during manufacture of a polygonal filter element.

The filter paper arranged as a polygon and secured is taken from the device using a hoisting unit or pulley and placed first into one of the covers on the front side for tight embedding of the filter paper with a sealing compound and then, after drying, into the other cover on the front side. During the same process the grating provided as an external protection of the filter is fastened to the cover by means of the sealing compound.

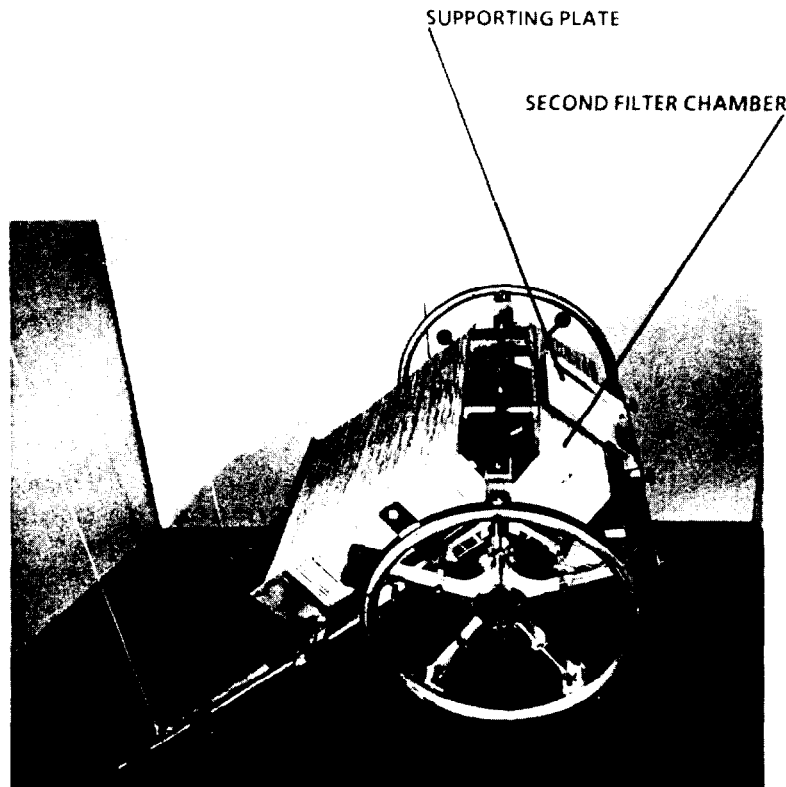


Fig. 4 Filter assembling device, separation of second filter chamber

- /1/ Jannakos, K., Potgeter, G., Legner, W., "Behavior of the Polygonal HEPA Filter Exposed to Water Droplets Carried by the Offgas Flow". Proceedings of the 21st DOE/NRC Nuclear Air Cleaning Conference, Vol. 2, 772 (1990).
- /2/ Jannakos, K., Potgeter, G., Mock, H., Furrer, J., "Advanced Filters for Nuclear Facilities and Filter Conditioning for Disposal". Proceedings of the 20th DOE/NRC Nuclear Air Cleaning Conference, Vol. 2, 1055 (1988).

THE APPLICATION OF HEPA FILTER UNITS IN GAS STREAMS OF  
HIGH DUST CONCENTRATIONS

H. Leibold, I. Döffert, T. Leiber, J.G. Wilhelm  
Kernforschungszentrum Karlsruhe GmbH  
Laboratorium für Aerosolphysik und Filtertechnik II  
Postfach 3640, D-7500 Karlsruhe 1  
Federal Republic of Germany

Abstract

Almost without exception, High Efficiency Particulate Air Filter (HEPA) units are currently employed for cleaning air and gas streams of very low dust concentrations where their high removal efficiencies reliably protect the environment. The high dust concentrations encountered during the modification and decommissioning of nuclear facilities, in the processing of contaminated scrap or in the incineration of radioactive waste have limited the use of HEPA filters to the role of final stage, clean-up filters.

Recleaning HEPA filter units in their service locations offers economic advantages compared with conventional combinations of multiple dust removal devices. Primarily fluid dynamic techniques come into consideration for the nondetrimental recleaning of inherently fragile, glass fiber filter media. This is explained by the relatively low mechanical stress induced during the required high-intensity recleaning processes, in comparison to beating or shaking methods.

Recleaning via low pressure reverse flow will be addressed in detail. The influence of reverse flow intensity and particle size on recleanability was studied in laboratory tests on specimens of HEPA filter media. The minimum required reverse flow intensity was determined on the basis of the residual pressure drop after recleaning. Measurements of local pressures in a single pleat and theoretically calculated flow patterns showed that airflows in conventional deep-pleat pack geometries during reverse flow recleaning are not uniformly distributed. The difference between the air velocities at the pleat inlet and the downstream end can vary by up to a factor of five at typical reverse flow intensities. This decreases the overall effectiveness of particle dislodgement from the filter medium which can result in a shortening of filter unit service life.

Finally, the results of field investigations into the recleanability of deep-pleat filter units during actual service conditions will be presented for three different dust types.

## I. Introduction

HEPA filters are used for the highly efficient removal of very fine dusts down into the range of particle sizes  $< 1 \mu\text{m}$  in nuclear technology, but also in conventional applications, such as the semiconductor industry, pharmaceutical industry, or in hospitals (1). However, the compact design and low pressure drop, which are additional advantages of HEPA filters, can be exploited only if the dust concentrations are comparatively low, on the order of a few  $\text{mg}/\text{m}^3$  or even less. Being accumulation filters without regeneration capability, HEPA filters very soon become uneconomical at high dust contents, because of their short service lives, and should therefore be used only as backup filters (2).

Due to their extremely high removal efficiency, however, HEPA filters should be installed also in those instances where very high dust concentrations up to several  $\text{g}/\text{m}^3$  arise. Typical applications of this kind are revision and decommissioning of nuclear power plants and other nuclear installations, treatment of contaminated scrap, and incineration of radioactive waste. HEPA filters can be operated economically under these conditions only if they can be cleaned repeatedly while installed, thus ensuring stable filtration (2).

In principle, filters installed can be cleaned by such mechanical procedures as beating or shaking of the filter units (3), or by aerodynamic cleaning techniques, such as low-pressure reverse flow, jet pulsing, or by shock waves. The mechanical procedures have been found to be ineffective. More effective cleaning techniques are required to dislodge the dust from the filter medium and remove it from the filter element.

## II. Requirements

Stable operation of HEPA filters over long periods of time in the presence of high dust concentrations raises two basic requirements: The removal efficiency of the filter unit must, at any point in time during the period of operation, attain at least 99.97 % for the DOP test aerosol of  $0.3 \mu\text{m}$  particle size.

Over the entire period of operation, the pressure drop of the filter must not exceed a given maximum level, i.e., filter clogging must be prevented reliably by the recleaning process. Various studies (2, 4, 5, 6) have indicated that very high velocities of up to 40 m/s are required to detach single particles by flow forces; these velocities increase greatly as the particle size decreases. If the dust has been deposited close to the surface as a continuous dust layer, the necessary flow velocities will be much lower, which would advocate surface filtration as a primary mode of operation. Soft cleaning at low reverse flow velocities should be endeavored also because fiberglass filter media are very sensitive mechanically and have only low tensile strengths. When high mechanical loads are applied, the filter medium is likely to be damaged and its removal efficiency reduced. In the light of these considerations, a suitable cleaning technique to be employed is low-pressure reverse flow. During the cleaning process, uniform cleaning of the filter unit over the entire pleating depth of the filter pack must be ensured.

Differences in the effectiveness of cleaning give rise to local differences in the flow conditions during the filtration phase and, ultimately, may cause the filter unit to be clogged.

III. Experimentals

Initially, plane specimens of filter media were subjected to laboratory-scale tests to find out the filtration velocities at which particles of submicron size can be deposited close to the surface. Also under laboratory conditions, the extent to which fiberglass filter media can be recleaned by reverse flow was studied, i.e., the filtration and cleaning conditions under which a constant residual pressure drop can be achieved after cleaning. These activities were supplemented by theoretical and experimental studies of the flow through a filter pleat during recleaning. Filter tests carried out in parallel with practice-related dusts at three different locations provided information about the transferability of laboratory data to specific dust removal problems and produced important findings about the cleanability of deep-pleat filter units.

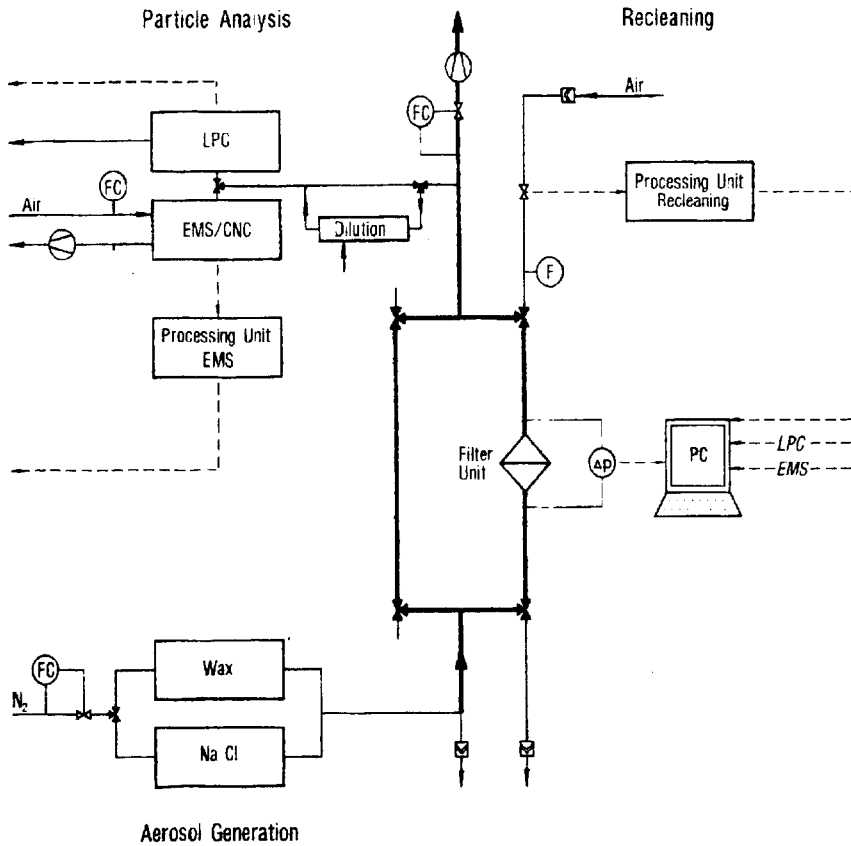


Fig. 1: Laboratory apparatus for studies of the recleanability of HEPA filter media.

## 22nd DOE/NRC NUCLEAR AIR CLEANING AND TREATMENT CONFERENCE

The first picture shows the laboratory apparatus used to study the filtration and removal of submicron-size particles from HEPA filter media. At face velocities between 0.5 and 5 cm/s, this apparatus can be loaded with plane filter specimens of 32 mm diameter carrying monodisperse and quasi-monodisperse test aerosols, respectively. In the range of particle diameters of 0.05-1  $\mu\text{m}$ , NaCl aerosol is used which is generated at temperatures between 500 and 700 °C in a Sinclair LaMer generator. The particles are spherical and are made up of amorphous NaCl, since dry nitrogen is used as a carrier gas. For the diameter range of 0.2-2  $\mu\text{m}$ , a condensation aerosol with spherical wax particles is produced also in a Sinclair LaMer generator. The numerical concentrations of both aerosols are on the order of  $10^6$  particles/cm<sup>3</sup>, with excellent constancy in time. The penetration and the pressure drop of the filter medium are measured continuously. For particle diameters > 0.2  $\mu\text{m}$ , a Laser Particle Counter (LPC) is used to determine penetration which allows the particles in the diameter range of 0.12-7.5  $\mu\text{m}$  to be classified in 16 channels. For smaller particles, penetration is determined by means of an Electromobility Spectrometer (EMS) in combination with a Condensation Nuclei Counter (CNC).

The apparatus branches into one duct section containing the test filter and an identical duct used to determine the raw gas concentration. This design of the apparatus allows high resolutions to be achieved in determining penetration. Penetration levels below  $10^{-9}$  can be determined continuously and with absolute reliability. When recleaning the loaded HEPA filter media, reverse flow velocities to a maximum of 2 m/s can be set.

Recleaning was initiated by triggering a solenoid valve above the test filter and may be carried out either at preset time intervals or after a preset filter pressure drop has been reached. To facilitate operation, especially in long-term experiments extending over several days, control and data acquisition are PC based.

The design of the test filter systems for practice-related experiments can be seen from Fig. 2. The filter systems were operated in the bypass mode at a maximum volume flow of 1000 m<sup>3</sup>/h. In the filtration phase, the raw gas passes first through the HEPA filter to be recleaned and then into the main air stream through a safety filter and the in-plant blower. Recleaning is performed off-line at a compressed air supply pressure of 3-6 bar by traversing the filter downstream side with a nozzle manifold oriented parallel to the pleats. The individual pleats are consecutively cleaned by exposure to the reverse air flow. The extracted airborne particles fall into the dust hopper. After a programmable sedimentation interval, the filtration cycle begins again.

Upstream of each filter unit, the dust concentration in the raw gas and the particle size distribution and particle shape are determined at specific sampling points. The raw gas concentration was measured gravimetrically, while the particle size distribution was determined by means of cascade impactors and in dust analysis

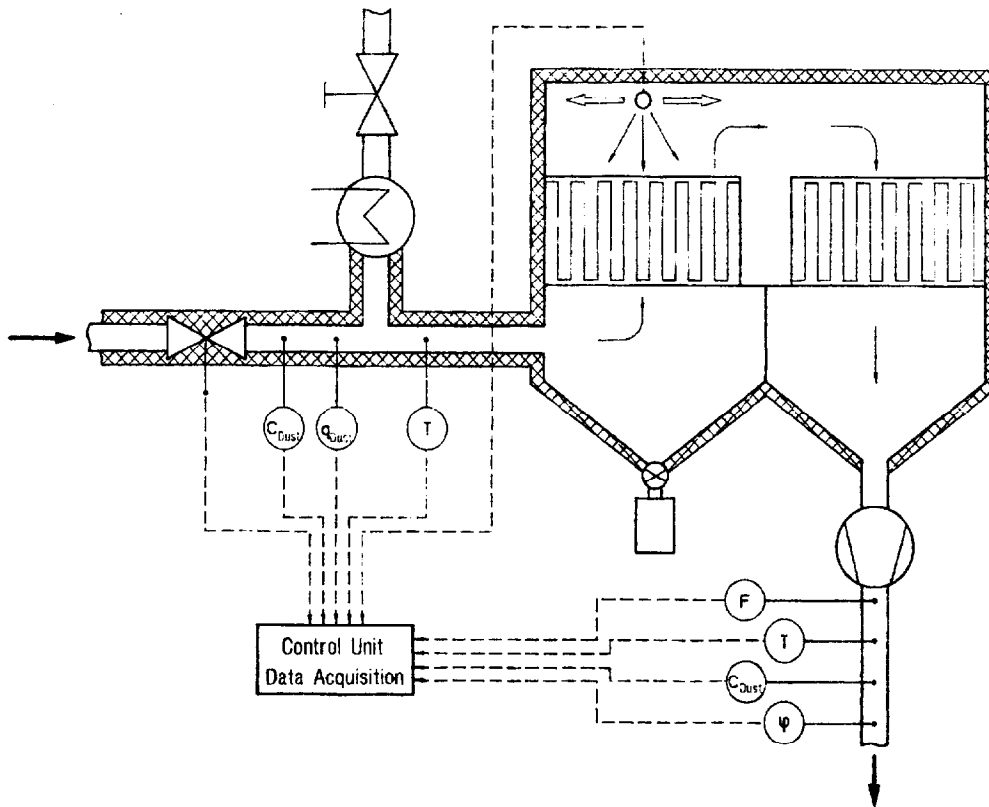


**Fig.2:** Design of the test filter systems for tests with complete filter units under practical conditions.

performed under the scanning electron microscope. Conditions on the upstream side can be seen from Table 1. On the downstream side, the throughput and the dust content of the clean gas were determined continuously. Concentrations were measured photometrically by dust photometers measuring in the forward direction. The gas temperature was continuously determined on the upstream side and, together with the relative humidity, also after the gas had passed through the filter.

**Table 1:** Operating conditions at the locations of the test filter systems.

Dust Source	MMD $\mu\text{m}$	$C_{\text{Dust}}$ $\text{mg}/\text{m}^3$	Temperature $^{\circ}\text{C}$	rel. Humidity %
Blasting Box	2-8	500-2000	25	65
Ag/Cd Smelter	< 1	< 500	55	30
Rotary Kiln	< 2	< 40	110	70

## 22nd DOE/NRC NUCLEAR AIR CLEANING AND TREATMENT CONFERENCE

Control of the test filter unit and continuous data acquisition were automated by means of a personal computer.

### IV. Results

To facilitate filter cleaning, the dust collected should be deposited as continuous surface layers. Such dust layers adhering to the surface support filtration and can be detached with less force than the dust penetrating into the filter medium. In dust deposition on the surface of a HEPA filter medium, a linear rise of the pressure drop with the mass of dust is observed. The diagram (Fig. 3) shows that, for particles  $> 0.4 \mu\text{m}$ , at a usual face velocity of 5 cm/s, this linear relationship can be observed; the pressure drop rises the faster, the smaller the particles are. For particles  $< 0.4 \mu\text{m}$ , there is first depth filtration over a long period of loading, which can be recognized from the progressive development of the pressure drop curve, before the deposition is shifted to the surface of the filter medium.

It is important to note that, in this range of particle sizes, no continuous dust layers can be detected even after long loading periods. Layers are formed only as isles along the fibers, while larger areas in between show little deposition.

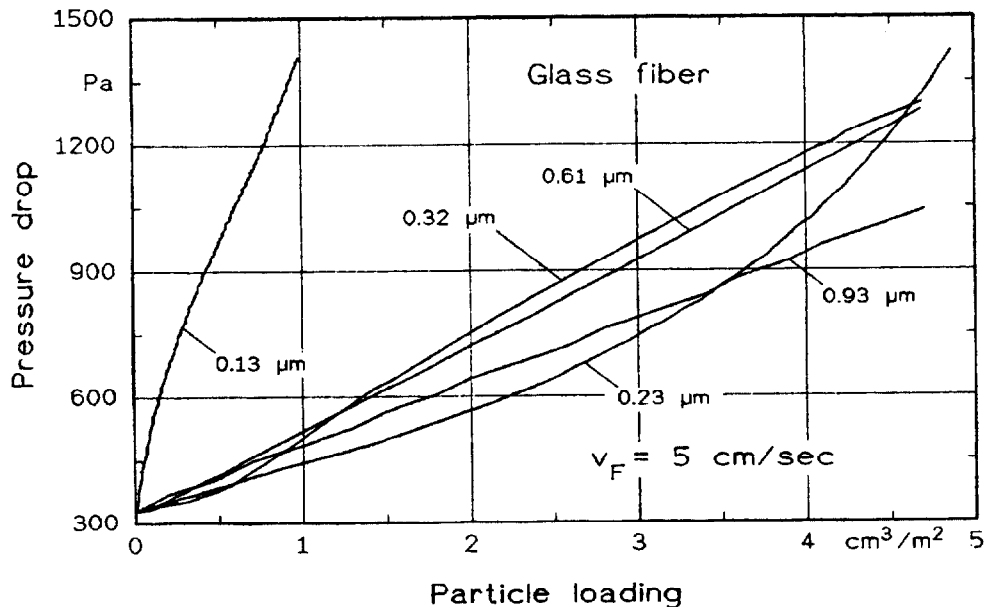


**Fig. 3:** Pressure drop curve of a HEPA filter medium loaded with monodisperse particles in the submicron range.

The pressure drop immediately after cleaning is the most important quantity in assessing the cleanability of HEPA filter media. This residual pressure drop therefore was used as the main criterion to assess stable filtration/cleaning modes of operation. The residual pressure drop is influenced primarily by the recleaning conditions, as represented by the reverse flow velocity, the development of the recleaning phase over time, and the properties of the adhering dust.

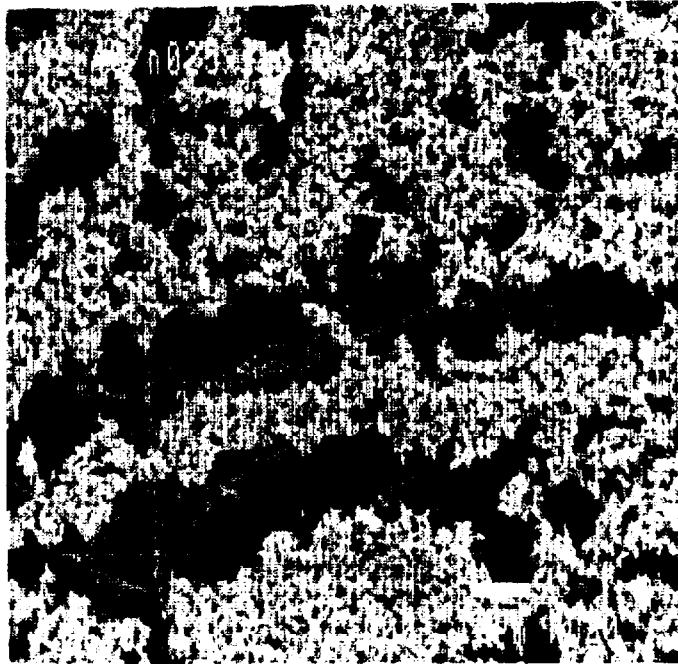


Fig. 4: Insular dust deposits for particles of  $0.15 \mu\text{m}$  in diameter (SEM micrograph).

Figure 5, by way of example, shows the influence of the reverse flow velocity on the residual pressure drop for particles of  $0.52 \mu\text{m}$  diameter for the range of technical interest above  $0.4 \mu\text{m}$ .

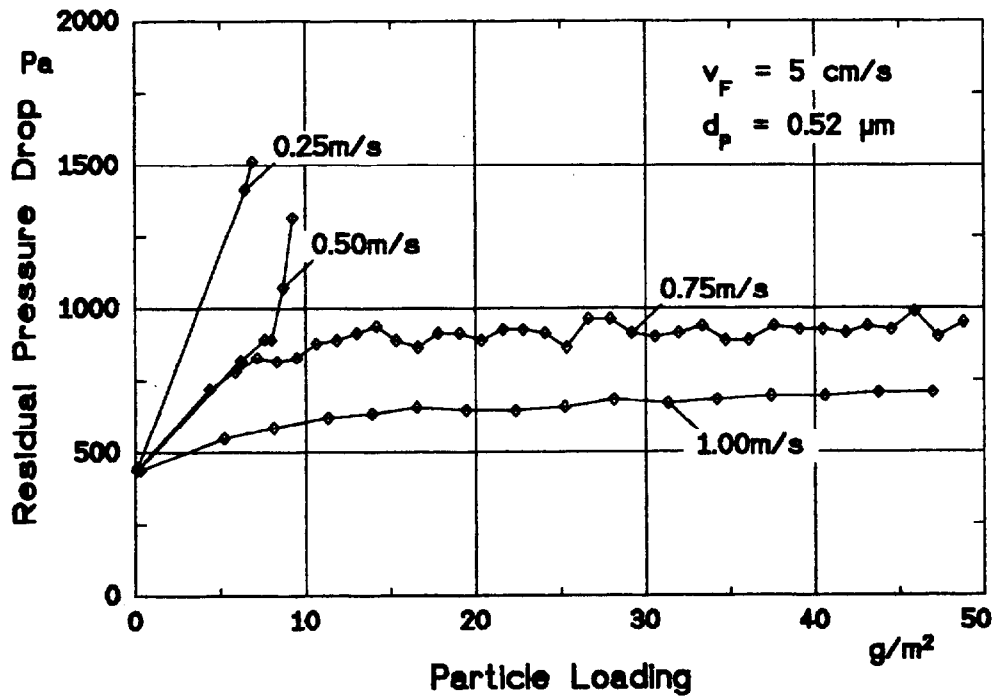


Fig. 5: Development of the residual pressure drop for recleaning  $0.52 \mu\text{m}$  particles at different reverse flow velocities.

## 22nd DOE/NRC NUCLEAR AIR CLEANING AND TREATMENT CONFERENCE

Cleaning was initiated whenever a pressure drop of 1500 Pa had been reached. For reverse flow velocities of 0.75 and 1 m/s, the residual pressure drop stabilizes at 710 and 930 Pa, respectively. It is seen that the filter medium becomes clogged very quickly at lower reverse flow velocities, thus making stable filter operation impossible.

For particles in the range of the removal minimum (diameters around  $0.2 \mu\text{m}$ ), which initially were deposited inside the filter medium in large numbers, the required minimum reverse flow velocity is 1 m/s. Much smaller particles are still under study.

For the particle range investigated the duration of the recleaning step has been found to have no impact on the recleaning performance of HEPA filter media.

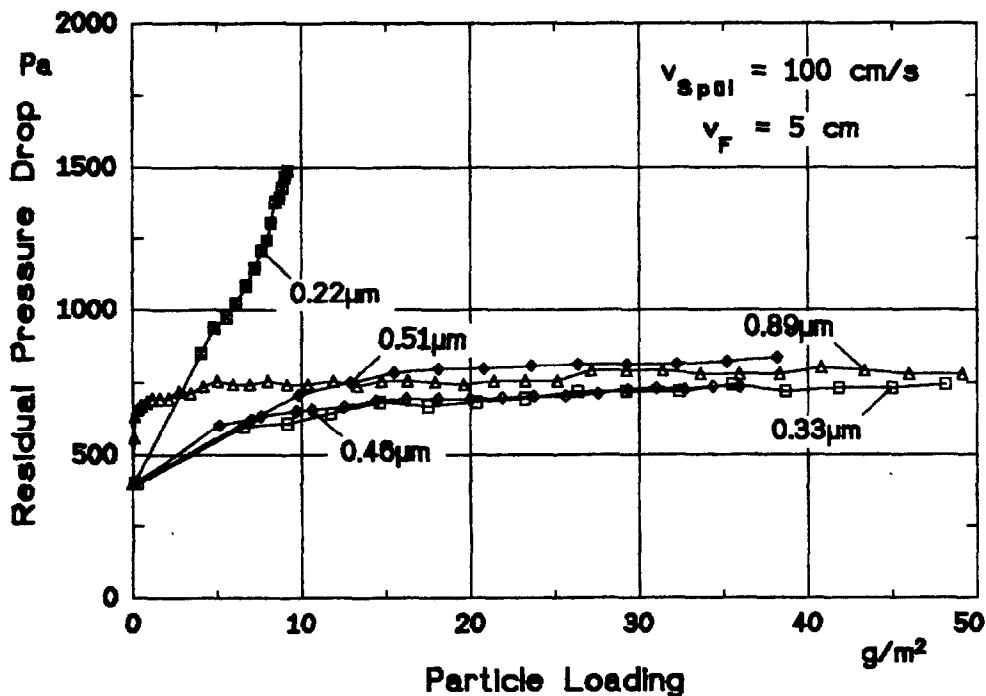


**Fig. 6:** Residual pressure drop for recleaning particles in the range of  $0.22\text{-}0.89 \mu\text{m}$  diameter.

In a deep pleat HEPA filter unit, the filter medium is not directly exposed to the reverse flow during the recleaning process. The air first passes straight into a filter pleat at high velocity and only then is deflected to the filter medium.

Figure 7 illustrates this process. To achieve optimum recleaning, the same reverse flow velocity must be generated at each point within the filter pack, and the air flow through the filter unit must be uniform over the entire pleat depth. If there are local differences in the degree of recleaning achieved, the well cleaned areas will show higher flow velocities in the ensuing filtration phase, thus allowing particles to penetrate to greater depths into the filter medium and aggravating recleaning at these points.

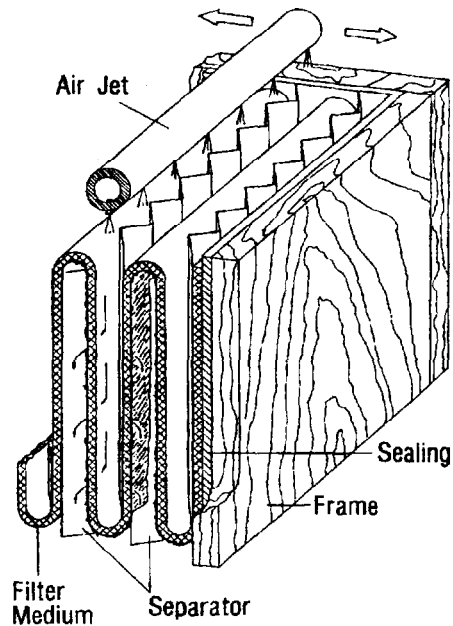


**Fig. 7:** Recleaning a HEPA filter unit by compressed air (schematic diagram).

Figures 8 and 9 indicate the influence of the air flow into a pleat upon the uniformity of the velocity through the filter medium along the pleat. The results are based on a computation model describing the pressure and velocity conditions in a triangular duct, of the type constituted in a HEPA filter pack by the filter medium and a separator (7). The diagram at the top indicates the situation under the usual filtering conditions, i.e.,  $1700 \text{ m}^3/\text{h}$  of volume flow per filter unit, corresponding to a filtration rate of some  $2.8 \text{ cm/s}$ . Along the whole pleat there is only a minor change in the filtration velocity.

On the other hand, reverse flow velocities on the order of those required for recleaning show significant irregularities in the flow distribution. The diagram shows the actual curve along a pleat for a mean reverse flow velocity of  $28 \text{ cm/s}$ . There is a significant increase in velocity at the closed end of the pleat, which is particularly pronounced for an unloaded filter medium. It can be seen that the velocity increase diminishes with rising preloading towards the end of the pleat, as the high pressure drop of the loaded filter paper has an equalizing effect. Yet, the difference in velocities between the pleat inlet and the pleat end, at preload up to  $2000 \text{ Pa}$ , is still more than a factor of 2. Model calculations show that the irregular distribution becomes more pronounced with increasing flow of recleaning air. Excessive flow of recleaning air consequently, merely for flow reasons, may have negative impacts because they give rise to very different cleaning conditions along a pleat, although they would be advantageous from the filtration point of view. In addition, the pleat ends on the downstream side of a filter pack are subjected to unusually high loads at very high recleaning flows, which finally causes the pleat ends to rupture.

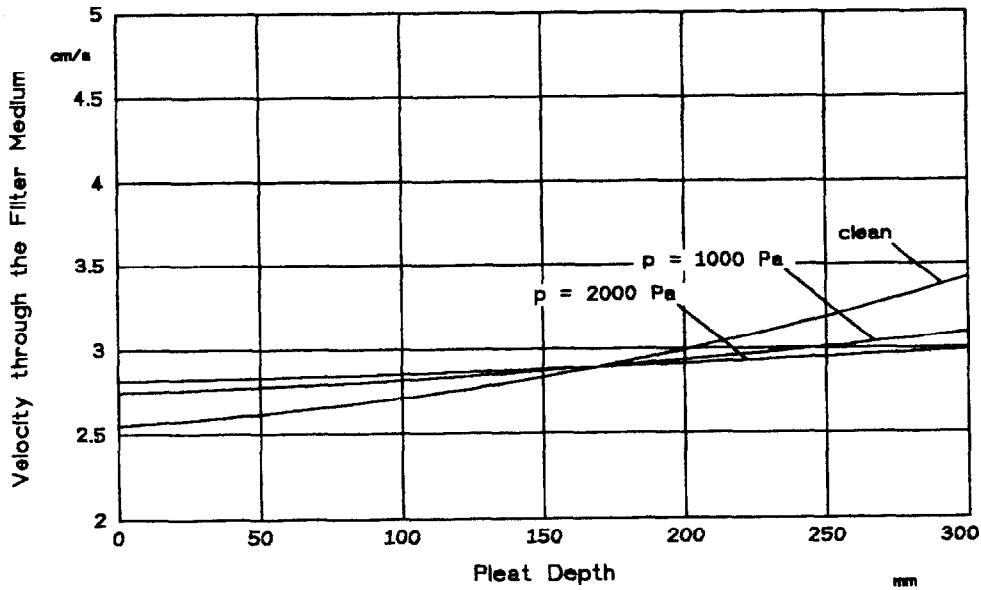


**Fig. 8:** Velocity through the filter medium along the upstream side of a filter pleat in a HEPA filter unit at design volume flow and various preloads.

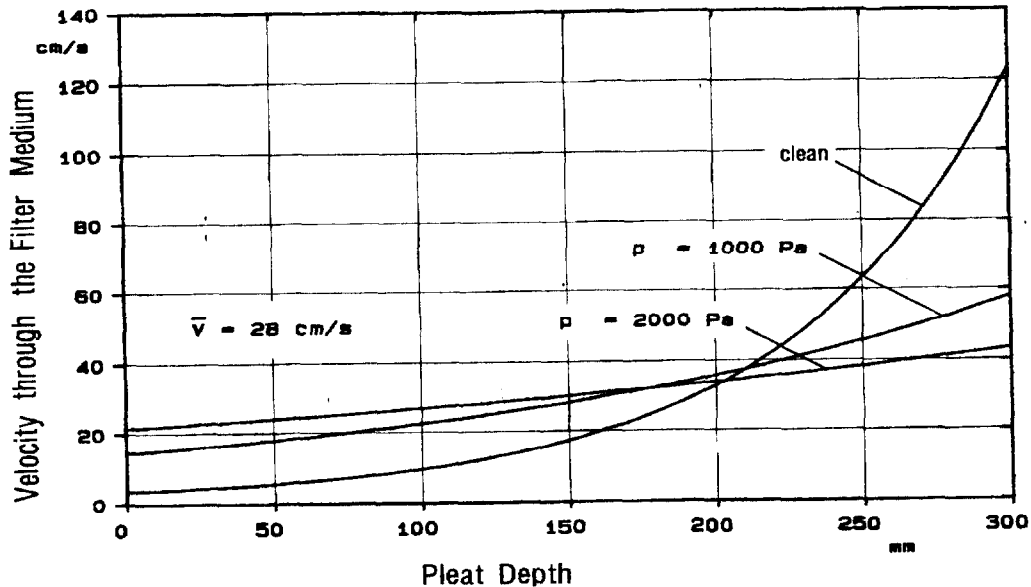


**Fig. 9:** Reverse flow velocity through the filter medium along the upstream side filter pleat of a HEPA filter unit at various preloads.

Due to the additional influence of pleating upon the local reverse flow velocities of the filter unit, the laboratory findings about the recleanability of filter media cannot readily be extrapolated to conditions in a filter unit. It must also be borne in mind that, in practice, dust normally has a broad distribution of

particle sizes not quite to be compared with the model dusts used. For the three types of dust chosen, which were filtered under practical conditions, recleanability is discussed below as compared to laboratory findings.

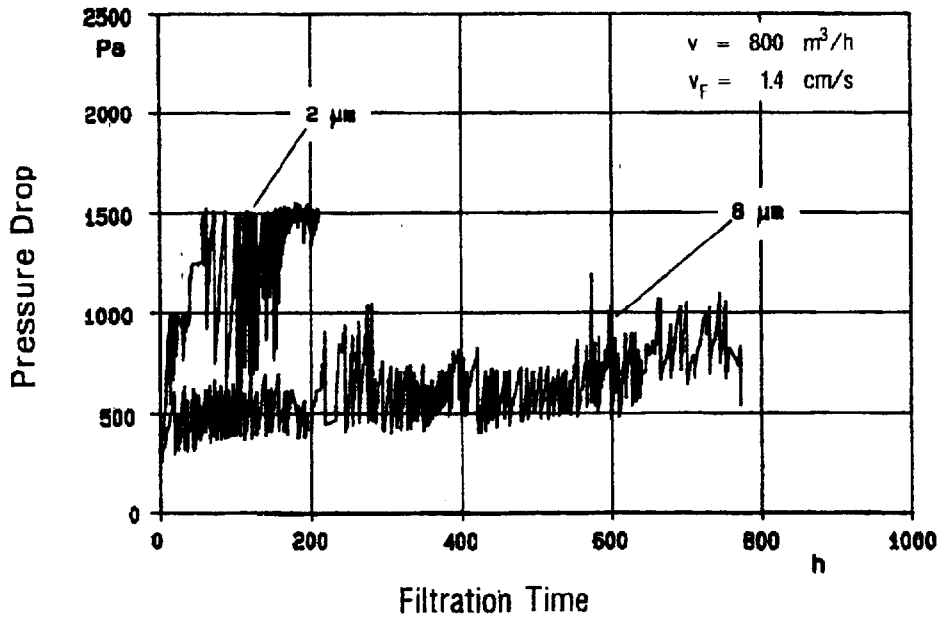


**Fig. 10:** Pressure drop curve of a HEPA filter for the filtration of fine dusts in a blast cleaning room.

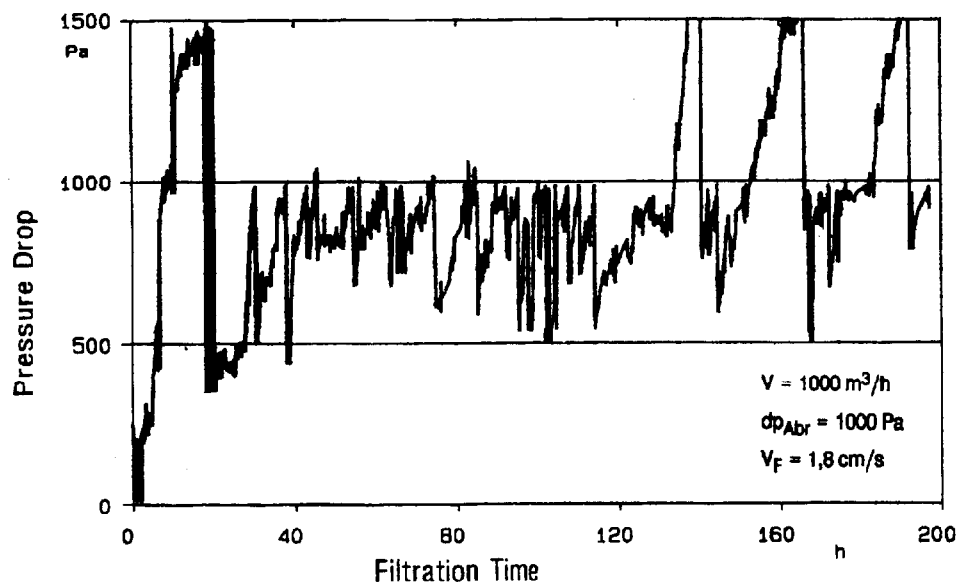


**Fig. 11:** Pressure drop curve of a HEPA filter for filtering fines in an Ag/Cd smelter.

## 22nd DOE/NRC NUCLEAR AIR CLEANING AND TREATMENT CONFERENCE

For dust arising in a blast cleaning room, the curves shown in Fig. 10 were recorded as a function of particle diameters. For the coarser dust fraction, quasi-stable filter operation is possible over for a long period of time, with the residual pressure drop gradually rising to five times its initial level during approximately 800 h. For the finer dust fraction, the filter needs to be replaced after only 200 h. Under the existing conditions no stable filter operation was achievable. It must be taken into account that, in this case, 20% by mass of the dust is in the submicron range and, consequently, relatively difficult to detach from the filter medium.

In the filtration of extremely fine dusts arising in smelters, the curve shown in Fig. 11 is measured for HEPA filter units. Under comparable operating conditions, a maximum residual pressure drop of 800 Pa is observed for this dust. The development is seen to be extremely non-uniform, with pronounced fluctuations in the residual pressure drop probably due to changes in the dust composition as a function of time. Also in this plant, filter service lives of at least 500 h are possible.

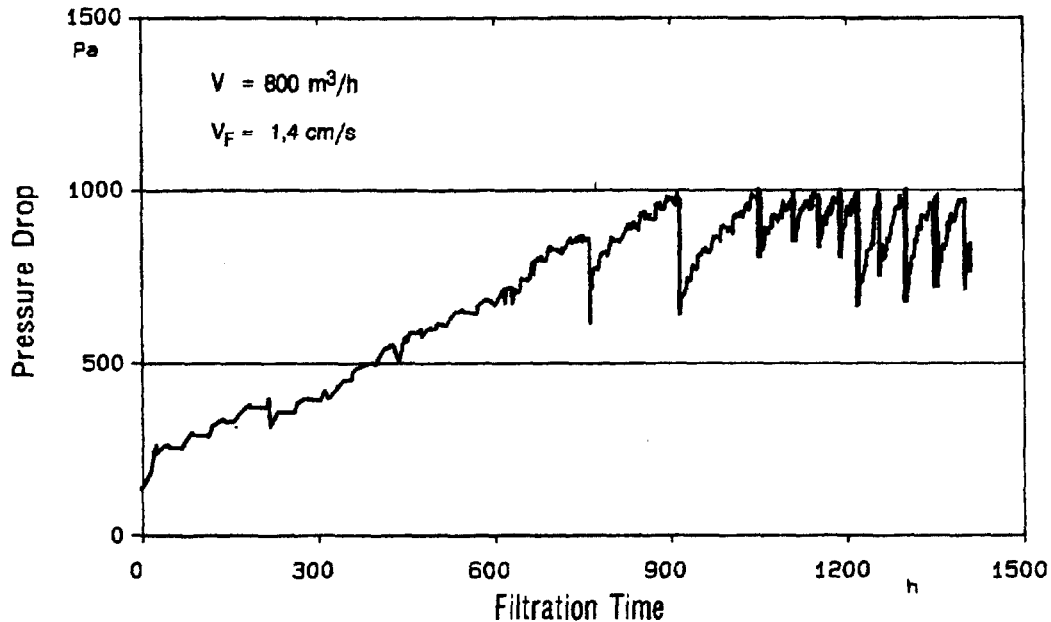


**Fig. 12:** Pressure drop curve of a HEPA filter for the filtration of cement dust.

Figure 12 shows the filter pressure drop plotted as a function of time under particularly difficult operating conditions. In this case, cement dust with particle diameters mainly in the submicron range was filtered. A special problem was posed by the high relative humidity of 70% at offgas temperatures of 110 °C. Due to the relatively low dust concentration, the pressure drop in the first filtration interval rises in an approximately linear fashion over a period of 750 h. Later, the typical sawtooth curve for the pressure drop of a recleanable filter can be seen. It is obvious that the residual pressure drop after recleaning fluctuates greatly also in this application, not exceeding a maximum residual pressure drop of 800 Pa. Compared to the two applications discussed above, the raw

## 22nd DOE/NRC NUCLEAR AIR CLEANING AND TREATMENT CONFERENCE

gas concentration of cement dust is relatively low, as a result of which a total of only 11 recleaning cycles were required up to dismantling of the filter, despite the long period of operation of 1000 h.

In comparing the residual pressure drop, which is approx. 800 Pa in the first three applications with nearly stable filter operation, with the corresponding laboratory levels, one finds the residual pressure drop to be three or four times higher. This is a clear indication of the insufficient overall recleaning efficiency of the filter unit. In addition, it must be taken into account that the narrow filter pleats may become clogged by dust, which has not been removed, which also contributes to an increase in the residual pressure drop. Nevertheless, it is apparent that an approximately stable residual pressure drop can be achieved for HEPA filters in a combined mode of filtration and recleaning over long periods of operation. In particular at high fines contents of up to several g/m<sup>3</sup>, this allows HEPA filters to be operated economically without the need for prefilters.

### V. Conclusions

The area of application for HEPA filters can be expanded to include cases involving high upstream concentrations of fine particles. Cost-effective operation is only feasible via periodic *in-situ* recleaning of the filter units. Experimental investigations into reverse flow recleaning on a laboratory scale have shown that reliable long-term filter service can be attained under cyclical operation conditions.

Optimization of filter pleat geometries appears to be a prerequisite for attaining the high cleaning-air velocities necessary to improve filter field performance.

### **References**

- (1) Dorman, R.G.; Dust control and air cleaning; Pergamon Press; Oxford; 1974.
- (2) Leibold, H.; Wilhelm, J.G.; "Entwicklung abreinigbarer Schwebstofffilter - Versuchstechnik und erste Ergebnisse"; Kfk-PEF 80; Vol. 2; p. 773-743; (1991).
- (3) Borho, K.; " Mehrstufiges Abscheiden von Stäuben mit Schwebstofffiltersystemen"; Maschinenmarkt; Vol. 90; p. 1266-1269; (1984).
- (4) Corn, M. and Silverman, L.; "Removal of solid particles from a solid surface by a turbulent air stream"; Am. Ind. Hyg. Assoc. J.; Vol. 21; p. 337-347; (1961).

## 22nd DOE/NRC NUCLEAR AIR CLEANING AND TREATMENT CONFERENCE

- (5) Löffler, F.; " Abblasen von an Filterfasern abgeschiedenen Feststoffteilchen"; Verfahrenstechnik: Vol. 6; p. 1-5; (1972).
- (6) Medjimarec, V.; Okuyama, K.; Payatakes, A.C.; "Estimation of the drag force acting on particle dendrites"; J. Colloid. Interf. Sci.: Vol. 82; p. 543-559; (1981).
- (7) Schlehuber, F.; Neuberger, M.; "HEPAFIL - ein Programm zur Berechnung der Strömungsgrößen am Schwebstofffilter"; KfK 4773; (1990).

### DISCUSSION

**ANON:** Were any measurements made to see if the filter is damaged by the reverse air jet?

**LIEBOLD:** Yes, we did it on a laboratory scale and in the practice-related filter tests. The laboratory scale penetration was measured during all the filtration cycles. No leakages could be detected. Maximum penetration occurred all the time immediately after the recleaning but it did not exceed the initial penetration of the medium. For the full-scale filter elements, the pleat ends are critical, but by optimizing air pressure, nozzle diameter, and distance between the nozzle manifold and the filter pack, damage of the filter medium can be avoided during filter servicing. We controlled the integrity of the filter units by continuous monitoring with a photometer measuring in the forward direction. These photometers detect dust concentrations down to  $0.2 \mu\text{g}/\text{m}^3$ .

PREDICTING MASS LOADING AS A FUNCTION OF PRESSURE DIFFERENCE  
ACROSS PREFILTER/HEPA FILTER SYSTEMS

V. J. Novick and J.F. Klassen\*  
Argonne National Laboratory  
Argonne, Illinois

and

P. R. Monson and T.A. Long  
Westinghouse Savannah River Company  
Aiken, South Carolina

Abstract

In many filtration scenarios, the need to estimate either the maximum mass that can be loaded onto a filter system or the corresponding pressure difference across a system for a known or expected mass loading, is a major concern for efficient design and for realistic risk assessment. Previous work has focused on determining the specific resistance of a filter for an aerosol of particular interest. Few attempts were made to determine the effects of particle density or diameter on the specific aerosol and filter combination that had been tested experimentally.

This work is an attempt to broaden the ability to predict the mass loading and pressure drop by accounting for the aerosol particle size and density effects on the specific resistance using empirical correlations. These correlations, along with measured efficiency characteristics for the particular prefilter, provide a more accurate method at estimating the mass loading and final pressure difference across the prefilter/HEPA filter system. The equations and methodology described also applies to predicting pressure differences based on known or expected mass loadings.

Results show the average difference between the measured and predicted total mass loading was 11.7% with a standard deviation of  $\pm 15.7\%$ , indicating that an estimate based on this technique can be expected to be 25% of the measured value due to the error in the correlations and the variation in particle size distribution between tests.

Introduction

The purpose of this work is to develop a methodology for predicting the mass loading and pressure drop effects on a prefilter/ HEPA filter system. The methodology relies on the use of empirical equations for the specific resistance of the aerosol loaded filter as a function of the particle diameter. These correlations relate the pressure difference across a filter to the mass loading on the filter and account for aerosol particle density effects. These predictions are necessary for the efficient design of new filtration systems and for risk assessment studies of existing filter systems. This work specifically addresses the prefilter/HEPA filter Airborne Activity Confinement Systems (AACS) (1), at the Savannah River Site. Other applications include air pollution control in factories, buildings or facilities where large quantities of aerosols may be released and must be contained. The AACS consists of a two-stage prefilter/HEPA filtration system in which the demister/prefilter is designed primarily to remove water droplets, but will also remove any other large aerosol particles, thereby

\*J.F. Klassen presently affiliated with ABB Impell Corporation

## 22nd DOE/NRC NUCLEAR AIR CLEANING AND TREATMENT CONFERENCE

reducing the mass loading on the High Efficiency Particulate Air (HEPA) filter and extending the service life of the HEPA filter.

In order to determine the mass loading on the system, it is necessary to establish the efficiency characteristics for the prefilter, the mass loading characteristics of the prefilter measured as a function of pressure difference across the prefilter, and the mass loading characteristics of the HEPA filter as a function of pressure difference across the filter. Furthermore, the efficiency and mass loading characteristics need to be determined as a function of the aerosol particle diameter. A review of the literature revealed that no previous work had been performed to characterize the prefilter material of interest.

The mass loading capacity of the HEPA filter was previously studied (2) (3) (4) (5). The direction of this research was to develop correlations to allow the prediction of either the final pressure difference across a loaded HEPA filter or the maximum mass that could be loaded onto a filter for a specified pressure difference. The experimental data from Novick, et al (2) (3), for the specific resistance were found to be well correlated with the mass median particle diameter and independent of the particle density.

In order to complete the foundation of information necessary to predict total mass loadings on prefilter/HEPA filter systems, it was necessary to determine the prefilter efficiency and mass loading characteristics. The measured prefilter characteristics combined with the previously determined HEPA filter characteristics allowed the resulting pressure difference across both filters to be predicted as a function of total particle mass for a given particle distribution. These predictions compare favorably to experimental measurements ( $\pm 25\%$ ).

### Theory

The total efficiency of a filter can be described by combining the individual theoretical efficiencies due to impaction, interception and diffusion. Theoretical equations exist for each of these mechanisms, but usually semi-empirical equations are used to improve the accuracy of the predicted efficiency. The combined single fiber efficiency is generally determined as the sum of the efficiency of each collection mechanism. Equations for the most important mechanisms, impaction (6), diffusion(6) and interception (7) are given.

$$\eta = \eta_i + \eta_D + \eta_I \quad (1)$$

$$\begin{aligned} \text{where } \eta_i &= \psi^3 / \{ \psi^3 + (0.77 \psi^2 + 0.22) \} \\ \psi &= \rho V d_p^2 C / 18 \mu d_f \\ \eta_D &= 6 Sc^{-2/3} Re^{-1/2} \\ Sc &= \mu / \rho D \\ Re &= V \rho d_f / \mu \\ \eta_I &= \{ 1/(2 Ku) \} \{ 2 (1+R) [\ln (1+R)] - (1+R) + [1/(1+R)] \} \\ Ku &= \alpha_f - [(\ln \alpha_f) / 2] - (3/4) - (\alpha_f^2 / 4) \end{aligned}$$

The theoretical collection efficiency of the filter (E) is then determined from the following equation given by Hinds (7).

## 22nd DOE/NRC NUCLEAR AIR CLEANING AND TREATMENT CONFERENCE

$$E = 1 - e^{-(f \eta)} \quad (2)$$

where  $f = 4 \alpha h / \pi d_f (1 - \alpha_f)$   
 $h =$  depth of filter material = 5.08 cm (2 in)

These theoretical efficiency equations hold for both solid particles as well as liquid particles providing the particle sticking coefficient is unity.

A simple model describing the total pressure increase across a filter due to solid particle mass loading can be written as the sum of the pressure increase across the clean filter plus the pressure increase across the filter cake due to particle loading. <sup>(8)</sup>

$$\Delta P = \Delta P_0 + \Delta P_c \quad (3)$$

This simple model is appropriate for HEPA filters because their high collection efficiency causes a particle cake to rapidly form on the surface of the filter. From D'Arcy's law,  $\Delta P_0$  can be written in terms of the gas media velocity times a constant and the gas media velocity times the mass loading per unit filter area times another constant. The first constant,  $K_1$ , depends upon the physical characteristics of the filter media such as the fiber diameter, filter porosity and thickness. The other constant,  $K_2$ , is identified as the specific resistance of loading material on the filter and depends primarily upon the particle diameter.

$$\Delta P_0 = K_1 V \quad (4a)$$

$$\Delta P_c = K_2 V M / A \quad (4b)$$

$K_2$  can be experimentally correlated with parameters that are known or easily estimated so that accurate predictions can be made for the pressure increase across a given filter as a function of mass loading. <sup>(4) (5) (9)</sup>

For a low efficiency filter, like a woven fiber prefilter, a particle cake never covers the entire surface of the prefilter. Most of the particles are removed inside the layers of the prefilter. As mass is collected on the prefilter, the specific resistance changes due to the particles becoming trapped inside the filter. The specific resistance, therefore, becomes a function of the particle mass per unit area being collected in the filter. A simple model can be postulated similar to that in Equation 4b,

$$\Delta P = (K_{1P} + K_{2P} M/A) V \quad (5)$$

where the subscript P denotes prefilter.

Mathematically, this equation is the same as Equation 3. As in the case of the HEPA filter model, an empirical correlation can be made that relates  $K_P$  to the particle diameter of the challenge aerosol.

For liquid aerosol mass lengths, models that predict the pressure difference across a filter are very sensitive to the geometry of the filter. These models differ from the solid mass loading models because as liquid aerosol is collected on the filter, an equilibrium develops between mass collected and

## 22nd DOE/NRC NUCLEAR AIR CLEANING AND TREATMENT CONFERENCE

mass removed by drainage. Therefore, the total liquid mass collected no longer contributes to the pressure difference across the prefilter, once the equilibrium value has been attained.

$$\Delta P_{we} / \Delta P_0 = A_1 [(d_f / \alpha_f h)^{0.561} (A t \cos \theta / Q \mu)^{0.477}] \quad (6)$$

Equation 6 relates the equilibrium pressure difference to the physical characteristics of the filter (10). In general, the contact angle of the droplet with respect to the fiber is usually unknown. In addition, for the Savannah River prefilter, the effective fiber diameter is an uncertain quantity due to the stranded nature of the woven fibers.

### Experimental

Particle collection efficiencies for the prefilter were tested using Savannah River Site prefilter material. The prefilter is formed from individual teflon fibers with nominal diameters of 0.02 mm. The individual fibers are bundled into strands with resulting diameters ranging between 0.78 mm and 1.3 mm. The strands are woven into a mesh-like structure with the addition of fine stainless steel wire. The prefilter mat contains 24 layers (12 double layers) of this material which is compressed to a thickness of two inches with a stainless steel frame. Many of the fibers have been broken from the strands and protrude at various angles from the strands.

For both the efficiency and the mass loading tests, the prefilter material was cut to a 10.2 cm x 12.7 cm (4 in. x 5 in.) rectangle and stacked together in a metal holder designed to hold the 12 double layers of material. This arrangement was designed to maintain the prefilter mat thickness of 2 inches. A metal frame covered the edges of the prefilter mat in the holder, leaving a rectangular face area of 7.6 cm x 10.2 cm (3 in. x 4 in.).

In the AACS, standard prefilter size is 0.6 m x 0.6 m (2 ft x 2 ft) with an effective filtration area of 56.8 cm x 56.8 cm or 3210 cm<sup>2</sup>. The nominal total flow rate through the AACS is about 100,000 to 120,000 cfm. The flow is distributed through 5 sets of compartments, each with 20 prefilter assemblies and 32 HEPA filters. The lower AACS flow would result in a flow rate of at least 1000 cfm through each prefilter assembly. Therefore, the resulting gas velocity through the prefilter in the AACS can be calculated to be approximately 150 cm/sec. For the laboratory scale filter with an effective area of 77.4 cm<sup>2</sup> (12 in<sup>2</sup>), the volumetric flowrate through the test assembly should be at least 24.6 cfm to simulate the AACS.

A HEPA filter with an effective filtration area (not cross sectional area) of 3855.5 cm<sup>2</sup> (4.15 ft<sup>2</sup>) was used in the test system downstream of the 77.4 cm<sup>2</sup> prefilter. The volumetric gas flowrate was controlled at 25 cfm resulting in a HEPA media velocity of 3 cm/s. The filtration velocities through each test filter are the same as those through the AACS filters.

Tests were conducted to establish efficiency characteristics for the prefilter and to measure mass loading characteristics as a function of pressure difference across the prefilter in order to develop a methodology for predicting the mass loading and pressure drop effects on a prefilter/HEPA filter system. To determine filtration efficiency of the prefilter for both solid and liquid particles, various nebulizing methods were used. A TSI Model 3075/3076 Constant Output Atomizer (COA) was used with a TSI Model 3071 Electrostatic Classifier (EC) to produce both solid and liquid particles with Mass Median Aerodynamic Diameters (MMAD's) less than 0.5 μm. Sodium chloride was chosen as the

## 22nd DOE/NRC NUCLEAR AIR CLEANING AND TREATMENT CONFERENCE

material for the small solid particles, and fluorescein was used as a tracer in solutions of ethylene glycol, diethylene glycol and dioctyl phthalate which were chosen for the small liquid particles. To generate solid and liquid particles greater than 1.5  $\mu\text{m}$  a TSI Model 3450 Vibrating Orifice Generator (VOG) was used. A sodium hydroxide and water solution with fluorescein was used to produce the solid particles, and the same solutions as listed above were again used to produce the liquid particles. A 3-jet Collison Nebulizer was used with a TSI Model 3072 Evaporation/Condensation Aerosol Conditioner (E/C) to generate liquid particles in the range between 0.5 micrometers and 2.5  $\mu\text{m}$ . Solutions of ethylene glycol, diethylene glycol and dioctyl phthalate with fluorescein tracer were again used to produce these liquid particles.

In tests utilizing sodium chloride particles, efficiencies were determined by counting particles with two Condensation Nucleus Counters (CNC), one sampling in the upstream flow of the aerosol and the other sampling in the downstream flow of the prefilter. Upstream and downstream particle counts were taken simultaneously for one minute. Several readings were taken to assure reproducibility and averaged to improve statistical accuracy. The downstream particle count was divided by the upstream particle count to determine the percent penetration of particles through the prefilter. The efficiency ratio was determined by subtracting the percent penetration from 100%.

In tests utilizing fluorescein as a tracer, the prefilter was rinsed in a sodium hydroxide/purified water solution following the test. The rinse solution was analyzed with the Model 111 Turner Fluorometer. The intensity of the light re-emitted by a sample exposed to a constant ultraviolet light source is directly proportional to the concentration of fluorescein in the solution. These fluorometric readings were multiplied by the amount of the rinse solution to obtain an equivalent mass. At least three rinses of each filter were made until the fluorometric reading was less than 10 times the background reading. The rinse results from each filter were summed to give separate equivalent mass results for the prefilter and the HEPA filter. The efficiency is the ratio of the equivalent mass on the prefilter to the total equivalent mass on the prefilter plus the HEPA filter.

Experimental measurements of the filtration efficiency as a function of particle diameter for both solid and liquid particles at a filtration velocity of 152 cm/s, are shown in Figure 1. Also shown in Figure 1 is a calculation of the expected theoretical efficiency based on Equations 1 and 2. The differences are primarily attributed to the non-uniform distribution of fibers in the prefilter due to its stranded construction.

The mass loading characteristics were determined as a function of pressure difference across the prefilter with respect to particle size and composition of the aerosol. The prefilter mass loading tests were done at a flow velocity of 152 cm/s. Pressure changes were monitored across the prefilter and across the HEPA filter. The clean prefilter and HEPA filter were initially weighed and placed into the test system. The filters were loaded with challenge aerosols until a desired total pressure difference across both filters was achieved. When the given target pressure difference was reached, both filters were carefully removed from the system and weighed again. The change in mass was used to determine the mass loading per unit filter area.

For liquid aerosol mass loading tests, the prefilter and HEPA filter were weighed when the first target  $\Delta P$  was reached. The drainage of liquid from the prefilter was also collected and weighed as part of the mass collected on the prefilter. The filters were carefully replaced into the system and the test continued until the next  $\Delta P$  was reached. This procedure was repeated until the final target  $\Delta P$  was reached.

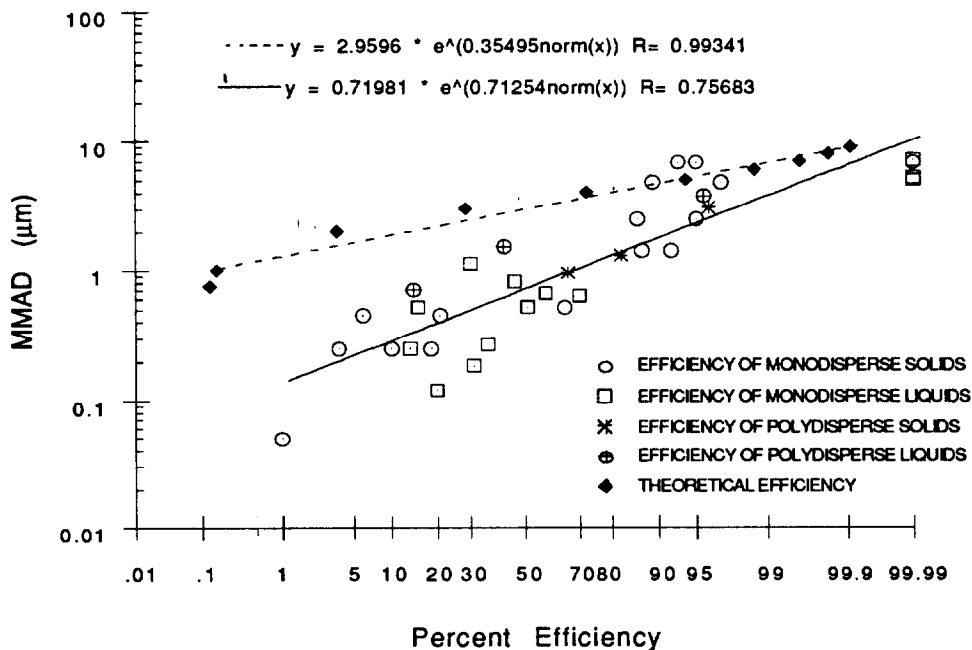


FIGURE 1 Theoretical and experimental collection efficiency curves for particles for the prefilter material at a face velocity of 152 cm/s. Experimental particle diameters are both solid and liquid particles.

In contrast to the liquid tests, the solid particles mass loading tests each had to be started from  $\Delta P_0$ , removed and weighed at the target  $\Delta P$ , and new filters used for the next target  $\Delta P$ . This procedure was required due to the change in particle cake structure of solid particles caused by handling the prefilters.

Three different aerosol generators were used to generate the three sizes of liquid particles. A BGI Inc. 6-jet Collison Atomizer was used to atomize a solution of 50% dioctyl phthalate (DOP) and 50% isopropyl alcohol generating particles with an MMAD of approximately 1.5  $\mu\text{m}$ . To generate particles with an MMAD less than 1.5  $\mu\text{m}$ , an evaporation-condensation aerosol generator was used in conjunction with a TSI Constant Output Atomizer (COA). The third liquid generation technique used three Bennett ultrasonic nebulizers to generate an aerosol with an MMAD greater than 1.5  $\mu\text{m}$ . A graph of the mass loading versus the net pressure change for liquid particles is shown in Figure 2. Note that there is no change in  $\Delta P$  with mass loading within the limits of the resolution of the pressure transducers.

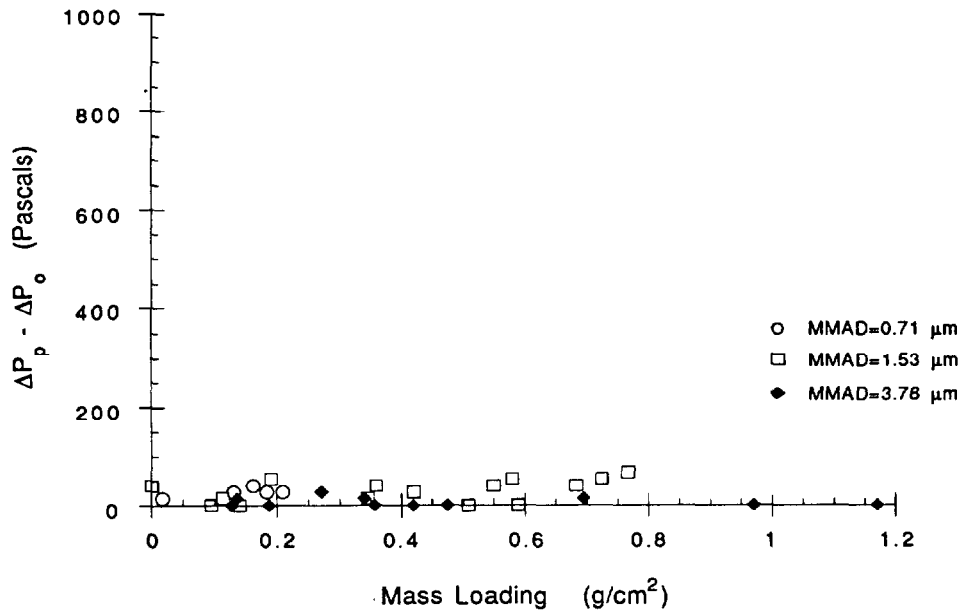


FIGURE 2 Mass loading -vs- net pressure change for liquid particles on the prefilter material at a face velocity of 152 cm/s. Three particle sizes were studied, each MMAD being the average of tests done for that specific size. Two liquid solutions were used, di-ethylene glycol and dioctyl phthalate.

Three distributions of solid particles were dispersed using a BGI Model WDF-II Wright Dust Feeder. Aluminum oxide powder was chosen to produce the solid particle aerosol. The output aerosol particle size is solely dependent on the size of the powder used down to a limit of about 0.1 μm. Figure 3 shows a graph of the mass loading versus the net pressure change for solid particles.

The specific resistance of the prefilter was determined from data obtained in the mass loading tests for solid particles. This was done by dividing the slope of each curve on the graph in Figure 3 by the filtration velocity. This data is plotted against the mass median particle diameter (MMD) and shown in Figure 4. The data was analyzed with a linear least squares curve fit resulting in the correlation,

$$\Delta P_p = \Delta P_o + [4.427 + (0.0001103 / d_p)] V M / A \quad (7)$$

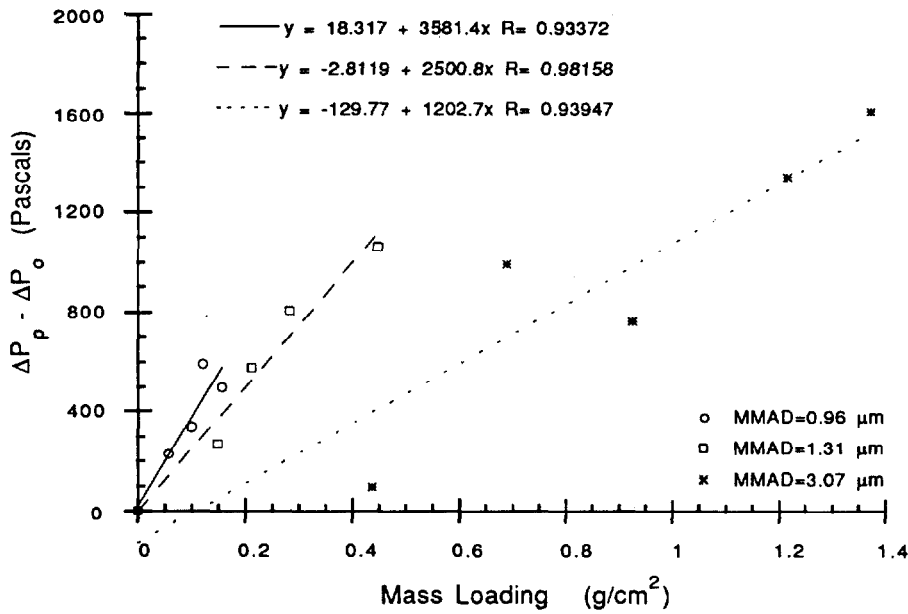


FIGURE 3 Mass loading -vs- the net pressure change for solid particles on the prefilter material at a face velocity of 152 cm/s. Three particles sizes of aluminum oxide powder were studied, each MMAD being the average of tests done for that specific size.

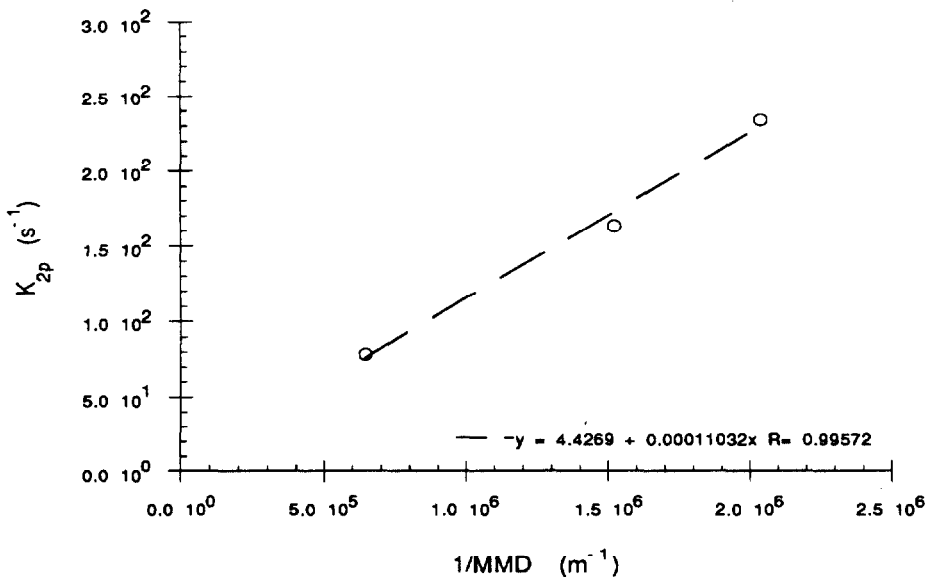


FIGURE 4 The specific resistance of aluminum oxide filter cakes plotted as a function of the inverse of the MMAD for the prefilter material.

## 22nd DOE/NRC NUCLEAR AIR CLEANING AND TREATMENT CONFERENCE

The MMD was chosen to describe the aerosol introduction, to be consistent with the HEPA filter correlation. This correlation will be used with the prefilter efficiency characterization to calculate the total predicted mass loading on a prefilter/HEPA filter system. To complete this calculation, the particles that penetrate the prefilter are loaded onto the HEPA filter and must be considered. Figure 5 presents the data that was used to previously determine the correlation for the specific resistance as a function of particle diameter for HEPA filters. (2) (3) (9)

$$\Delta P_H = \Delta P_0 + [-1.586 \times 10^5 + (0.9494 / d_p)] V M / A \quad (8)$$

where the subscript H denotes HEPA filter and  $d_p$  is the MMD required to determine the specific resistance ( $K_2$ ) of the HEPA filter .

This correlation allows the  $\Delta P$  to be calculated for a given mass loading of an aerosol distribution with a known mass median particle diameter.

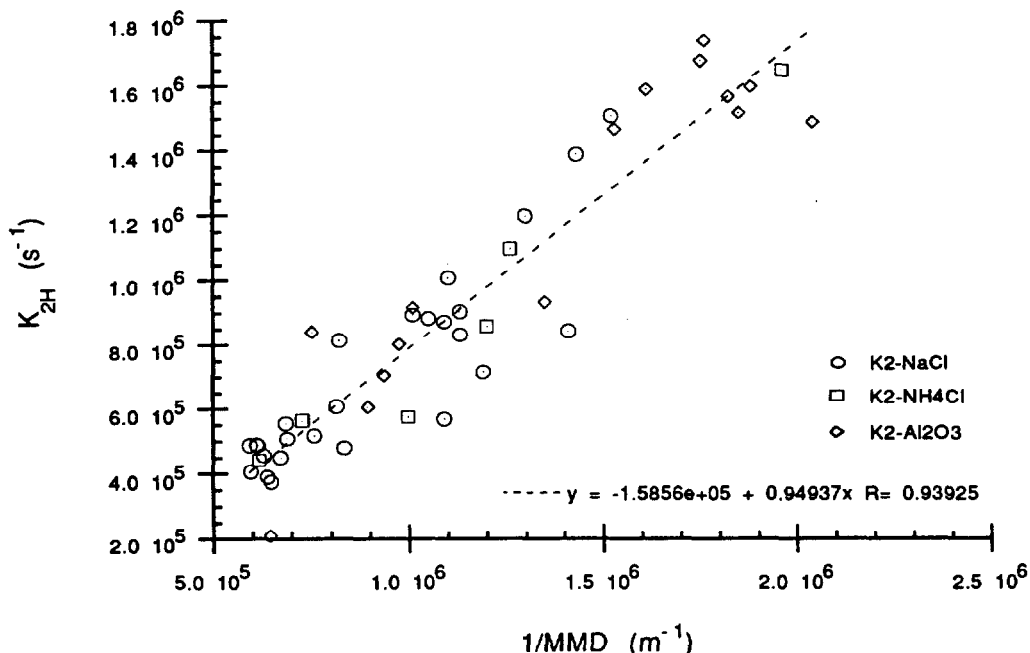


FIGURE 5 The specific resistance of sodium chloride, ammonium chloride and aluminum oxide filter cakes on the HEPA filter media plotted as a function of the inverse of the MMAD.

### Predicting Loading on Prefilter/HEPA Filter Systems

The mass loading on a prefilter/HEPA filter system can be predicted by empirical correlations for the prefilter efficiency, prefilter mass loading and HEPA filter mass loading. These correlations provide an accurate method of estimating the mass loading and final pressure difference across the

## 22nd DOE/NRC NUCLEAR AIR CLEANING AND TREATMENT CONFERENCE

prefilter/HEPA filter system. Separate expressions were developed for liquid and solid particles because of the difference in the structure of the accumulated particles on the filters.

### Solid Particles

In order to model the behavior of the total aerosol mass collected on a system for a given pressure drop as a function of particle diameter, three fundamental equations are necessary. These equations will then be combined with the correlations developed experimentally. The total pressure difference in the prefilter/HEPA filter system can be expressed as

$$\Delta P_{\text{SYSTEM}} = \Delta P_H + \Delta P_P + (\Delta P_0)_H + (\Delta P_0)_P \quad (9)$$

The efficiency of the prefilter can be expressed in terms of mass loading,

$$E = M_P / M_P + M_H \quad (10)$$

And the specific resistance of either filter can be expressed,

$$K_2 = (\Delta P - \Delta P_0) A / V M \quad (11)$$

From Figures 4 and 5 in the previous section, the specific resistance,  $K_2$ , can be correlated with the mass median aerosol diameter challenge in the prefilter and HEPA filter.

$$K_{2H} = -1.586 \times 10^5 + 0.9494 / \text{MMD}_H \quad (12)$$

$$K_{2P} = 4.427 + 0.0001103 / \text{MMD}_P \quad (13)$$

In this series of equations, the surface area,  $A$ , of the prefilter and HEPA filter are both known quantities. The velocity,  $V$ , through the prefilter and HEPA filter are parameters initially set for the system. The initial  $\Delta P$  across the prefilter and HEPA filters are both measurable quantities based on the velocity. The final or design limit  $\Delta P$  of the system is an assumed value based on the system that is being studied. The mass collected on the HEPA filter,  $M_H$  and the mass collected on the prefilter,  $M_P$  are both unknown quantities. The  $\Delta P$  across the prefilter and the  $\Delta P$  across the HEPA filter are also unknown quantities. The efficiency of the prefilter is a quantity established from the prefilter efficiency characteristics tests. The mass median diameter,  $\text{MMD}_P$ , of particles collected on the prefilter is a known value based on the measured or assumed aerosol distribution challenging the system. However, the particle size distribution,  $\text{MMD}_H$ , for the particles collected on the HEPA filter is an unknown quantity.

The key to solving the system of equations is to determine the MMD of the aerosol distribution reaching the HEPA filter. The first step is to divide the known or assumed initial aerosol distribution into segments. In this work, the initial aerosol distribution was assumed to be the average of the measured Mass Median Aerodynamic Diameters (MMAD's) for each distribution tested, and the geometric standard deviation was assumed to be 2.0. The reason the measured distributions were not used to generate the calculated values of mass loading and pressure difference was to provide an indication of the magnitude of the error that might be expected using this methodology in a predictive

## 22nd DOE/NRC NUCLEAR AIR CLEANING AND TREATMENT CONFERENCE

manner using reasonable initial assumptions. The segments of the initial distribution can be arbitrarily chosen. For our calculations, the mid points of each segment were based on the cut points (ECD's) of a cascade impactor. Once the midpoint of each segment is determined, the penetration efficiency of the particles in that segment can be determined from the efficiency curve of the prefilter. The penetrating aerosol distribution is determined by multiplying the efficiency by the quantity of aerosol in each segment. In this case, the mass of aerosol was used to define the distribution since the mass loading is the ultimate quantity of interest. Once the distribution of the aerosol that penetrates the prefilter, and therefore challenges the HEPA filter, is determined, the mass median diameter ( $MMD_H$ ) of the distribution can be calculated. The  $MMD_H$  is then used to determine  $K_{2H}$  from Equation 12. The specific resistance of the prefilter ( $K_{2P}$ ) is determined for Equation 13 by calculating the MMD of the initial aerosol distribution from the known or assumed MMAD, by dividing the MMAD by the square root of the particle density.

Knowledge of the specific resistances reduces the problem to a set of four equations and four unknowns. The equations to be solved are (8), (9) and (10), where Equation (10) is written once for the HEPA filter and again for the prefilter. The four unknowns are the mass collected in the HEPA,  $M_H$ , the mass collected on the prefilter,  $M_P$ , the final  $\Delta P$  of the HEPA,  $\Delta P_H$ , and the final  $\Delta P$  of the prefilter,  $\Delta P_P$ . A comparison between the actual mass collected on the HEPA filters in the laboratory experiments, and the mass that was calculated from the methodology presented above, is given in Table 1. The average of the absolute value of the differences between the calculated and measured masses is 11.7%.

Table 2 compares the calculated pressure increases and the measured pressure increases on the filters used in these experiments. The average difference for the prefilter pressure increase is 12.9% and the corresponding average difference for the HEPA filter pressure increase is 20.6%.

Calculations predicting the mass loading capabilities of the AACS are based on the following initial conditions and assumptions.

Total $\Delta P$ of System:	$\Delta P_{System} = 1750 \text{ Pa}$
Initial $\Delta P$ across HEPA filter:	$\Delta(P_0)_H = 228.2 \text{ Pa}$
Initial $\Delta P$ across Prefilter:	$\Delta(P_0)_P = 187.9 \text{ Pa}$
Surface area of HEPA filter:	$A_H = 2229.7 \text{ m}^2$
Surface area of Prefilter:	$A_P = 32.12 \text{ m}^2$
Velocity through HEPA filter:	$V_H = 0.0254 \text{ m/s}$
Velocity through Prefilter:	$V_P = 1.76 \text{ m/s}$

The predicted total mass of solid particles collected by the system with a given total pressure drop of 1750 Pa, as a function of the MMAD is shown in Figure 6.

Figure 7 compares the predicted total mass of solid particles that are expected to be collected by the AACS when calculated using the above methodology to extrapolated experimental test data. The experimental data was scaled by the AACS/experimental filter area ratios to obtain the extrapolated AACS values.

Table 1. Measured vs. calculated mass loadings on the prefilters and HEPA filters used in the laboratory tests

Initial MMAD ( $\mu\text{m}$ )	Initial MMD ( $\mu\text{m}$ )	Penetrating MMD ( $\mu\text{m}$ )	Calc. Pre-filter Efficiency	Calc. Pre-filter Mass (g)	Calc. HEPA Mass (g)	Calc. Total Mass (g)	Meas. HEPA Mass (g)	Meas. Pre-filter Mass (g)	Total Meas. Mass (g)	Calc. vs. Meas. Total Mass Diff (%)
3.34	1.69	0.71	0.98	33.87	0.55	34.42	0.65	33.85	34.50	- 0.2
3.16	1.60	0.71	0.98	66.30	1.27	67.57	4.95	71.60	76.55	-11.7
3.13	1.58	0.71	0.98	72.63	1.46	74.09	1.75	53.35	55.10	34.5
3.13	1.58	0.71	0.98	121.40	2.44	123.84	6.25	106.35	112.60	10.0
2.65	1.34	0.71	0.97	79.37	2.49	79.37	2.40	94.20	96.60	-17.8
1.38	0.70	0.41	0.85	11.70	2.05	13.75	2.60	11.50	14.10	- 2.5
1.35	0.68	0.41	0.84	31.22	5.78	37.00	6.90	34.60	41.50	-10.8
1.21	0.61	0.41	0.81	20.00	4.67	24.68	4.65	21.90	26.55	- 7.1
1.21	0.61	0.41	0.81	13.32	3.11	16.43	3.60	16.35	19.95	-17.6
0.99	0.50	0.33	0.74	4.50	1.62	6.11	1.95	4.45	6.40	- 4.5
1.00	0.51	0.33	0.74	7.92	2.80	10.72	3.35	7.75	11.10	- 3.5
0.83	0.42	0.33	0.66	12.02	6.22	18.24	7.25	12.10	19.35	- 5.7
1.02	0.52	0.33	0.75	14.15	4.83	18.99	5.65	9.40	15.05	26.2
Difference										11.7
Standard Deviation										15.7

Table 2. Measured vs. calculated pressure increases across the prefilter and HEPA filter used in the laboratory tests

Initial MMAD ( $\mu\text{m}$ )	Total System $\Delta\text{P}$ (Pa)	Measured $\Delta\text{P}_H-\Delta\text{P}_0$ on HEPA (Pa)	Measured $\Delta\text{P}_P-\Delta\text{P}_0$ on Prefilter (Pa)	Calculated $\Delta\text{P}_H-\Delta\text{P}_0$ on HEPA (Pa)	Calculated $\Delta\text{P}_P-\Delta\text{P}_0$ on Prefilter (Pa)	HEPA Difference (%)	Prefilter Difference (%)
3.34	930	93	492	51	463	-45.6	- 5.8
3.16	1488	359	757	117	955	-67.5	26.2
3.13	1606	146	983	134	1056	- 8.1	7.4
3.13	2405	385	1595	224	1765	-41.7	10.6
2.65	1953	173	1329	229	1308	32.4	- 1.6
1.38	1134	306	266	345	373	12.8	40.1
1.35	2405	944	1050	972	1016	3.0	- 3.2
1.21	1927	718	797	786	725	9.5	- 9.1
1.21	1422	425	571	524	482	23.2	-15.5
0.99	957	332	226	343	198	3.2	-12.3
1.00	1355	625	332	593	346	- 5.1	4.1
0.83	2365	1488	492	1319	630	-11.4	28.1
1.02	2047	1076	585	1025	606	- 4.7	3.6
						Difference	Average
						Standard Deviation	20.6
							28.4
							12.9
							16.8

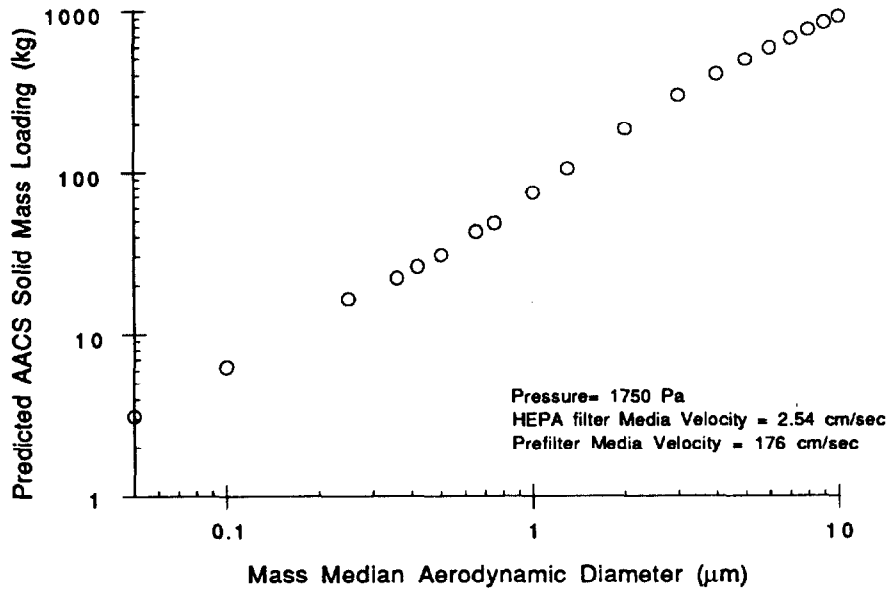


FIGURE 6 Predicted AACS mass loading for solid particles as a function of particle size.

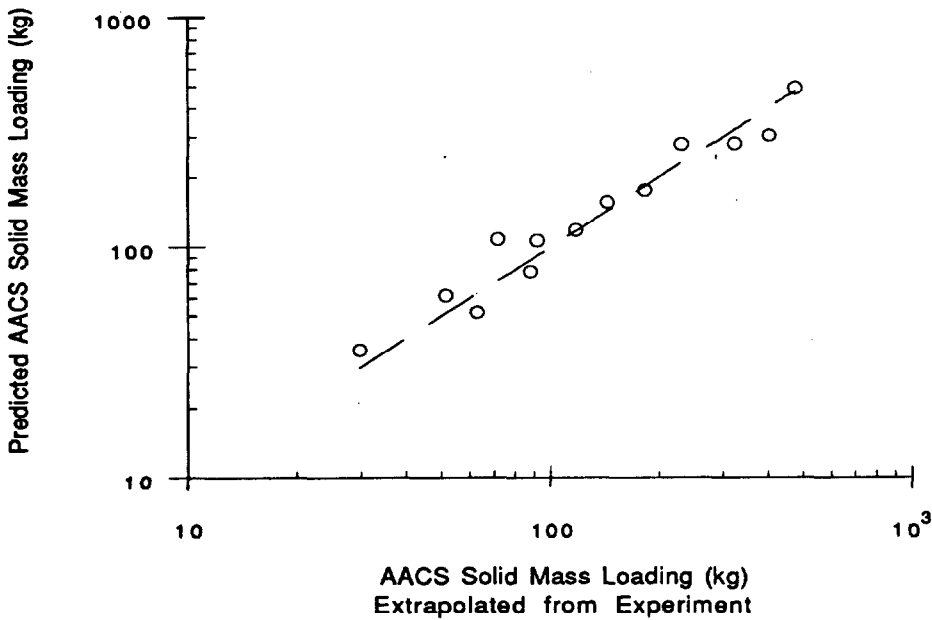


FIGURE 7 Comparison between the maximum solid aerosol mass loading predicted for the AACS determined by calculation and by extrapolation of the experimental results scaled by the respective AACS/Experimental filtration area ratios. The dashed line represents perfect agreement.

Liquid Particles

A similar type of strategy can be developed for predicting the liquid mass loaded onto a system. However, in the liquid model an equation cannot be written for  $K_2$  because no cake is formed. Instead, a graph of net pressure change versus the liquid mass loading on the HEPA filter, Figure 8, was used to determine an average mass loading for a liquid at a given  $\Delta P$  regardless of the particle diameter. The assumption is that the liquid particles will coalesce and coat the fibers with a liquid film after attaining a critical volume. Therefore, the first order relationship between mass loading and  $\Delta P$  should not be a function of droplet size. Note that since the prefilter drains excess liquid mass away from the prefilter fibers, the equilibrium pressure difference across the prefilter is a constant. Therefore, the HEPA filter always determines the limit of the system  $\Delta P$ .

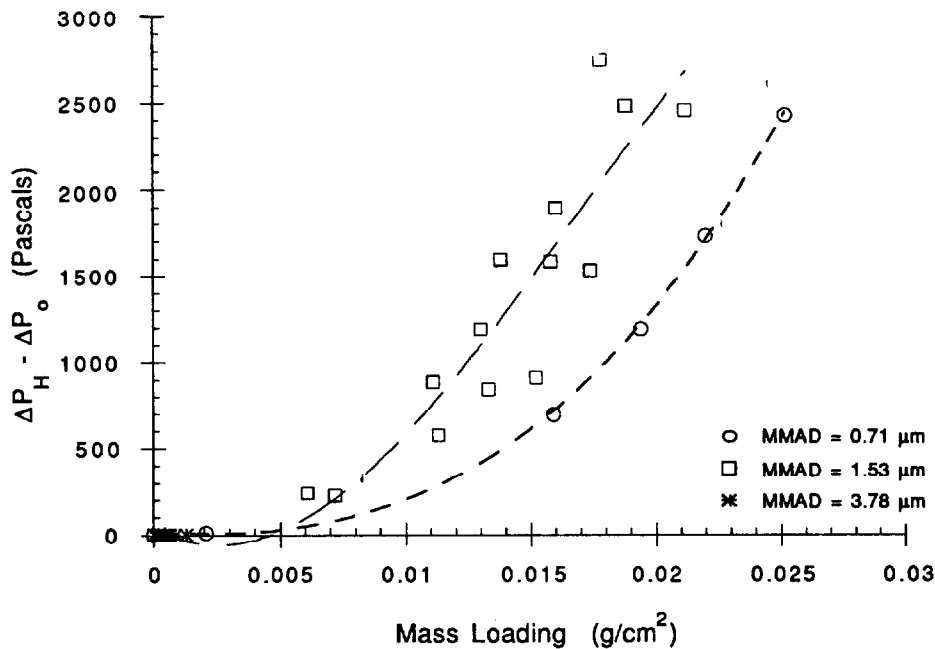


FIGURE 8 Mass loading -vs- net pressure change for liquid particles on the HEPA filter media at a face velocity of 3 cm/s. Three particle sizes were studied, each MMAD being the average of tests done for that specific size. Two liquid solutions were used, di-ethylene glycol and dioctyl phthalate.

In addition,  $\Delta P_P - (\Delta P_o)_P$  is assumed to be zero based on the results presented in Figure 2. This results in only two unknowns,  $\Delta P_H$  which can now be calculated directly from Equation 8 with a known target pressure and initial pressure drops across the filters, and  $M_P$  which can be calculated directly from Equation 9 after determining the efficiency from Figure 1.

Using the AACS parameters as an example, the average mass loading per unit area of the HEPA filter, for a pressure difference of 1550 Pa, is determined to be 0.018 grams/sq cm. Since the total area of the HEPA filter media in the system is 22,297,000 sq cm, the amount of mass the HEPA

filters in the system could collect is 401 kg. This amount of liquid mass depends only on the total HEPA filter filtration area and the design  $\Delta P$  limit. The prefilter will remove mass in relation to its efficiency. For example, for a particle distribution with an MMAD of 1 micrometer, the prefilter efficiency is 0.68, as determined from Figure 1. Therefore, for a design limit system pressure difference of 1750 Pa across the prefilters and HEPA filters, the total mass of 1  $\mu\text{m}$  aerosol that could be collected on the system is 1253 kg. The predicted total mass of liquid particles collected by the AACS with a given total pressure drop of 1750 Pa, as a function of the MMAD is shown in Figure 9. No comparison is made between the measured and predicted liquid mass loadings due to the number of common parameters.

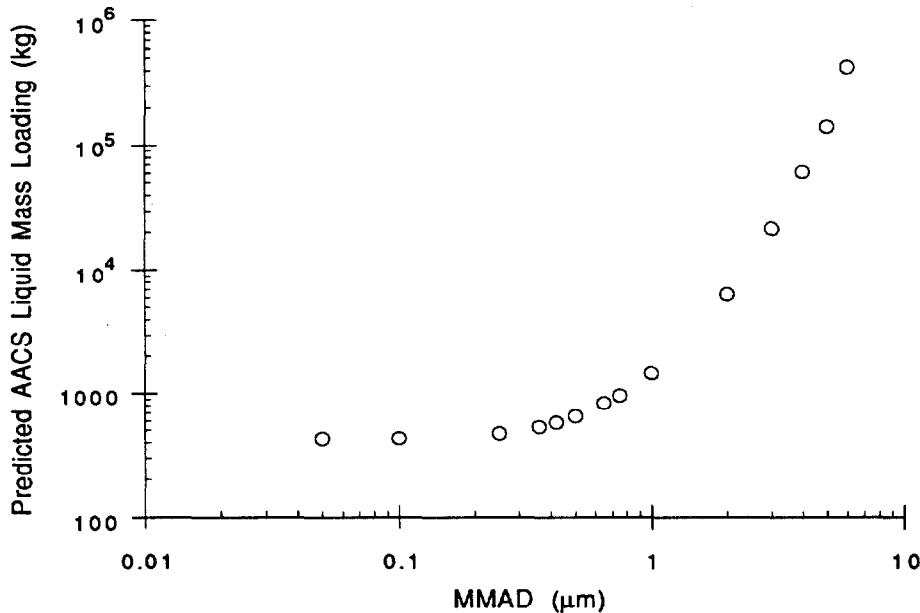


FIGURE 9 Predicted AACS mass loading as a function of liquid particle size based on experimental data from efficiency and mass loading tests for a total pressure difference of 1750 Pa, prefilter velocity of 152 cm/s and a HEPA velocity of 3 cm/s.

### Conclusions

As expected, this method of predicting the total mass of solid particles collected by a prefilter/HEPA filter system shows that the small particle region the system mass is limited by the specific resistance of the HEPA filter. As the particle diameter increases, the specific resistance of the prefilter becomes the dominating factor. Comparisons between the predictive model for solid particles with scaled aluminum oxide experiments results in the average of the absolute value of the difference between the mass predicted from calculations and the mass measured from the experimental data of 11.7%, with a standard deviation of  $\pm 15.7\%$ .

Although this is not a completely independent comparison because of the experimental data used to

## 22nd DOE/NRC NUCLEAR AIR CLEANING AND TREATMENT CONFERENCE

determine  $K_2$  for the prefilter, the remaining parameters are independent and lead to the conclusion that relatively accurate predictions of system mass loading can be made as a function of postulated particle diameter and density.

The predicted liquid mass loading on a system as a function of MMAD indicates that the higher mass loading in the small particle region is dominated by the HEPA filter. As the particle diameter is increased, the prefilter efficiency increases but the total  $\Delta P$  is still controlled solely by the HEPA. Eventually very little aerosol reaches the HEPA filter so the total mass collected by the system becomes limited only by the capacity of the prefilter drain or trap.

The methodology presented in this paper allows predictions of pressure increases resulting from loading aerosols on a prefilter/ HEPA filter system as a function of particle size. The accuracy of these predictions is generally better than 25% which is significantly better than other methods of estimation. These results represent the boundary cases of mass loading on a system for pure solid aerosols and pure liquid aerosols, but do not necessarily represent the limits of mass loading for a mixed solid and liquid aerosol.

### Acknowledgements

The authors would like to thank Robert Haglund and Jeffrey Sciortino for their assistance in performing some of the experiments. We would like to acknowledge the U. S. Department of Energy, Nuclear Group, for supporting this work under Contract No. W-31-109-ENG-38 with ANL and Contract No. DE-AC09-89SR18035 with WSRC. We would also like to thank ABB Impell Corporation for their cooperation and assistance during preparation of this paper.

## 22nd DOE/NRC NUCLEAR AIR CLEANING AND TREATMENT CONFERENCE

### References

1. Hyder, M.L., "The severe accident analysis program for the Savannah River nuclear production reactors," Nuclear Safety, Vol. 32, No. 4, pp. 502-510 (1991).
2. Novick, V. J., Abrahamson, C. A., and Richardson, W. B., "Relationship between the pressure drop across the Savannah River Site's HEPA filter material and aerosol mass loading," WSRC-RP-90-779 (1990).
3. Novick, V. J., Higgins, P. J., Dierkschiede, B., Abrahamson, C., Richardson, W. B., Monson, P.R. and Ellison, P.E., "Efficiency and mass loading characteristics of a typical HEPA filter media material," 21st DOE Nuclear Air Cleaning Conference (1990).
4. Bergman, W., Taylor, R. D., Miller, H. H., Biermann, A. H., Hebard, H. D., da Roza, R. A., Lum, B. Y., "Enhanced filtration program at LLNL. A progress report," 15th DOE Nuclear Air Cleaning Conference, CONF-780819, Boston (1978).
5. Gunn, C. A. and Eaton, D. M., "HEPA filter performance comparative study," 14th ERDA Air Cleaning Conference, CONF 760822 (1976).
6. Strauss, W., *Industrial Gas Cleaning*, Pergamon Press, Oxford, 1975.
7. Hinds, W. C., *Aerosol Technology - Properties, Behavior, and Measurement of Airborne Particles*, John Wiley & Sons, Inc., New York, 1982.
8. Wakeman, R.J., *Progress in Filtration and Separation*, Elsevier, Amsterdam, 1986.
9. Novick, V. J., Monson, P. R. and Ellison, P. E., "The effect of solid particle mass loading on the pressure drop of HEPA filters," Journal of Aerosol Science, Vol. 23, No.6, pp. 657-665 (1992).
10. Liew, T. P. and Conder, J. R., Journal of Aerosol Science, Vol 16, No. 6, pp. 497-509 (1985).

Nomenclature

A	=	surface area of the filter
$A_1$	=	Liew and Condor correlation coefficient
C	=	slip correction factor
D	=	diffusion coefficient
$d_f$	=	fiber diameter
$d_p$	=	diameter of particle
E	=	filtration efficiency
h	=	depth of filter material
$K_1$	=	constant depending on filter parameters
$K_2$	=	specific resistance of the cake
Ku	=	Kuwabara hydrodynamic factor
M	=	mass collected on filter
$\Delta P$	=	total pressure difference
$\Delta P_c$	=	pressure difference due to particle cake on filter
$\Delta P_0$	=	pressure difference across clean filter
$\Delta P_{we}$	=	equilibrium pressure difference across the wet filter
Q	=	volumetric gas flowrate
R	=	$d_p/d_f$
Re	=	Reynolds number
Sc	=	Schmidt number
t	=	surface tension of the liquid
V	=	velocity
$\alpha_f$	=	filter solidity, or packing (volume) density
$\eta$	=	single fiber efficiency
$\eta_i$	=	single fiber efficiency due to impaction
$\eta_d$	=	single fiber efficiency due to diffusion
$\eta_l$	=	single fiber efficiency due to interception
$\mu$	=	gas viscosity
$\rho$	=	particle density
$\theta$	=	contact angle of a droplet with respect to the fiber's surface
$\psi$	=	Stokes number

DISCUSSION

**DYMENT:** I am talking about solid particles, not liquid particles. Did you find that the particle size distributions of the particles which penetrate through the prefilter vary as a function of time? I think it has been reported in the past that certain filters do change their efficiency characteristics as they begin to load with particles. There is often a need to make a decision as to whether there is an economic benefit in the use of a prefilter in conjunction with a HEPA filter. Does your work enable you to conclude that there is an economic advantage in using prefilters in conjunction with HEPA filters, and if so, roughly speaking, what efficiency of prefilters should one aim to use.

**NOVICK:** 1) Prefilter efficiencies were measured for clean prefilters. One measurement was performed on a loaded prefilter. The resulting efficiency did not differ significantly from the clean prefilter. This may be attributed to the fact that the HEPA prefilter system studied in these tests were terminated before reaching a total delta P of 8 in. of H<sub>2</sub>O due to the AACS limitations at Savannah River. These particle loading levels did not obscure the basic structure of the prefilter. Therefore, the efficiency remained essentially unchanged. Obviously, at some point in time (i.e., mass loading) the efficiency would be affected.

2) The focus of this work was on the environmental benefit of maintaining the integrity of the AACS under severe accident conditions, rather than focusing on the economics of when to use a prefilter. However, this work can be used as input to an economic analysis for a specific application. For example, in applications where micron-sized droplets are required to be filtered, this work clearly shows the advantage of adding a prefilter.

**KOVACH:** You started out the paper by stating that this work was done to either verify the utility of your installation or give you design data for modification of the Savannah River confinement filter system. What is your conclusion, are you going to change it and if, yes, how are you going to use these data in relation to the original intention of the project?

**KLASSEN:** The intention was to study the system, it wasn't necessarily to change it. The scope of this project didn't involve recommendations for change. The results were turned over to Savannah River and then it became their decision whether or not to make changes.

**HYDER:** Just a comment on this last question. The purpose of the study was to develop data for computer modeling of the AACS system. The results were useful for that purpose.

APPLICATION of HIGH EFFICIENCY METAL FIBER FILTERS  
in VENTILATION SYSTEMS of NON-REACTOR NUCLEAR FACILITIES

Gurinder Grewal, Zoran Milatovic and Frank L. Landon  
Advanced Technology Business Unit  
Fluor Daniel Inc.  
Irvine, California  
and  
William M. Harty  
Westinghouse Hanford Co.  
Richland, Washington

Abstract

Sand filters, Deep Bed Glass Fiber filters, and remotely replaceable High Efficiency Particulate Air filters have been successfully used for filtration of exhaust air from highly contaminated exhaust air streams. However, none of these technologies satisfy all requirements of an optimum filtration system design. The basic requirements of a nuclear filtration system are a high decontamination factor, low pressure drop, long operating life, sturdiness during normal operation, ability to withstand Design Basis Accidents, minimize generation of waste, minimum maintenance, high radiation resistance, ease of decontamination and decommissioning, and low life cycle cost. High Efficiency Metal Fiber filters are a new technology and provide a suitable alternative to the currently used nuclear air filtration technologies. This article investigates the advantages and disadvantages of the current air filtration technologies and compares them with those of the High Efficiency Metal Fiber filters. High Efficiency Metal Fiber filters system design considerations for non-reactor nuclear facilities are also discussed in this article. The design considerations include, but are not limited to, physical configuration, space requirements, pressure drop, decontamination factors, dust holding capacity, in-place cleanability, cleaning procedures, in-place testing, and other support equipment.

I. Introduction

Nuclear facilities are designed to minimize their impact on the environment. All exhaust air from these facilities is filtered to minimize the release of radioactivity to the environment. The nuclear air cleaning filters have minimum efficiency requirement of 99.97% for 0.3 micrometer size particles. Nuclear grade High Efficiency Particulate Air (HEPA) filters provide this efficiency and have been used satisfactorily in nuclear air cleaning applications. HEPA filters are fragile and can fail due to overpressurization caused by high concentration of water droplets or dust in the air. HEPA filters are disposable type and must be replaced periodically. HEPA filter failure is always a concern in severe service applications, such as offgas cleaning, exhaust air

## 22nd DOE/NRC NUCLEAR AIR CLEANING AND TREATMENT CONFERENCE

filtration from highly contaminated process enclosures, and safety related facility exhaust systems. HEPA filters exposed to high radioactivity, severe acids, and moisture are protected by scrubbers, High Efficiency Mist Eliminators, and heaters to assure that moisture accumulation on the filters will not cause overpressurization and failure. Multiple HEPA filter banks are provided in series and in parallel for reliability and safety. HEPA filters in high radioactivity service are designed for remote maintenance to reduce operating personnel radiation exposure. Highly radioactive HEPA filters are difficult to dispose of. Sand filters and Deep Bed Glass Fiber (DBGF) filters have been used as alternatives to HEPA filters for severe applications in the U.S. Department of Energy (DOE) nuclear facilities for many years. They are described in detail in the Nuclear Air Cleaning Handbook<sup>(1)</sup> and the proceedings of the DOE/NRC Nuclear Air Cleaning Conferences. The sand filters and the DBGF filters are non-replaceable types and are designed to last the life of the facility. Their design is empirical and performance is difficult to predict in advance. The sand filters and the DBGF filters are normally designed for a target efficiency of 99.95%, but the efficiency is difficult to test reliably due to their large size. The sand filters provide excellent protection from explosions and fire because of the enormous mass of sand, but are difficult to qualify for Design Basis Earthquake (DBE). The decontamination and decommissioning requirements for the sand filters and DBGF filters have not been defined, and no suitable methods of decontamination and decommissioning have been demonstrated.

Owens Corning Fiberglass type 115K was found to be the most suitable media for the DBGF filters<sup>(1)</sup>. No DBGF filters have been constructed in recent years and this media is not commercially available.

High Efficiency Metal Fiber (HEMF) filters have many desirable characteristics of HEPA filters, sand filters, and DBGF filters. They have high efficiency of HEPA filters, and the permanence and ruggedness of the sand filters and the DBGF filters. HEMF filters would not be damaged by large amounts of moisture droplets, heavy dust, and burning embers in the air stream. HEMF filters are non-replaceable type and are cleaned in-place using water, nitric acid or other chemical solutions compatible with the process application. The resulting liquid waste is treated by the facility radioactive liquid waste treatment system. HEMF filters are constructed of stainless steel and they can be DBE qualified. Presently, the capital cost of the HEMF filter systems is competitive with other filter systems (i.e., remotely replaceable HEPA filters, sand filter, etc.) for filtration of high radioactivity, high temperature, and high moisture content gas streams. The operating, maintenance and disposal cost of HEMF filters will be lower than that of HEPA filters, sand filters and DBGF filters.

The HEMF filter media is relatively new to the industry,

## 22nd DOE/NRC NUCLEAR AIR CLEANING AND TREATMENT CONFERENCE

having been commercially available in the U.S. A. for only about past six years. HEMF filters have been successfully used in Europe for high efficiency filtration of gases in the chemical and food industries. These filters have the following potential gas cleaning applications in the nuclear industry:

1. Highly radioactive off-gas systems.
2. Air exhaust from highly contaminated processing cells.
3. Vent filters for radioactive waste storage tanks.
4. Exhaust from Plutonium processing glove boxes.
5. Incinerator off-gas.

HEMF filters are manufactured by Pall Trinity Micro Corporation, Cortland, N.Y.

### II. HEMF Construction

All welded stainless steel construction of the HEMF filters

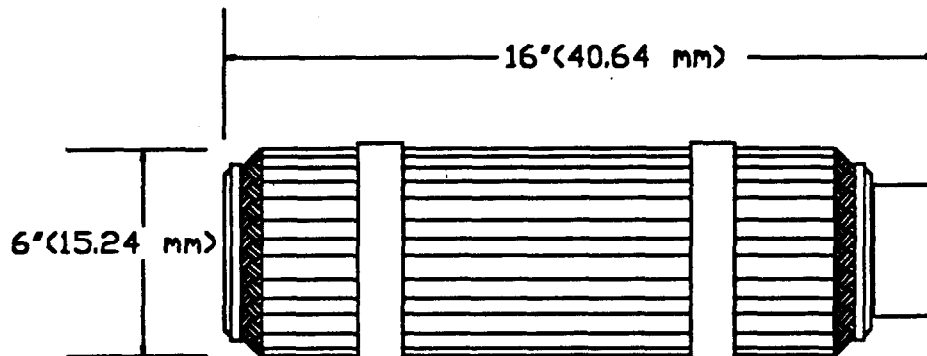


Figure 1 - High Efficiency Metal Fiber Filter Module

provides high mechanical strength, integrity, and corrosion resistance. A large number of very fine 316L stainless steel fibers are sintered at their points of contact to produce a uniform strong multilayered filter media. The sintering process strengthens the filter media and fixes the pore size. The filter media is pleated into cylindrical modules as shown in Figure 1. The cylindrical modules are welded together to produce long tubes. These tubes are welded to a tube sheet and installed in a cylindrical vessel to make a filter unit as shown in Figure 2.

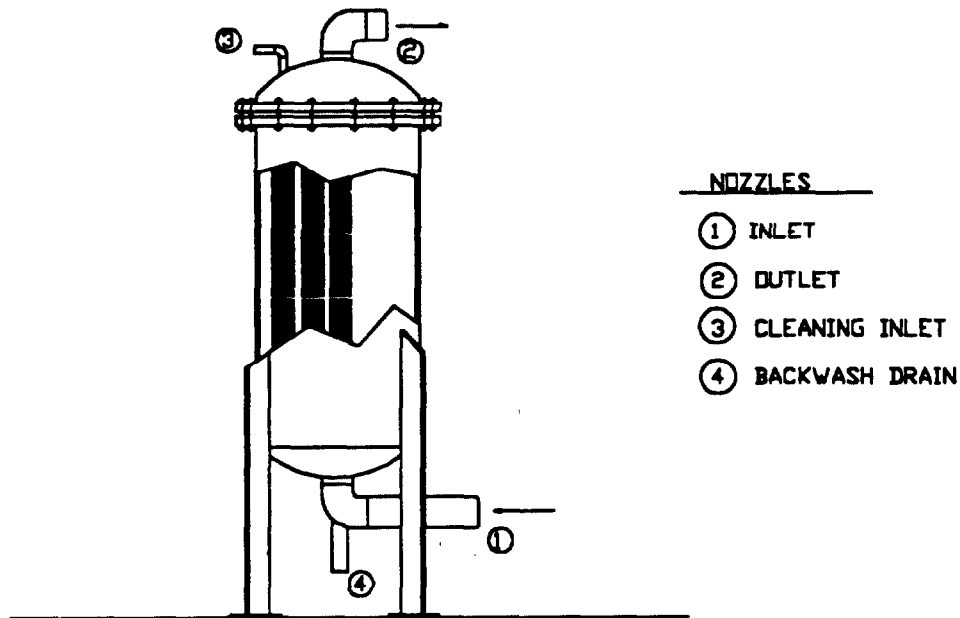


Figure 2 - High Efficiency Metal Fiber Filter Unit

### III. Filter Performance

#### A. Pressure Drop

Pressure drop is an important filter performance parameter. The system power requirement and energy consumption depend on the filter pressure drop. The HEMF filter's high void volume and small pore size give it a combination of high efficiency and low pressure drop. The HEMF filter clean pressure drop can be designed to meet system pressure drop requirements by optimizing the filter media surface area.

#### B. Dust Holding Capacity

The dust holding capacity parameter of a filter relates the pressure drop increase at constant airflow to the weight of contaminants being captured by the filter. The expected frequency of filter replacement or cleaning is estimated from:

1. Concentration of contaminants (i.e. weight/unit volume) in the gas stream
2. Filter replacement or cleaning pressure drop

The desired filter pressure drop and dirt holding capacity of HEMF filter units are achieved for a specific application by optimizing the filter media surface area, the unit geometry and construction of the upstream, downstream, and filter medium drainage layers.

## 22nd DOE/NRC NUCLEAR AIR CLEANING AND TREATMENT CONFERENCE

### C. Temperature

The nuclear air cleaning systems can experience high temperature air streams during upset or accident conditions. HEPA filters can be damaged by high temperature airstreams due to deterioration of the filter media binders, unless protected with cool down sprays and mist eliminators.

The HEMF filters contain no synthetic bonding materials and can be subjected to high temperature airstream without any damage to the filter media integrity. According to the HEMF filter manufacturer, these filters can operate continuously at 750°F (400°C), and for 10 minutes at 1000°F (538°C) without any loss of efficiency and the media integrity.

### D. Moisture

The nuclear exhaust air filters can be exposed to high concentrations of moisture during upset and accident conditions. HEMF filters are not weakened by condensed moisture on the media like HEPA filters and can be subjected to high pressure differential without media blow-through. HEPA filters are protected from moisture condensation on the media by mist eliminators and, if needed, with heaters. The air flow in the sand filters is upwards through the media and condensed moisture drains back prior to carryover through the media. The HEMF filter test data presented in the literature indicate no degradation in filter efficiencies when exposed to high moisture air streams<sup>(2)</sup>. However, if exposure to moisture saturates the media, the contaminants may pass through by wicking and/or a dissolution process. The prolonged exposure of HEMF filters to moisture combined with acids may corrode the metal fibers and make cleaning of the media difficult. The HEMF media should be water washed and dried as soon as possible following a high moisture upset to avoid corrosion of the fibers by absorption of acidic species from the gas stream by the water phase and to prevent water-induced migration of contaminants through the media. HEMF filters should be operated dry to assure high filtration efficiency.

### E. Filter Efficiency

A HEMF filter module was tested by the U.S. DOE Filter Testing Facility at Oak Ridge, Tennessee and has exhibited an efficiency exceeding 99.97% for 0.3 micrometer DOP particles. Since HEMF and HEPA filter media consist of micrometer size fibers, both filter media are presumed to have similar filtration mechanisms. According to the manufacturer, a single stage of HEMF filters can be designed to provide equivalent filtration efficiency of at least two stages of HEPA filters.

### F. Corrosion

Corrosion of the HEMF filter media is possible due to

prolonged localized condensation of acids in the gas stream or if correct cleaning procedures are not followed. The HEMF manufacturing process includes the use of high purity materials and annealing in a dry hydrogen atmosphere after welding to improve corrosion resistance. According to the manufacturer, the HEMF filter elements are now under corrosion test at the U.S. DOE Idaho Chemical Processing Plant, Idaho Falls. The knowledge of the HEMF filter corrosion rate is important and so far no corrosion test data on the stainless steel HEMF filters has been published.

IV. Design Considerations

A. Physical orientation

The following design is based on a 120,000 cubic feet per minute (203,880 m<sup>3</sup>/h) exhaust air capacity system of a high level radioactive waste processing facility. Ten HEMF filter units of 12,000 cfm (20,400 m<sup>3</sup>/h) capacity each are required in this application.

The HEMF filter units in this application will become highly radioactive during operation and are located in shielded concrete cell. The exhaust air filtration concept using HEMF filters is shown in Figure 3. The exhaust air from the hot cells enters the HEMF filter units at the bottom as shown in Figure 2, distributes amongst the filter module tubes, and flows through the media from

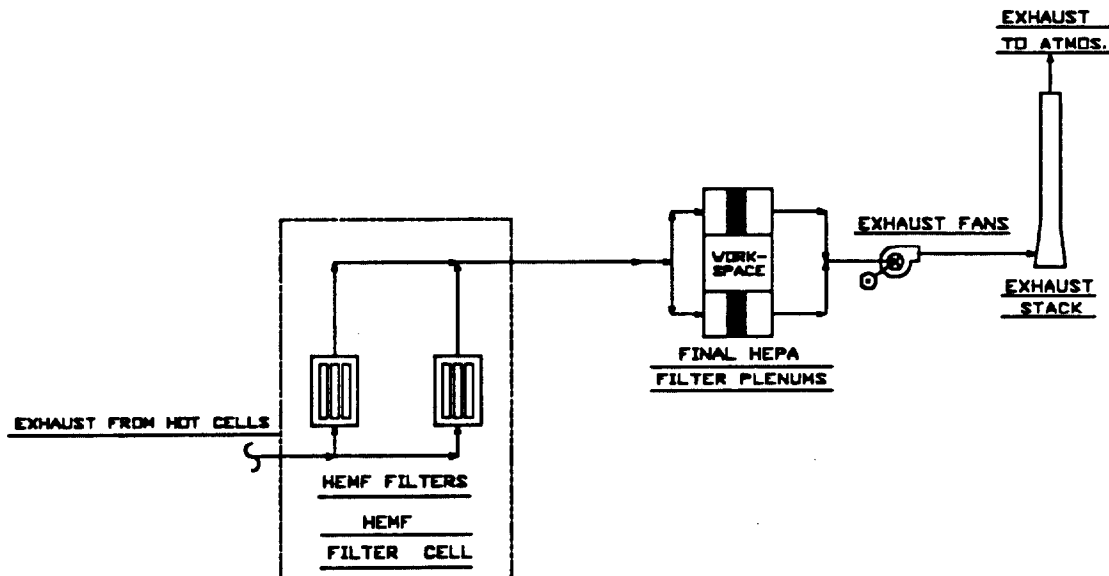


Figure 3 - Exhaust Air Filtration Using HEMF Filters

## 22nd DOE/NRC NUCLEAR AIR CLEANING AND TREATMENT CONFERENCE

the outside in. Rising through the tubesheets, the filtered air leaves the housing through the outlet duct at the top of the filter units. From the HEMF filter units, the exhaust air passes through final HEPA filter plenums, and is exhausted through a stack by exhaust fans. The high particulate removal efficiency of the upstream HEMF filters will result in very slow dust loading of the HEPA filters. The final HEPA filters prevent release of any contaminants from the HEMF filters either due to wetting of the media or after cleanup procedure.

A 12,000 cfm (20,400 m<sup>3</sup>/h) HEMF filter unit is a vertical cylindrical vessel of approximately 54" (138cm) diameter by 112" (285cm) overall height. Approximately 30 feet (9.2m) clear space is required in the filter cell to accommodate the filter units, isolation valves, and inlet and outlet ductwork. The top head of the vessel is flanged and is removable. The in-place cleanup procedure of the HEMF filters do not require removal of the top head. A tube sheet mounted between the top head flanges supports the internal module tubes, and separates the upstream and downstream compartments of the housing. The use of all welded components eliminates the need for the gaskets and sealants.

The support equipment required for in-place cleaning of the filter units is a cleaning liquid storage tank, pumps, liquid waste collection tanks, compressed air tank, drying air fan and associated air heater. In-place cleaning equipment including controls, and valve operators, are located outside the filter cell. All cleaning operations are performed without requiring personnel entry into the filter cell.

### B. Maintenance

HEMF filter systems in nuclear air cleaning applications are designed to be cleaned in-place due to high radiation hazards. The preliminary estimates show that these filters would require cleaning every two to three years in hot cell exhaust air filtration applications. The cleaning interval can be extended by HEPA filtering the hot cell supply air and by increasing the filter surface area. Standby filtration units are provided to maintain continuous operation of the exhaust system during the cleaning operation.

A schematic piping diagram for in-place cleaning of a filter unit is shown in Figure 4.

The following are the basic steps in cleaning of the filter unit:

1. Isolate the filter unit by closing inlet and outlet air valves (V1 and V2).
2. Open the demineralized water supply valve (V6) and vent valve (V3), allow the vessel to be filled with water to the overflow then close the water supply valve, and the vent valve. Allow the filter to soak.

3. Open pressurizing air valve (V4 & V7) and let the air pressure to build up to 80 psi (550 kPa).

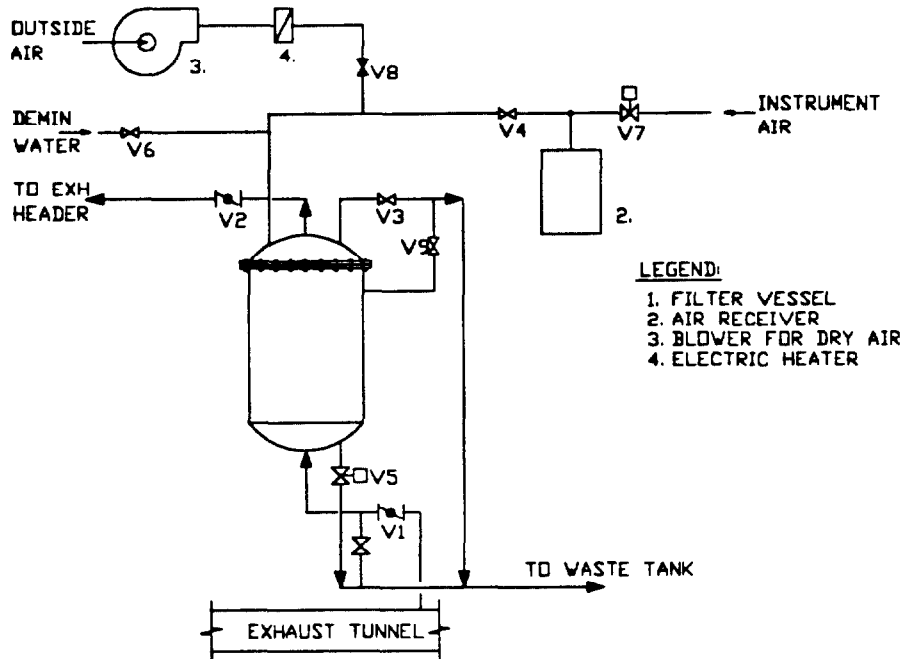


Figure 4 - Piping Diagram for Cleaning an HEMF Filter

4. Open drain valve (V5) and drain the vessel. Flush the vessel with water with approximately 1-3 gallons (4-11 liters) per filter module.
5. Drain all water.
6. Open drying air supply valve (V8) and supply hot air at a rate of approximately 1000 cfm (1700 m<sup>3</sup>/h). A dewpoint sensor in the exit air stream indicates when the filter unit is dry.
7. Close water drain valve (V5) and hot drying air supply valve (V8). Open the air inlet and outlet isolation valves (V1 and V2) to return the filter unit into service.

This cleaning procedure using demineralized water for soaking and backflushing of the HEMF filter unit is expected to be 85% to 95% effective by the manufacturer. The effectiveness of filter cleaning is directly related to filter application, the off-gas composition, and the filter design. Chemical agents, such as nitric acid, can be used to enhance cleaning efficiencies by partially dissolving particulate trapped in the media. HEMF filters have potential to last the life of the facility in this type of application.

To date there has not been any in-place cleaning experience of this size HEMF filter unit in nuclear applications. Therefore, it is prudent to withhold final judgement on the effectiveness of in-place cleaning of the HEMF filter units until the filter design is

tested in a simulated off-gas stream application.

### C. In-place Testing

Nuclear air cleaning filters are required to be tested in-place periodically. The HEMF filter units will be tested for efficiency prior to shipment and after installation. These filters will also be tested after each cleaning cycle to assure that they continue to meet the efficiency requirements. The design and procedures for in-place DOP testing of HEPA filter housings are described in ASME Standards N509 and N510. The guide lines of these ASME Standards and experience of the testing personnel will be used to develop design features and methods for in-place DOP testing of the HEMF filter units. The in-place testing of the filter units will be done remotely to prevent radiation exposure to the testing personnel.

### D. Instrumentation and Controls

Most instrumentation and controls associated with the HEMF filter unit, in-place DOP testing, and in-place cleaning equipment will be located outside the filter cell in the operating gallery.

The following are typical instrumentation and controls associated with the HEMF filter units:

1. Operators of the air isolation valves upstream and downstream of the filter unit.
2. Water supply isolation valves
3. Compressed air isolation valves
4. Valve limit switches
5. Air flow indication through the filter unit
6. Pressure differential indication across the filter unit
7. Negative pressure differential between the filter unit and atmosphere during the cleaning cycle
8. Dew point measurements downstream of the filter unit during the drying cycle

Additional instrumentation and controls may be required to satisfy unique application requirements.

### E. Decontamination and Disposal

The HEMF filter units can be decontaminated and disposed of using conventional techniques applicable to other Stainless Steel vessels in hot cells. Remotely operated equipment will be used to disconnect the entire unit from the ductwork and piping, and to open the filter housing to remove the filter module assembly. The empty filter housing and the filter module tube assembly will be thoroughly decontaminated using standard decontamination procedures for contaminated equipment. The decontaminated filter units will be removed and shipped to a radioactive waste burial site.

V. Operational Readiness

A. Testing for Nuclear Applications

The HEMF filters have not been used for nuclear air cleaning in the U.S.A. Demonstration testing is in progress of a 1,000 cfm, HEMF filter unit at the U.S. DOE Y12 Plant at Oak Ridge, Tennessee and a 300 cfm HEMF filter unit for the Hanford Waste Vitrification Plant melter off-gas system at Richland, Washington. The manufacturer has a number of non-nuclear gas cleaning applications to demonstrate that the HEMF filter module assembly performance and efficiency can be reliably scaled up from the performance of a single filter module.

B. Compatibility of Materials with Process Applications

The fully welded 316L Stainless Steel construction of the HEMF filter media, modules, and housings should be suitable for most nuclear air cleaning.

C. Vulnerability to accidents and Upsets

Fire

HEMF filters are made entirely of Stainless Steel and contain no flammable components. They are inherently resistant to high temperatures and over-pressurization. Although the finely divided filter media will not resist direct flame impingement, the media would not be destroyed by burning embers. The filters would get loaded with soot and other products of combustion and would experience high pressure differential. The manufacturer has indicated that HEMF filters can operate continuously at 125 psi (860 kPa) differential pressure and 750° F (400° C), and for 10 minutes at 1000° F (535° C).

Seismic

All the welded construction Stainless Steel of the HEMF filter modules and pressure vessel type construction of the filter unit assembly results in high mechanical strength. None of the HEMF filter units have been so far seismically qualified, but because of their rugged construction HEMF filters should be able to meet all DBE seismic requirements.

Operational Upsets

The impingement of water-saturated process gas and/or liquid droplets is a credible operating upset that would affect the HEMF filter units. Other credible accident scenarios may involve a sudden upset that can produce a large cloud of particulate in the air stream. Such operational upsets would lead to rapid plugging and overpressurization of the filters. The HEMF filter elements

## 22nd DOE/NRC NUCLEAR AIR CLEANING AND TREATMENT CONFERENCE

can resist high overpressure credibly produced by the exhaust fans.

### VI. Conclusion

HEMF filters have the following advantages over HEPA filters, sand filters, and DBGF filters:

1. Filtration Efficiency in excess of 99.97 percent for 0.3  $\mu\text{m}$  particles.
2. Higher resistance to overpressurization due to moisture loading than HEPA filters.
3. Can be DBE qualified in contrast to sand filters.
4. Lower operation and maintenance cost compared to HEPA filters.
5. Lower decontamination and decommissioning cost compared to HEPA filters, sand filters, and DBGF filters.

The ability to clean HEMF filters in-place repeatedly without loss of efficiency is an important parameter for their application in the nuclear industry. To date there has not been any in-place cleaning experience of HEMF filters in nuclear applications. However, several tests on these filters are currently in progress at U.S. DOE facilities.

### VII References

1. C.A. Burchsted, A.B. Fuller, and J.E. Kahn, Nuclear Air Cleaning Handbook (ERDA 76-21), Second Edition, Oak Ridge National Laboratory, Oak Ridge, Tennessee.
2. H. Randahn, B. Gotlinsky, S. Tousi, "The Development of All Metal Filters for Use in the Nuclear Industry", Proceedings of the 20<sup>th</sup> DOE/NRC Nuclear Conference, NUREG/CP-0098-Vol.2.

## 22nd DOE/NRC NUCLEAR AIR CLEANING AND TREATMENT CONFERENCE

### DISCUSSION

**PORCO:** There are no test data in your paper. Do you have test data available for the dust loading, holding capacity, moisture, over-pressure, etc.

**MILATOVIC:** The paper concentrated mainly on the application of High Efficiency Metal Fiber Filters. However, a test of dust holding capacity and filter efficiency of a Pall HEMF filter was performed per ASHRAE Standard 52-76, by the Air Filter Testing Laboratories, Inc. (AFTL), Crestwood, KY.

**PORCO:** On the cleaning of the filter, were you able to come back to the initial clean pressure drop?

**MILATOVIC:** There is no in-place cleaning experience for this size HEMF filter in nuclear application. Based on experience in pharmaceutical and food industries, a cleaning effectiveness of 85% to 95%, over several successive cycles, is achievable. However, filter cleaning in these industries is not done in-place. The filters are usually sent to the manufacturer for cleaning.

**PARKER, WAYNE:** Have you prepared any type of life cycle cost analysis to compare these filters with any other type of HEPA filter arrangements?

**MILATOVIC:** There were no life cycle cost analysis prepared for this paper. However, life cycle cost analysis was prepared for the project where HEMF filters are being considered. The data relating to this project are of proprietary nature and cannot be disclosed.

DEVELOPMENT AND EVALUATION OF A CLEANABLE HIGH  
EFFICIENCY STEEL FILTER\*

by

W. Bergman, G. Larsen, F. Weber, P. Wilson, R. Lopez, G. Valha,  
J. Conner, J. Garr, K. Williams, A. Biermann, K. Wilson, P. Moore,  
C. Gellner, D. Rapchun

Lawrence Livermore National Laboratory  
P. O. Box 808, Livermore, CA 94550

and

K. Simon, J. Turley, L. Frye and D. Monroe  
Martin Marrietta Energy Systems  
Oak Ridge, TN 37831

ABSTRACT

We have developed a high efficiency steel filter that can be cleaned in-situ by reverse air pulses. The filter consists of 64 pleated cylindrical filter elements packaged into a 610x610x292 mm (24x24x11.5 in.) aluminum frame and has 13.5 m<sup>2</sup> (145 square feet) of filter area. The filter media consists of a sintered steel fiber mat using 2 μm diameter fibers. We conducted an optimization study for filter efficiency and pressure drop to determine the filter design parameters of pleat width, pleat depth, outside diameter of the cylinder, and the total number of cylinders. Several prototype cylinders were then built and evaluated in terms of filter cleaning by reverse air pulses. The results of these studies were used to build the high efficiency steel filter.

We evaluated the prototype filter for efficiency and cleanability. The DOP filter certification test<sup>(1)</sup> showed the filter has a passing efficiency of 99.99% but a failing pressure drop of 0.80 kPa (3.2 in w.g.) at 1,700 m<sup>3</sup>/hr (1,000 cfm). Since we were not able to achieve a pressure drop less than 0.25 kPa (1 inch w.g.), the steel filter does not meet all the criteria for a HEPA filter.<sup>(2)</sup> Filter loading and cleaning tests using AC Fine dust showed the filter could be

\*This work was performed under the auspices of the U.S. Department of Energy by Lawrence Livermore National Laboratory under contract no. W-7405-eng.48. The work was supported by DOE's Office of Technology Development, EM-50.

repeatedly cleaned by reverse air pulses.

The next phase of the prototype evaluation consisted of installing the unit and support housing in the exhaust duct work of a uranium grit blaster for a field evaluation at the Y-12 Plant in Oak Ridge, TN. The grit blaster is used to clean the surface of uranium parts and generates a cloud of  $UO_2$  aerosols. We used a 1,700  $m^3/hr$  (1,000 cfm) slip stream from the 10,200  $m^3/hr$  (6,000 cfm) exhaust system.

### I. Introduction

This study is a continuation of our investigation on using high efficiency steel filters for nuclear air cleaning that was reported at the 21st DOE/NRC Nuclear Air Cleaning Conference.<sup>(3)</sup> The motivation for that study was to improve the reliability of the present glass fiber HEPA filter. The present glass HEPA filter is subject to structural damage when the filter is exposed to high air flows, shock waves, high temperatures, high humidities, and heavy particle deposits. Replacing the structurally weak glass fiber medium with a stainless steel medium overcomes these failure modes. The focus of our previous work was on improving the reliability of high efficiency air filters. This was also the motivation of Dillmann et al<sup>(4-6)</sup>, Klein et al<sup>(7)</sup> and Randhahn et al<sup>(8)</sup> who had previously conducted investigations of high efficiency steel filters.

Although improved filter reliability is still an important driving force, our present research is focused on cleanable steel filters to reduce the cost of filtration. Air filtration in the nuclear industry is based primarily on disposable HEPA filters. The cost to replace these filters and dispose of the used filters is estimated to be \$55 million per year for Department of Energy (DOE) facilities.<sup>(9)</sup> Moore et al<sup>(9)</sup> estimate that \$50 million of the \$55 million annual cost is due to waste handling. By developing a cleanable steel HEPA filter, we believe that a large fraction of the waste disposal costs can be saved.

Cleanable air filtration systems are used extensively in the non-nuclear industry. For example, bag house filters and electrostatic precipitators have proven to be a cost effective means for cleaning exhaust emissions from factories. However these air cleaning systems do not have the required HEPA filter efficiency, nor the reliability for use in nuclear exhaust cleaning. Our study is an initial effort to develop cleanable steel HEPA filters for use in the nuclear industry.

## II. Cost Analysis

Moore et al<sup>(9)</sup> have completed a survey of HEPA filtration costs in the U.S. DOE facilities. They found that DOE facilities use an average of 11,500 HEPA filters per year. The average purchase, handling and disposal cost per HEPA filter is \$4,750. DOE therefore spends \$55 million per year for HEPA filters.

We used the life-cycle cost of the standard glass-paper HEPA filter to compare with the estimated life cycle cost of the steel HEPA filter as shown in Table 1. We assumed that after several years of development the cost of the steel HEPA filter, not including the cleaning system, will drop to \$5,000 (the present cost is \$50,000). We also assumed that the maintenance and disposal for both filters will be \$4,450 and that the steel HEPA filter can be cleaned repeatedly to yield an effective life of 15 times the life of a glass HEPA filter prior to disposal. The cleaning cost for the steel HEPA filter is assumed to be \$400 for the life of an equivalent glass HEPA filter, plus an initial cost of \$1,500 to retrofit the cleaning system hardware into the filter housing. The total cleaning cost for the life of the steel filter is \$7,500. Using these figures, we estimate the total annual cost to DOE is \$55M for the glass-paper HEPA filter and \$13M for the cleanable steel HEPA filter, a savings of \$42M.

Table 1. Comparison of life-cycle costs for glass-paper and stainless steel cleanable HEPA filters.

	Glass-paper HEPA	Stainless steel HEPA
Filter element (1000 ft <sup>3</sup> /min)	\$300	\$5,000 <sup>a</sup>
Installation, test, removal, and disposal	\$4,450	\$4,450
Cleaning	---	\$7,500 (15 x HEPA life)
Annual number of filters used by DOE facilities	11,500	767
Total annual costs	\$55M	\$13M

<sup>a</sup>Estimated cost for one steel HEPA filter after additional development. Current cost is \$50,000 per filter.

### III. Conceptual Design of a Cleanable Steel HEPA Filter

Our design of a cleanable steel HEPA filter follows the same design that has been used for many years in industrial applications, including a few applications in the nuclear industry. Schurr<sup>(10)</sup> described a cleanable sintered metal filter for use in hot off-gas systems from radioactive waste calciners. Kirstein et al<sup>(11)</sup> evaluated the use of cleanable sintered metal filters for filtering the exhaust from incinerators burning radioactive wastes. These cleanable stainless steel filters were used as prefilters to extend the life of HEPA filters. These filters were made from sintered powder metal and were formed into smooth tubes. They had high pressure drops [over 2 kPa (8 inches w.g.) at 2 cm/s (4 feet per minute) air velocity] and low efficiencies (about 65%) when clean. The pressure drop and efficiency increased as particle deposits formed on the filter. Our previous study<sup>(3)</sup> demonstrated that these sintered-powder filters had higher pressure drops and lower efficiencies than sintered fiber filters.

The design concept of a cleanable steel HEPA filter that we selected is illustrated in Figures 1 and 2. The filter consists of multiple filter cartridge elements connected together as shown in Figure 1. Each filter cartridge is a closed cylinder with pleated filter media. Dirty air enters the exterior of the cartridge element where the suspended particles are removed. Clean air then passes through the hollow interior and exits on the clean air side of the filter. As the dirty air is cleaned, particle deposits form on the surface of the filter and cause the pressure drop to increase. After the filter reaches a preset pressure drop, a reverse air pulse blows back through several of the filter elements to dislodge the particle deposits, which are then collected in a hopper or barrel as shown in Figure 2. In this configuration it is possible to clean a few of the filter elements while still filtering dirty air in the remaining elements. A fraction of the particle deposits that are blown off the cartridges being cleaned will be redeposited on neighboring cylinders that are operating in the filtration mode. Incomplete cartridge cleaning and redeposited dirt limit the reverse air pulse to only partial cleaning of the filter.

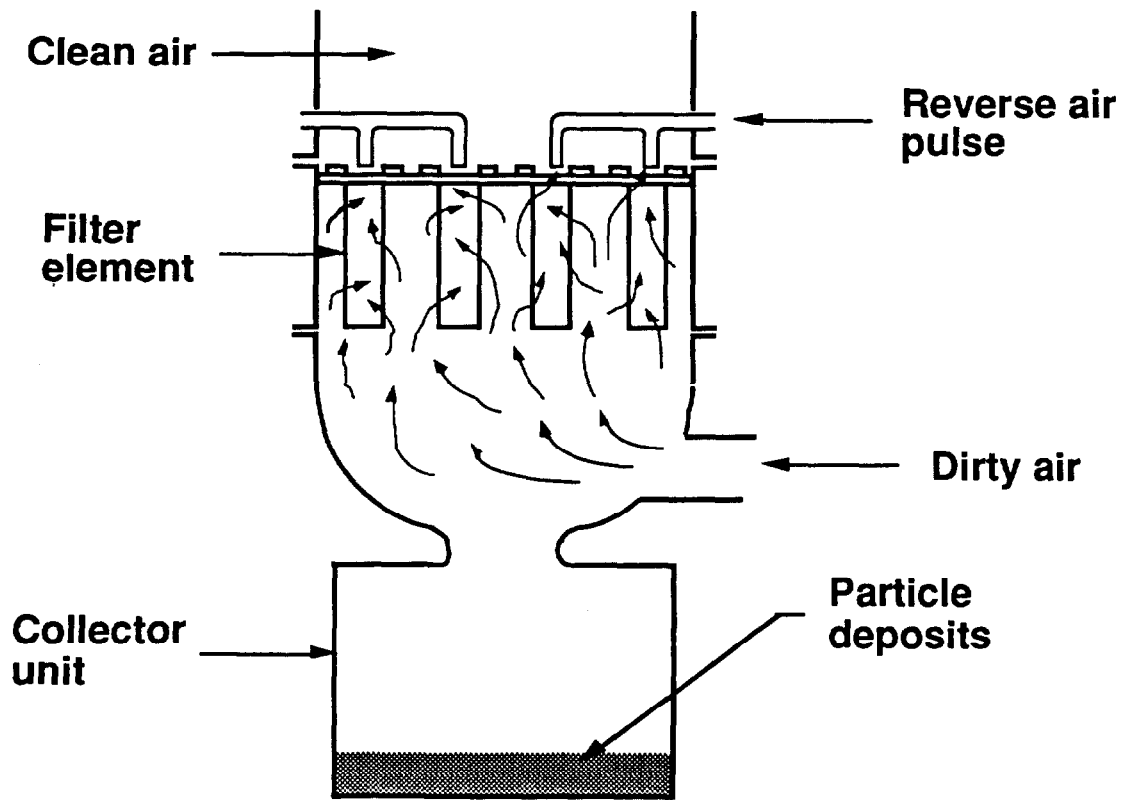


Figure 1 Filtration cycle for steel HEPA filter.

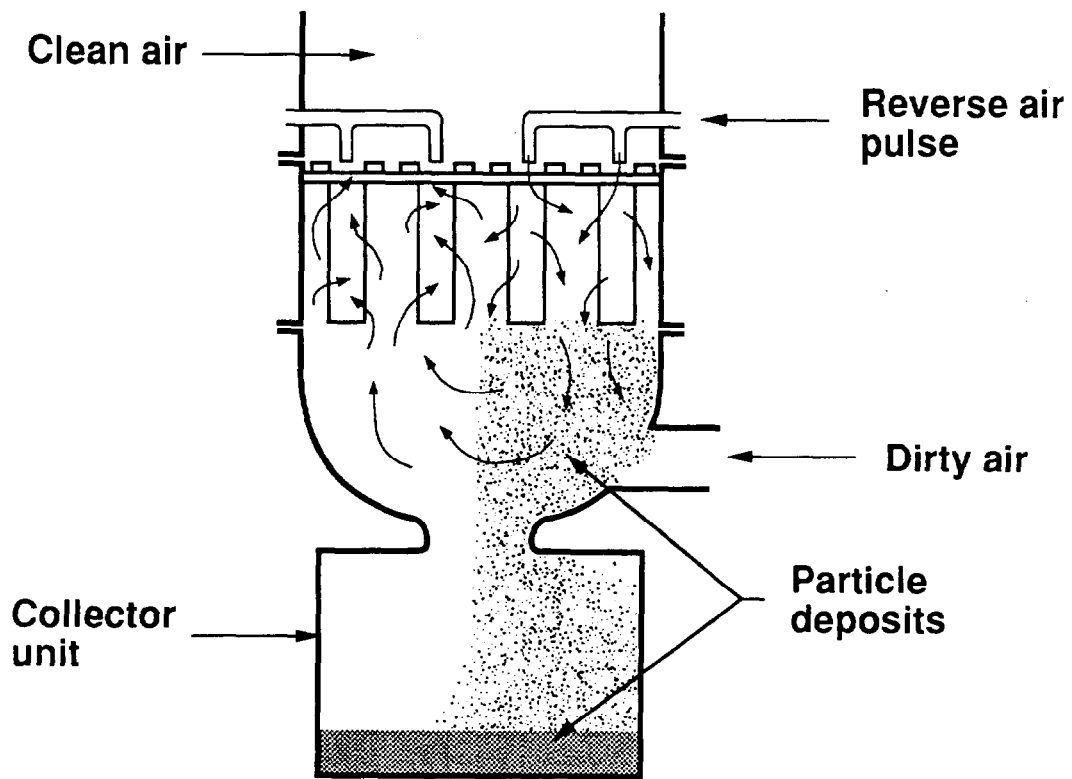


Figure 2 Cleaning cycle for steel HEPA filter.

Other filter cleaning methods can also be used in place of the reverse air pulse illustrated in Figure 2. It is possible to use liquid sprays to clean the filters. The selection of the solvent (eg. acid, base detergents, etc.) or sequence of solvents (eg. cleaning and rinsing solvents) would depend on the particular application. If liquids are used for cleaning, then a liquid handling system would be required to collect the contaminated liquid and recycle it for re-use. For extremely difficult cleaning, the filter can also be removed from the housing and washed in the appropriate liquid.

The final design concept that we incorporated into the cleanable steel HEPA filter was to package the multiple filter cartridges into the standard HEPA dimensions of 610x610x292 mm (24x24x11.5 in.). This choice of multiple filter cartridges housed in the standard HEPA frame represents the unique feature of our design. It is also possible to fabricate a steel HEPA filter using the standard HEPA designs, eg. deep pleat, mini pleat, etc., by substituting the glass fiber medium with the steel fiber medium.

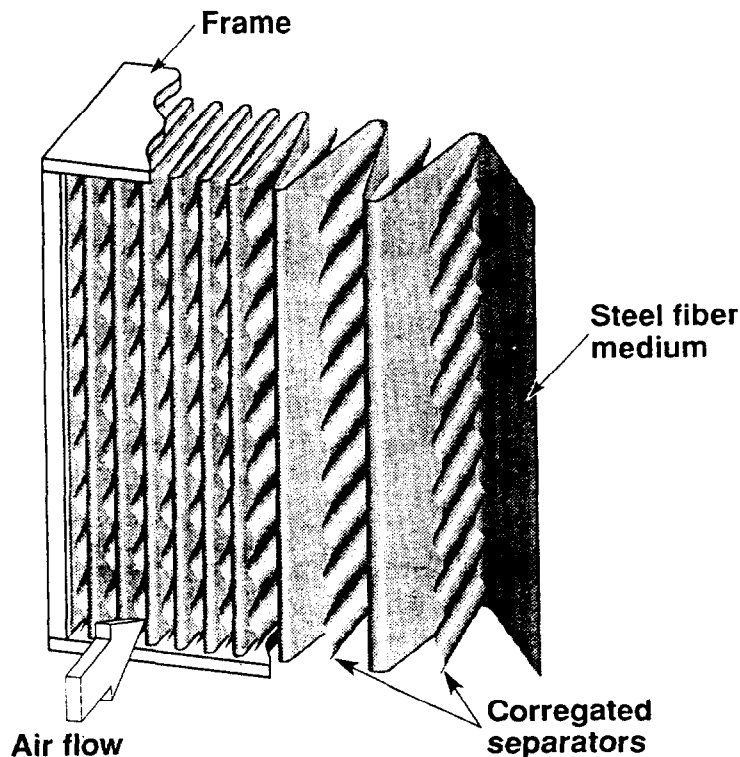


Figure 3 Cleanable steel HEPA filter in the deep pleat configuration.

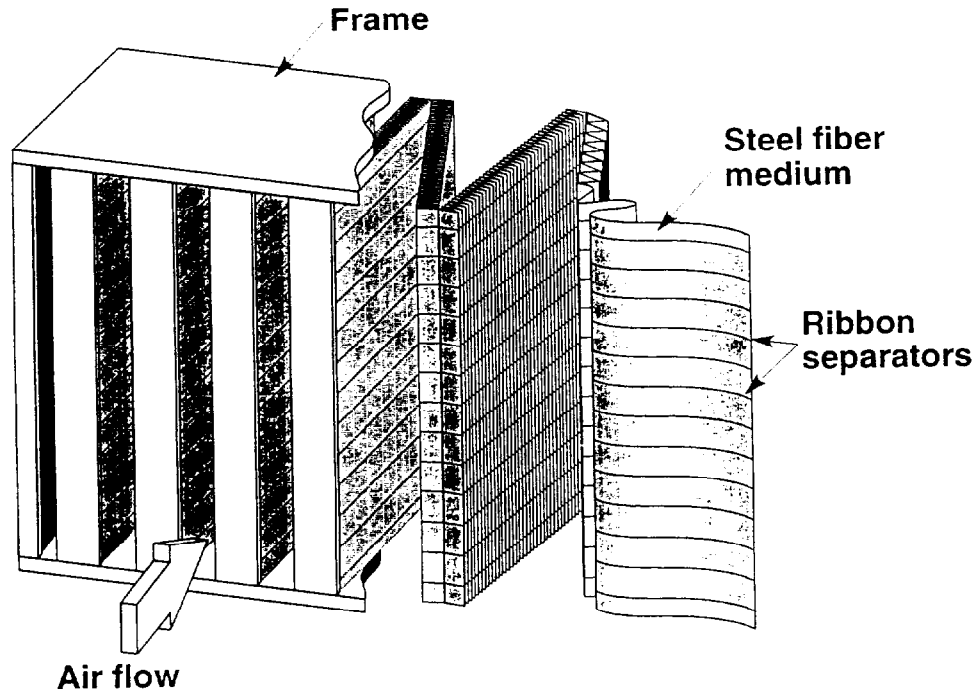


Figure 4 Cleanable steel HEPA in the mini-pleat configuration.

Figure 3 illustrates the fabrication of a cleanable steel HEPA using the standard deep pleat design with corrugated separators. Other deep pleat designs without separators are also possible.<sup>(12)</sup> The minipleat design is illustrated in Figure 4.

We selected the pleated cartridge design because it is the standard design for metal filters in the filter industry and would be the easiest to commercialize. We also believe the pleated cartridge filter with shallow pleats would be easier to clean by reverse air pulses than the deep pleated or mini pleat filter because the particle deposits would be easier to dislodge in the shallow pleats. Of course, if the filter is removed from the housing, it is possible to remove deposits from any filter design with the proper selection of cleaning agents.

#### IV. Optimization of the Cleanable Steel Filter

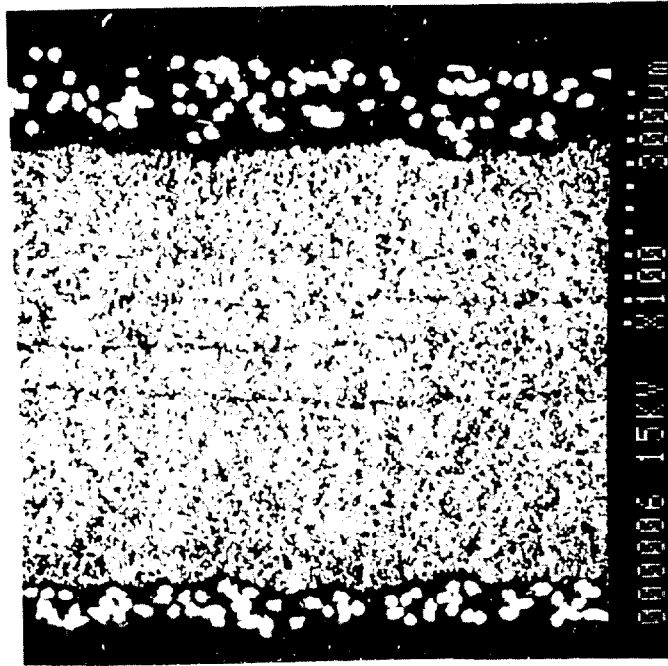
We optimized the pleated cartridge design through a combination of experiments and theoretical analysis. Pleating the media in a cartridge maximizes the surface area contained within the filter box. Our objective was to have a filter that met the efficiency requirement of a HEPA filter (99.97% for 0.3  $\mu\text{m}$  DOP aerosols) and

Detail



H  
4μm

Overall



H  
60μm

Figure 5. Cross section of the Pall Steel fiber medium used in our study.

also have the lowest possible pressure drop. We already knew from our previous studies<sup>(3)</sup> that the steel fiber media we had developed with industry had the same efficiency as the glass fiber HEPA media, but with three times the pressure drop. Figure 5 shows a cross section of the Pall filter medium that was used in our study.

We developed a mathematical model that showed variations of pleat depth, pleat width, cylinder diameter, number of cylinders and the total filter area. Our preliminary analysis showed that for the available filter media, we could only package 13.9 m<sup>2</sup> (150 ft<sup>2</sup>) into the standard HEPA frame. In contrast, a standard glass fiber HEPA filter uses over 18.6 m<sup>2</sup> (200 ft<sup>2</sup>) of media.

We then used our mathematical model (Figure 6) to show all possible variations of pleat depth, pleat width, and number of pleats to yield 13.9 m<sup>2</sup> (150 ft<sup>2</sup>) of area. Using that model, we selected three different combinations of the three parameters as indicated by A, B, and C in Figure 6 for fabricating experimental filters. Another important factor in the optimization was the number of cartridges to be used in the prototype filter; fewer cartridges would simplify the cleaning process. Figure 7 shows the number of cartridges as a function of pleat width and pleat depth and the three combinations of parameters used in Figure 6. We fabricated three different filter cartridges using the specifications given by A, B, and C. Figure 8 shows cartridge A.

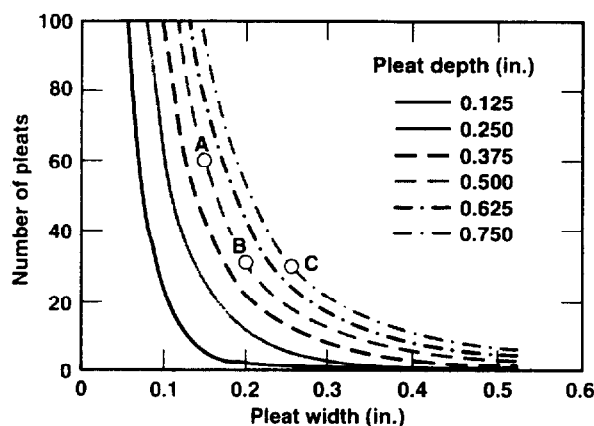


Figure 6 Possible combinations of pleat depth, pleat width, and number of pleats to yield 13.9 m<sup>2</sup> (150 ft<sup>2</sup>) of area. We selected the combinations indicated by A, B, and C for fabricating three different filter cartridges.

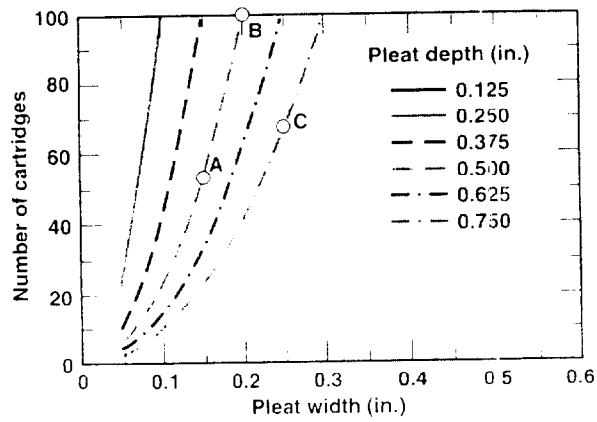


Figure 7 Calculation of number of cartridges to be used in the prototype filter, based on the parameters chosen from Figure 6.

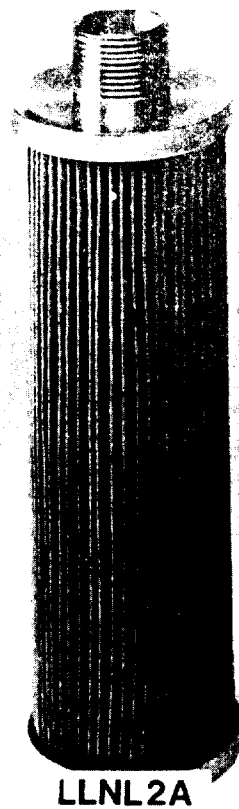


Figure 8 Filter cartridge A.

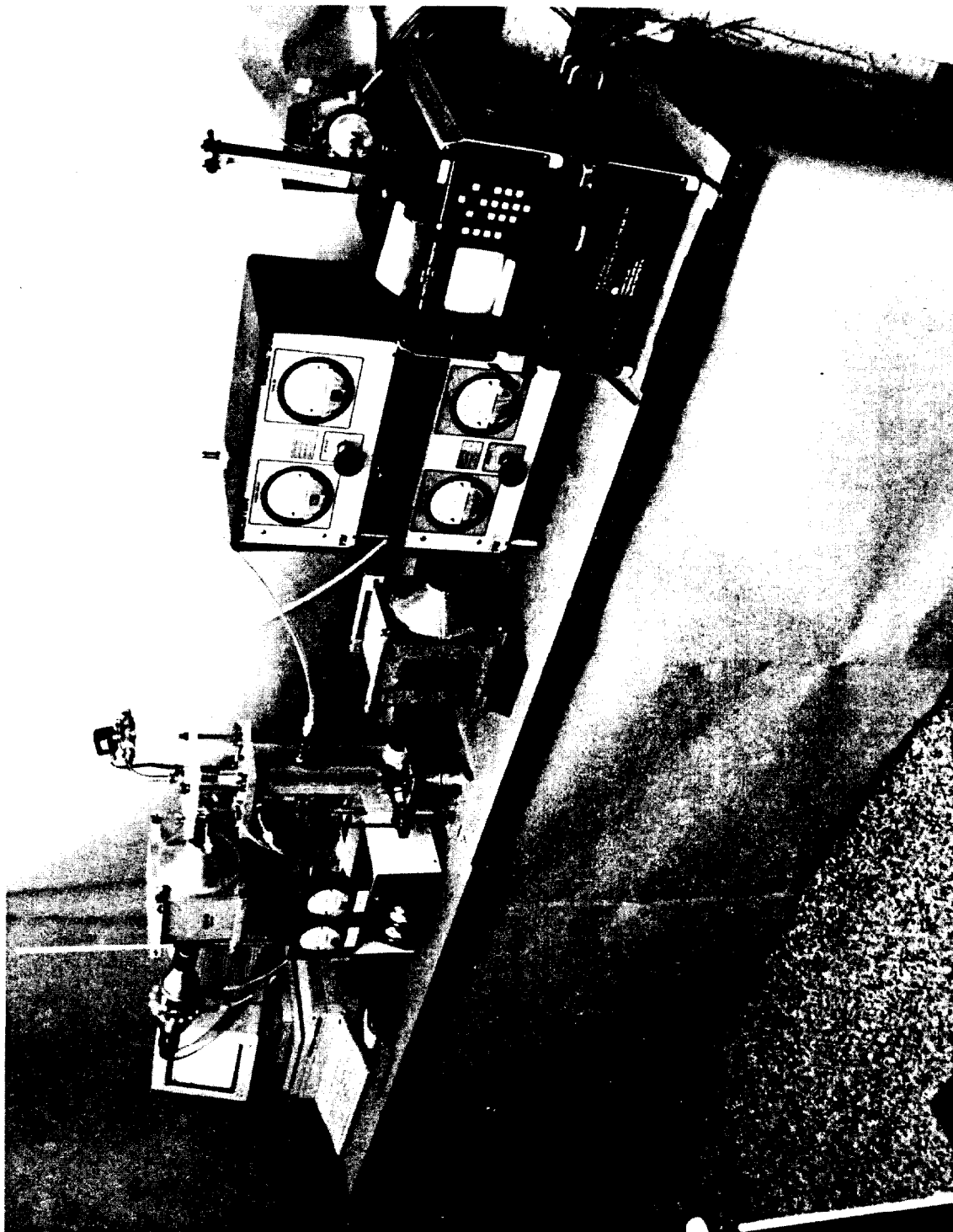


Figure 9 Test apparatus for studying filter efficiency and cleaning.

We tested the three filter cartridges for efficiency and cleaning using the test apparatus shown in Figure 9. We used a laser particle counter, model HS LAS-32, from Particle Measuring Systems (PMS) for the filter efficiency measurements. Details of the filter efficiency test were described in our previous report<sup>(3)</sup>. The cartridges were cleaned by applying a reverse air pulse on the filter to dislodge the particle deposits. Pleat geometry seemed to have minimal effect on the efficiency of the cartridges; all three had efficiencies of about 99.97%. However, pleat depth had a definite impact on the ability to clean the cartridge; the one with the deepest pleat (1.9 cm, 0.75 in.) had a higher relative pressure drop after loading and cleaning, and also had a faster loading rate than either of the other two cartridges. It is possible that the poor results obtained with the filter cartridge having the deepest pleat were partly due to the individual pleats being blinded because they were not properly spaced apart. We did not use a support screen in our model filters as is the common practice in industry. However, even if the additional wire screen would keep the media pleats from touching, the screens would be touching and make filter cleaning more difficult than wider spaced pleats. Optimizing the filter design with respect to filter cleaning will require more work than was possible in this study.

Using the data generated for the three filter cartridges and the curves in Figure 6, we calculated specifications that would give the desired efficiency and pressure drop, and also have the minimum number of cartridges to yield 13.9 m<sup>2</sup> (150 ft<sup>2</sup>). These specifications [pleat depth = 1.27 cm (0.5 in.), pleat width = 0.64 cm (0.25 in.), and 32 pleats] were given to Pall Corp. and Memtec Corp., who built prototype cartridges for testing. With these cartridge specifications, the cleanable steel filter would have an array of 64 cartridges.

### V. Filter Cartridge Performance

We conducted filter efficiency and cleaning tests on the prototype cartridges. The efficiency test consisted of measuring the particle concentration as a function of size using the PMS laser shown in Figure 9. We used dioctyl sebacate (DOS) aerosols generated by a Laskin nozzle in our efficiency tests so that direct comparisons could be made with the official DOP certification test.<sup>(1)</sup> A close-up of the filter test housing is shown in Figure 10. The filter test housing consists of three chambers: a lower chamber that functions as a hopper to collect particle deposits, a middle chamber that houses the filter cartridge and an upper chamber that has the reverse air pulse system. Challenge air enters into the lower part of the middle

chamber, passes through the filter cartridge into the upper chamber and then leaves through an exit port shown in the upper left of Figure 10. Sampling probes for the filter efficiency measurements can be seen in the middle and upper chambers. The differential pressure probes are also shown near the plate separating the upper and middle chambers.

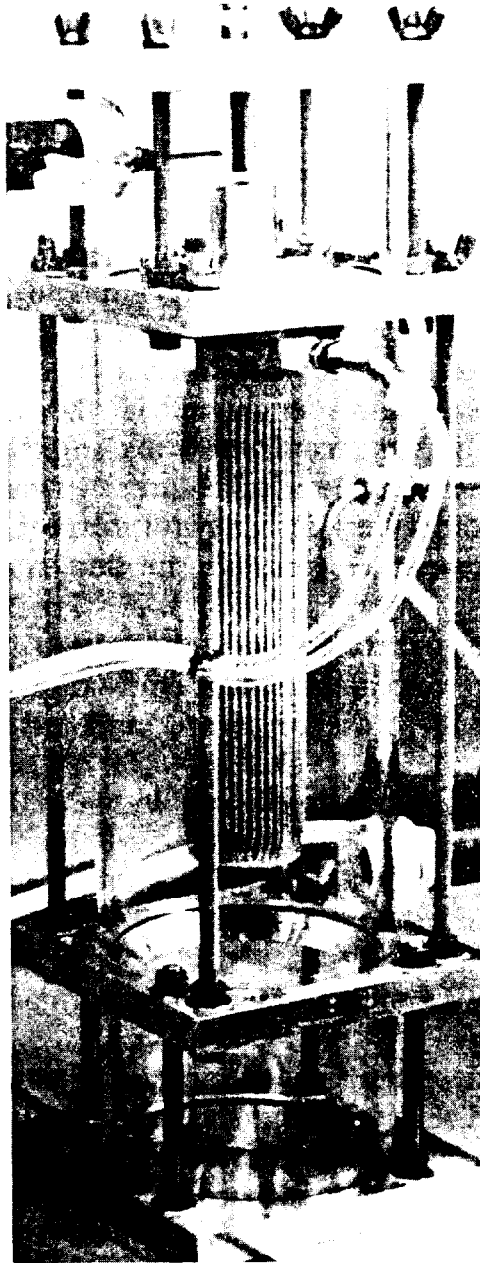


Figure 10 Filter test housing used for efficiency and cleaning tests.

Figure 11 shows the results of our efficiency measurements on one of the 64 Pall filter cartridges tested at  $26.5 \text{ m}^3/\text{hr}$  (15.6 cfm).

This flow rate corresponds to the fraction of the total flow at 1,700 m<sup>3</sup>/hr (1,000 cfm) through one of the 64 filter cartridges. The maximum penetration at 0.17 μm diameter is 0.05%. However, at 0.3 μm diameter the penetration is only 0.01%. The remaining Pall filter cartridges gave similar results. Since the DOP certification test allows a penetration up to 0.03%, the steel filter will easily pass the test. Unfortunately the pressure drop at 0.82 kPa (3.3 inches w.g.) is too high to qualify the steel filter as a HEPA filter according to MIL-F-51068.<sup>(2)</sup> The Memtec filter cartridges were also tested and gave similar results. Further development is required to reduce the pressure drop.

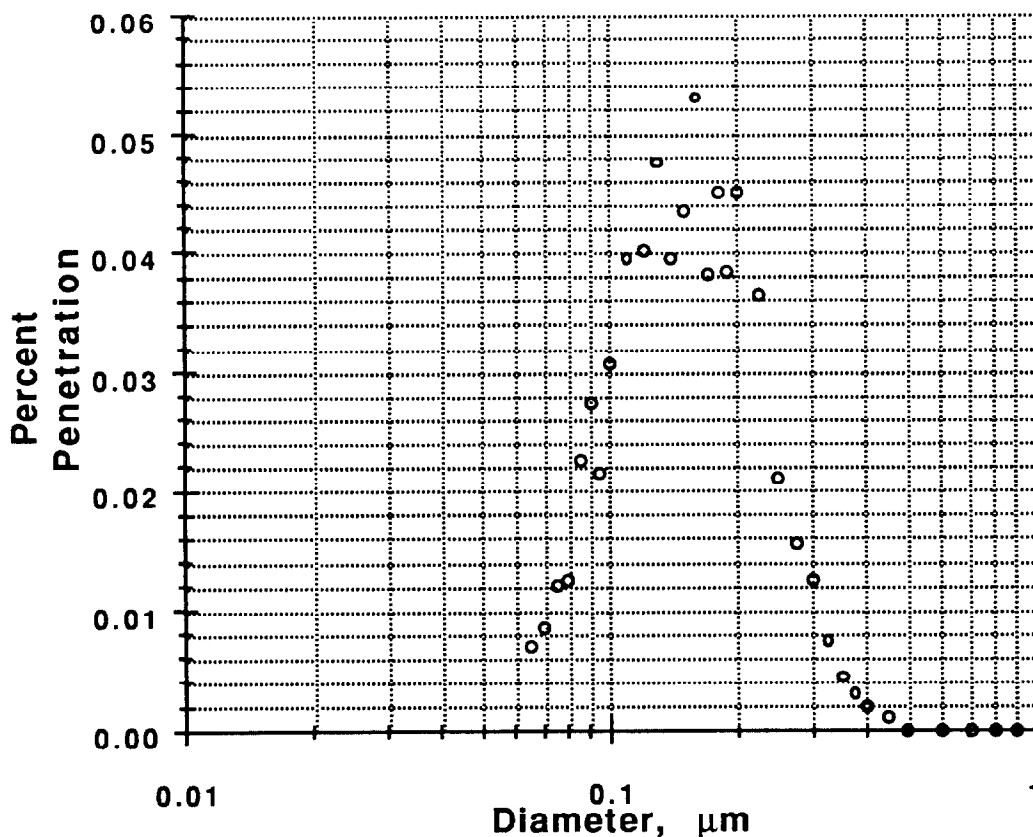


Figure 11 Penetration of DOS aerosols as a function of particle size through Pall filter cartridge.  $\Delta P = 0.82$  kPa (3.3 in. w.g.) at 26.5 m<sup>3</sup>/hr (15.6 cfm).

For the filter cleaning tests, we set up a reverse air pulse system consisting of a dust generator for accelerated filter plugging,

a single cartridge housing, and a solenoid-actuated reverse air pulse. The experimental apparatus is shown in Figures 9 and 10. We used AC Fine dust in our filter cleaning tests, since it represents a similar, although more severe, challenge compared to the uranium oxide dust measured in the Y-12 Plant. The filter cleaning test consists of loading the cartridge with dust until the pressure drop across the cartridge reaches 1.7 kPa (7 in. of water). At that point, the pressure solenoid valve is automatically opened and the air pulse blows off the particle deposits. In separate tests, we determined that the optimum cleaning pulse is 0.6 seconds at 276 kPa (40 psig).

The results from a sequence of 19 filter clogging and cleaning cycles are shown in Figure 12. The breaks in the clogging and cleaning cycles occurred when the aerosol generator was depleted. We estimate that about three glass HEPA filters would be clogged during a similar particle challenge. Since the glass HEPA filters cannot be cleaned, the corresponding test with glass HEPA filters would require about three filter replacements. We have conducted up to 100 filter clogging and cleaning cycles on a single steel cartridge, which corresponds to an equivalent service life of about 15 glass HEPA filters.

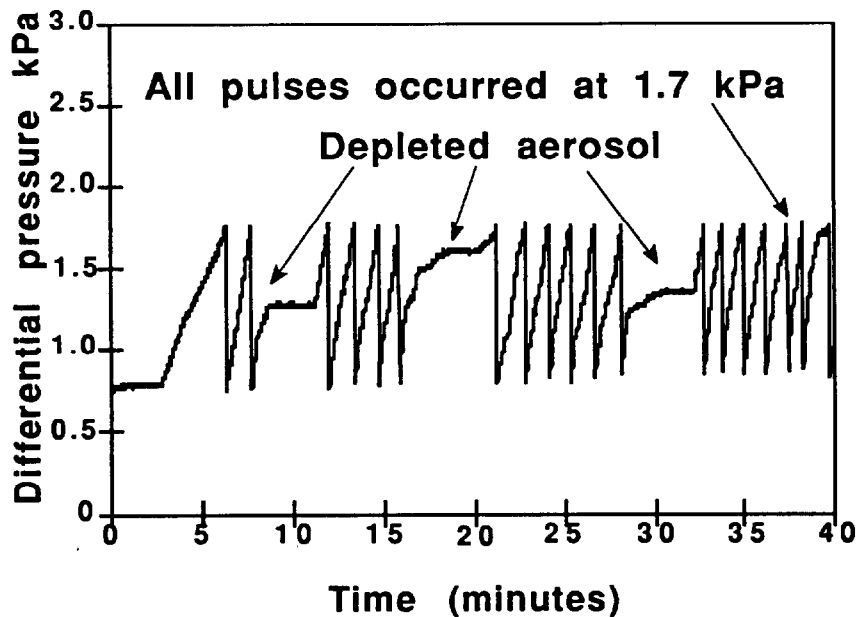


Figure 12 Results from a sequence of 19 clogging and cleaning cycles using one steel filter cartridge from Pall. About three glass filters would be needed for similar challenge.

IV. Fabrication and Evaluation of Cleanable Steel Filter

Fabrication

After verifying the performance of the Pall and Memtec filter cartridges, we completed the design and fabrication of the cleanable steel filter. Figure 13 shows one of the filter cartridges from Pall Inc. and Memtec Inc.. Note the threaded end on the filter cartridges. The individual filter cartridges are threaded into an end plate of a 610x610x292 mm (24x24x11.5 in.) housing. Figure 14 is a photograph of the assembled cleanable steel filter contains 64 Memtec cartridges. The weight of the fully assembled filter containing the Pall and Memtec cartridges were 102 kg (225 pounds) and 95 kg (210 pounds) respectively. Figure 15 shows a close up of a second steel filter containing Pall cartridges.

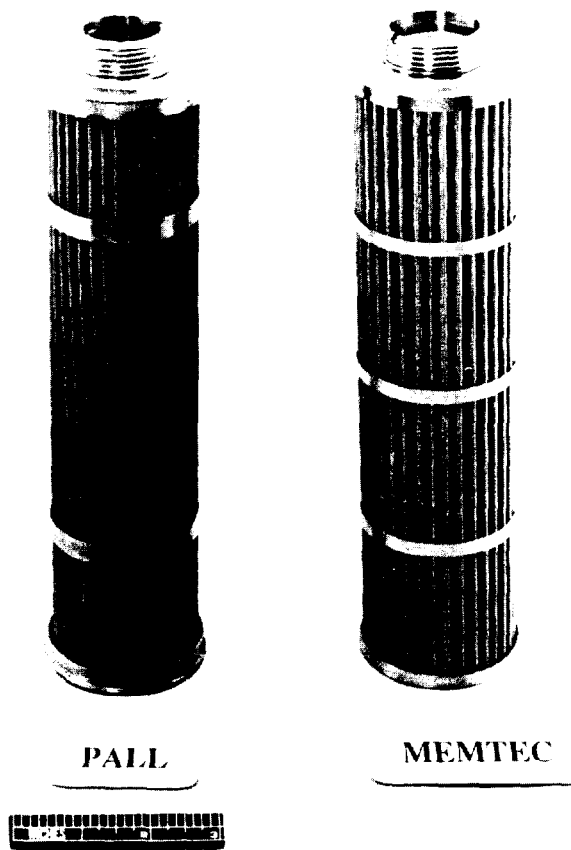


Figure 13 Filter cartridges from Pall and Memtec

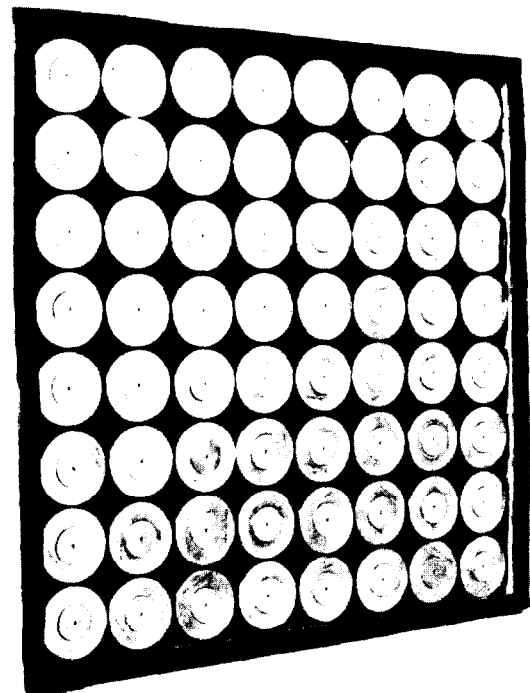


Figure 14 Photograph of the assembled cleanable steel filter with 64 Memtec cartridges.

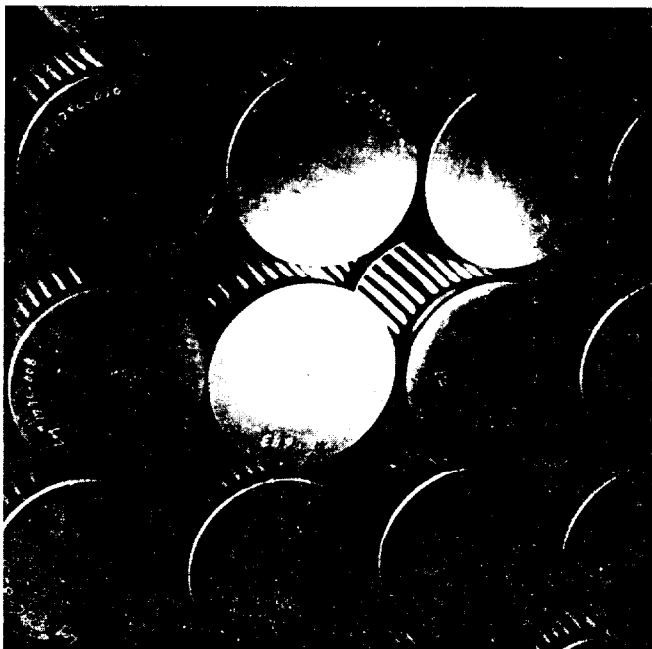


Figure 15 Close up of the filter cartridges from Pall Corp. in the assembled filter.

### Penetration Measurements

We installed the filter in our 1,700 m<sup>3</sup>/hr (1,000 cfm) test duct as shown in Figure 16 and measured the penetration with DOS aerosols, using the same laser particle counter used in our cartridge tests. To generate sufficient DOS challenge in the 1,700 m<sup>3</sup>/hr (1,000 cfm) test duct, we used an aerosol generator having six Laskin nozzles (Phoenix Precision). Figure 17 shows the percent penetration of DOS as a function of particle diameter for the steel filter with Pall cartridges. The filter has a maximum penetration of 0.115% at 0.17 μm diameter but still meets the requirement of less than 0.03% penetration at 0.3 μm diameter as required by the DOP certification test.<sup>(1)</sup> As we noted previously, the pressure drop at 0.77 kPa (3.1 inches w.g.) is too high to qualify the cleanable steel filter as a HEPA filter according to MIL-F51068.<sup>(2)</sup>

The penetration measurements for the cleanable steel filter using Memtec cartridges is shown in Figure 18. The penetration is 0.046% at 0.17 μm diameter and 0.01% at 0.3 μm diameter and therefore meets the requirements of MIL-F-51068.<sup>(2)</sup> However the pressure drop is too high at 0.77 kPa (3.1 inches of water) to qualify as a HEPA filter.

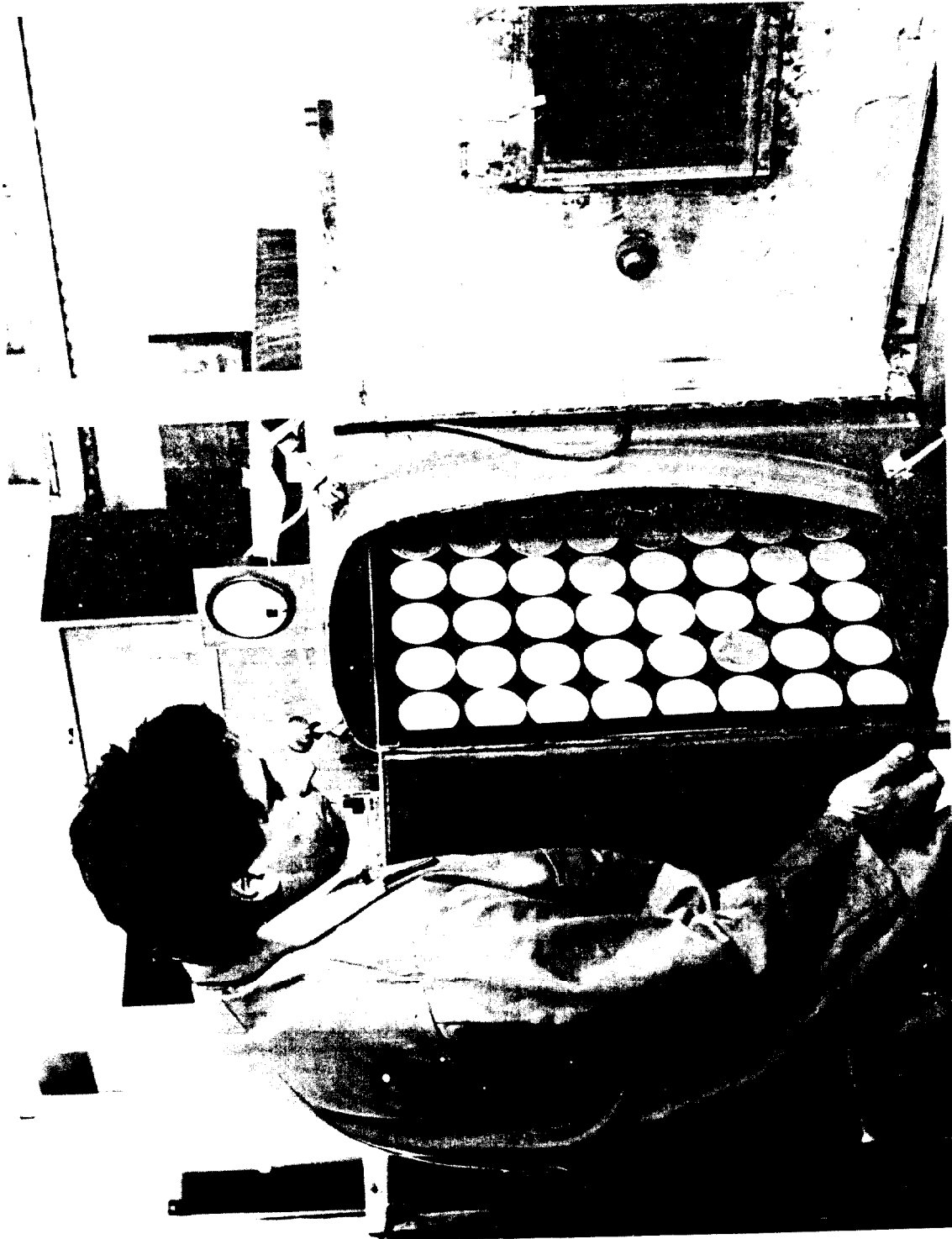


Figure 16 Installation of cleanable steel filter in 1,700 m<sup>3</sup>/hr (1,000 cfm) test duct.

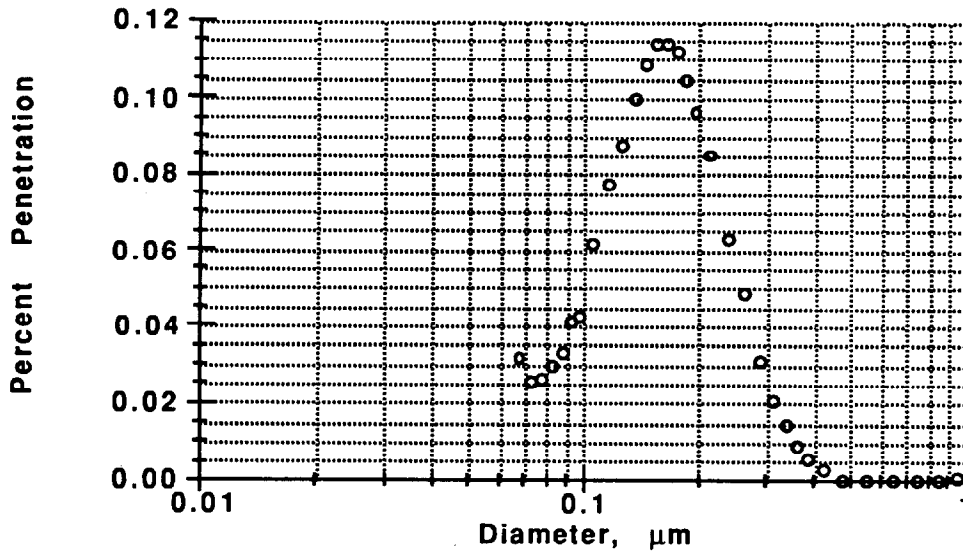


Figure 17 Penetration of DOS aerosols as a function of particle diameter through a cleanable steel filter using Pall cartridges.  $\Delta P = 0.77$  kPa (3.1 in. w.g.) at  $1,700$  m<sup>3</sup>/hr (1,000 cfm).

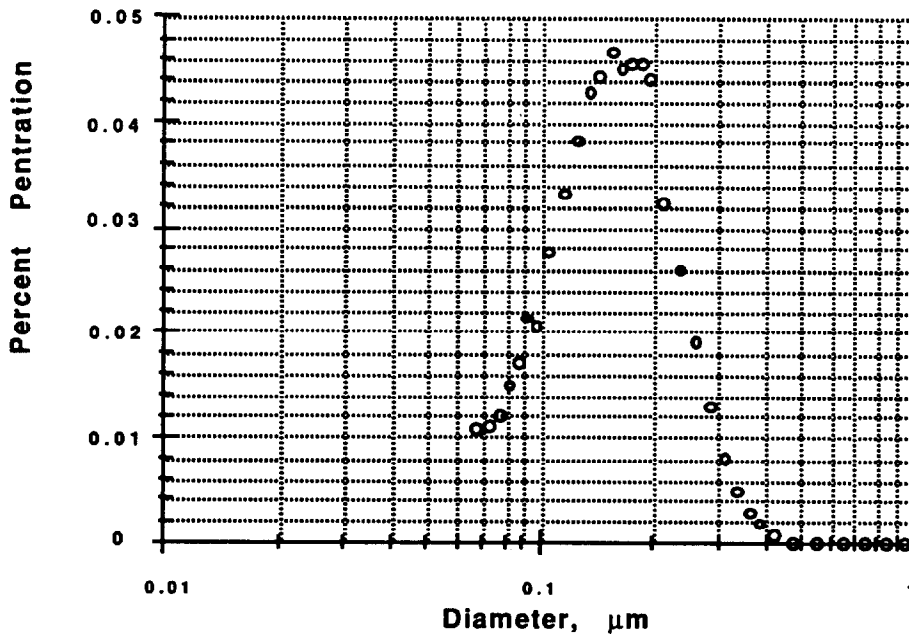


Figure 18 Penetration of DOS aerosols as a function of particle diameter through a cleanable steel filter using Memtec cartridges.  $\Delta P = 0.77$  kPa (3.1 in. w.g.) at  $1,700$  m<sup>3</sup>/hr (1,000 cfm).

We also had the two steel filters tested using the official DOP HEPA certification test.<sup>(1)</sup> The filters were tested at the DOE filter certification laboratory in Oak Ridge, TN. Test results show the DOP penetration was 0.01% for both the filter with Pall cartridges and the filter with Memtec cartridges when tested at 1,700 m<sup>3</sup>/hr (1,000 cfm). The corresponding pressure drops were 0.80 kPa (3.2 inches w.g.) for the Pall filter and 0.72 kPa (2.9 inches at w.g.) for the Memtec filter.

### Cleanability Tests

After establishing the filter efficiency, we ran a series of tests to establish the cleanability of the filter. These tests were similar to the small scale tests described previously for the individual filter cartridges. However to evaluate the cleanability of the entire filter consisting of 64 cartridges, we used a filter housing and blower assembly that we designed and built for use in our field demonstration at the Y-12 Plant in Oak Ridge, TN.

The filter housing and blower assembly, shown in Figure 19, is an independent filtration system for demonstrating the performance of the cleanable steel filter. The housing assembly was designed to meet seismic and mechanical safety standards. A photograph of the assembly is shown in Figure 20. The housing assembly will pull exhaust from the uranium grit blaster at the Y-12 Plant through the entrance pipe shown on the right side of the figures. The radioactively contaminated exhaust will then be passed through filters, first through the cleanable steel filter and then through a conventional glass filter, before exiting through the exhaust pipe at the top of the housing assembly. The clean exhaust is then passed through a variable speed blower and discharged into an existing baghouse filter at the Y-12 Plant. Figure 21 shows the steel filter, being inserted into the housing with the aid of a support table. Since the steel filter weighs about 100 kg (220 pounds), it is not possible to manually install the filter as is done with standard HEPA filters. However with further development, we estimate that the weight can be reduced to 41 kg (90 pounds) and allow manual installation of the filter.

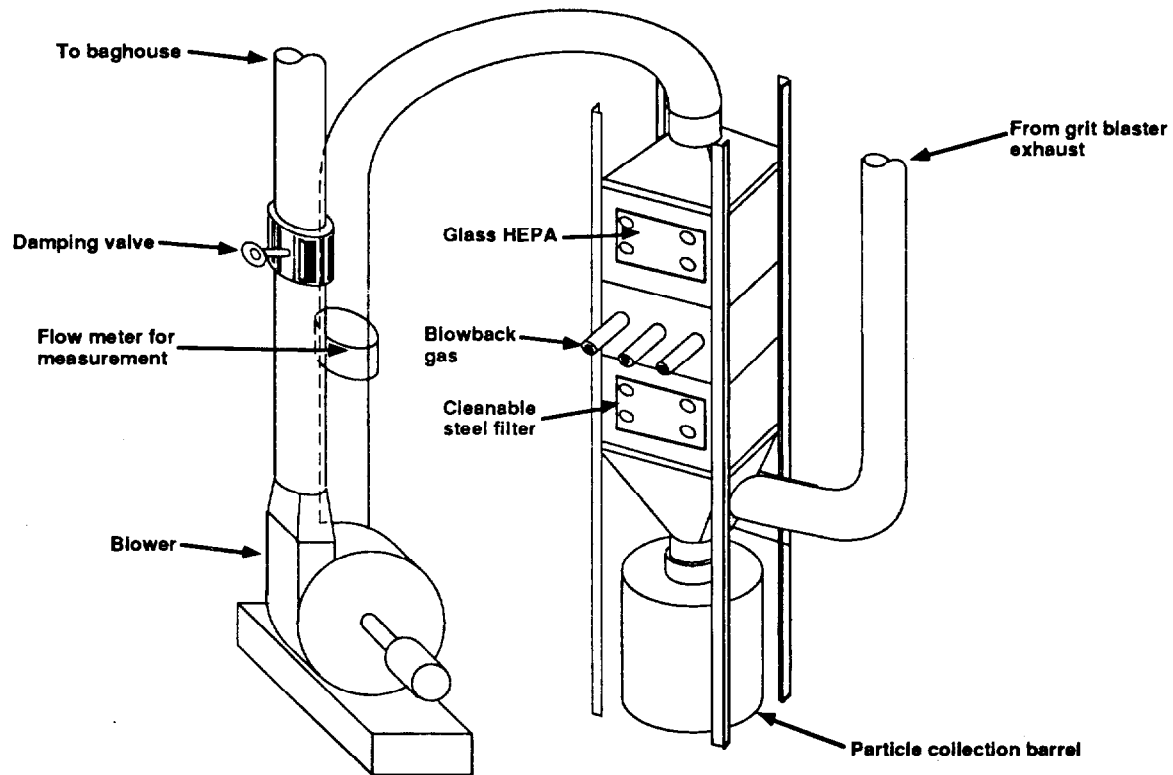


Figure 19 Design of the filter housing and blower assembly for a field test at the Y-12 Plant.

The filter-cleaning system is mounted inside the filter housing assembly between the steel filter and the glass HEPA filter. This cleaning system consists of 64 individual nozzles and solenoids to generate reverse air pulses for each of the filter cartridges. We initially evaluated various manifold combinations (primarily four- and eight-nozzle configurations), but none proved satisfactory. The filter-cleaning tests on the single cartridge tester shown in Figure 10 were not successful using the manifold configurations, apparently due to poor flow distribution and lack of an adequate shock wave. Because of time constraints, we abandoned the manifold design and used a separate air pulse line for each of the 64 cartridge filters. This system is overly complex, expensive and prone to failures. An efficient filter cleaning system is another area for further development.

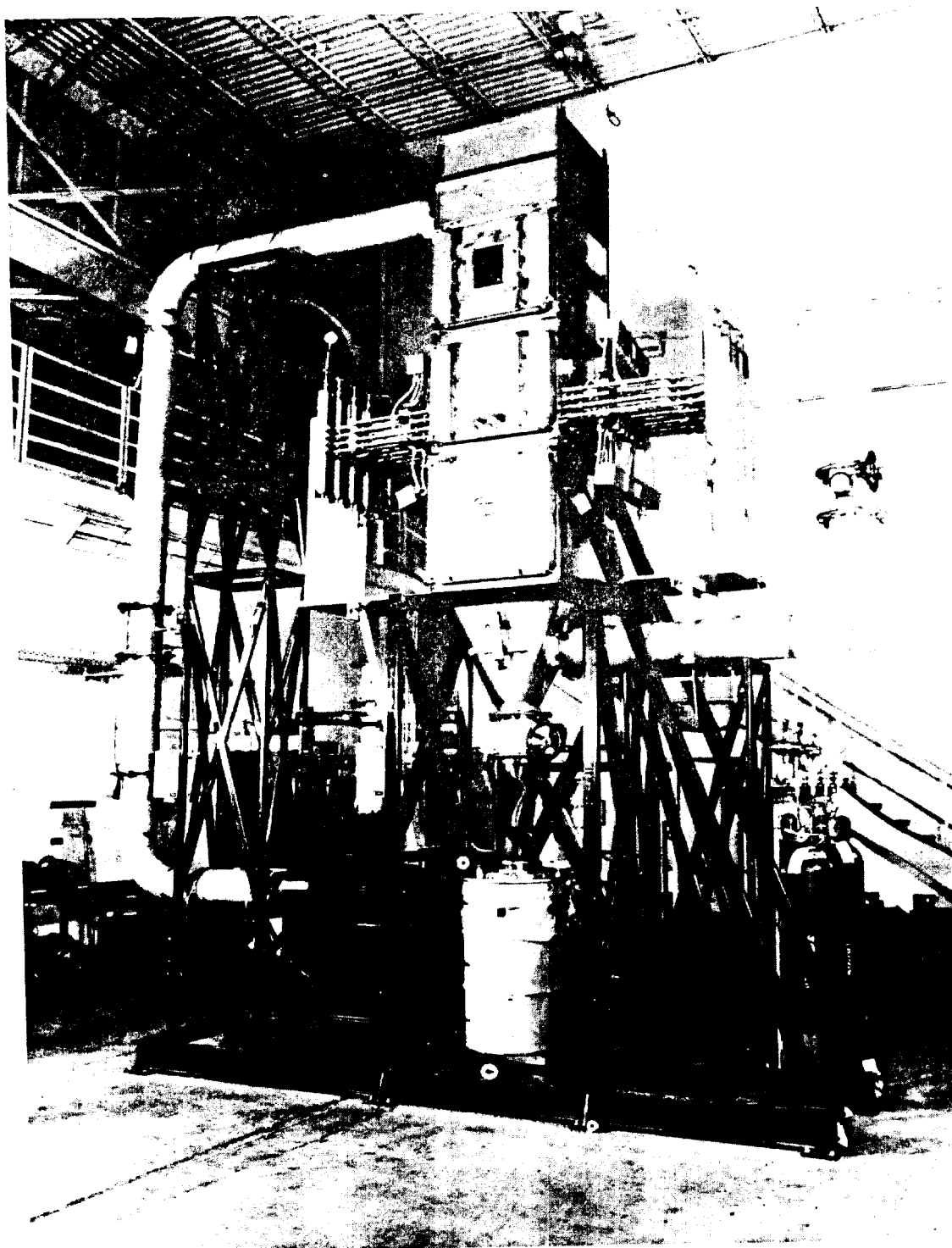


Figure 20 Photograph of the filter housing and blower assembly.



Figure 21 Cleanable steel filter being inserted into filter housing.

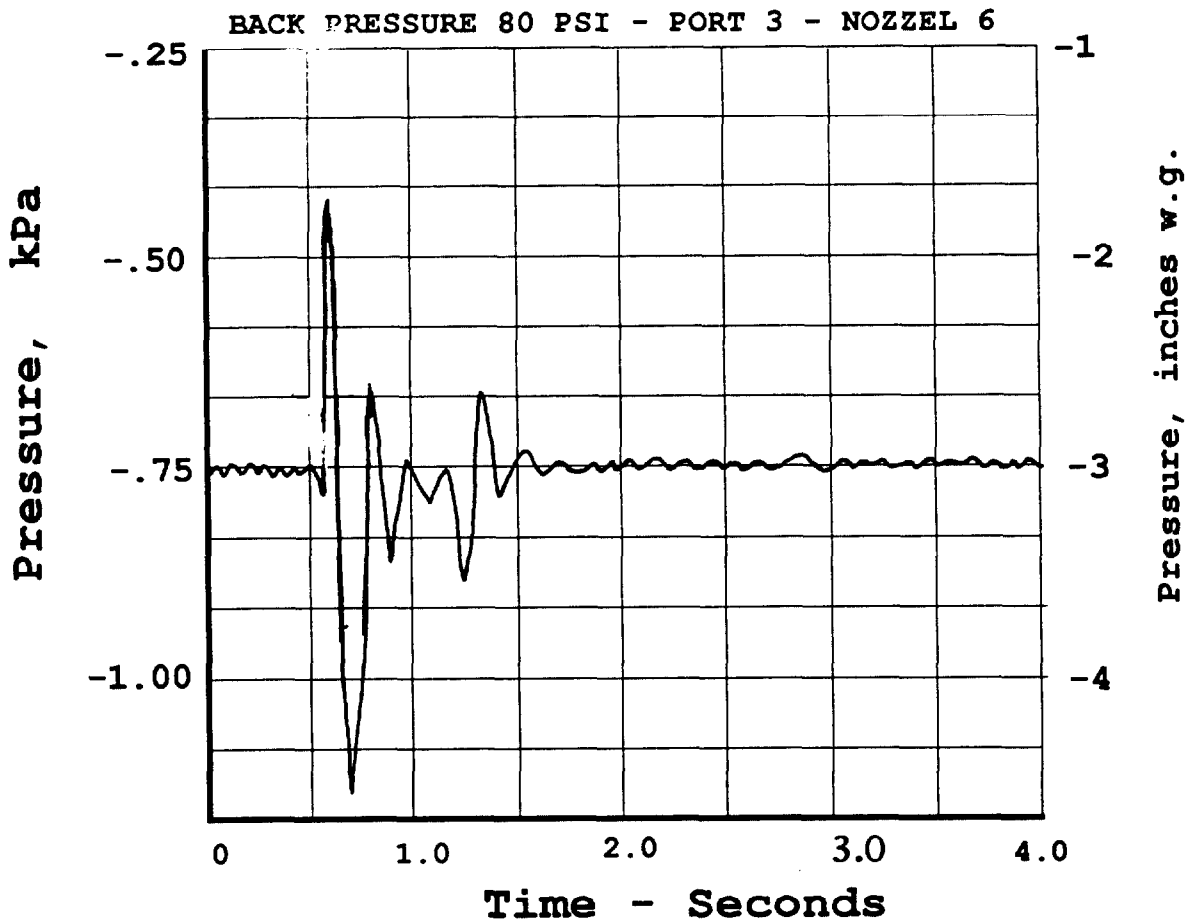


Figure 22 Transient pressure measurements inside filter housing during reverse air pulse.

We then conducted filter cleaning tests that consisted of a series of filter clogging and cleaning cycles. We used AC Fine dust (Powder Technology Inc.) in these tests as was done previously with the individual cartridges. The results of our cleaning tests are shown in Figure 23. Note that the filter pressure drop after each cleaning is only reduced to 1.4 kPa (5.5 inches w.g.). This increased pressure drop (compared to the clean filter) shows that we are not able to remove all of the particle deposits during a cleaning cycle as was done in our single cartridge tests. The deposits that remain on the filter cartridge after pulse cleaning is due to the lower cleaning efficiency of the air pulses in the multi cylinder unit and due to the redeposition of particles blown off one cartridge onto another cartridge. Figure 24 shows that the steel filter has a significant particle deposit that remains after this pulse cleaning. The filter cleaning system requires further development.

We then conducted filter cleaning tests that consisted of a series of filter clogging and cleaning cycles. We used AC Fine dust (Powder Technology Inc.) in these tests as was done previously with the individual cartridges. The results of our cleaning tests are shown in Figure 23. Note that the filter pressure drop after each cleaning is only reduced to 1.4 kPa (5.5 inches w.g.). This increased pressure drop (compared to the clean filter) shows that we are not able to remove all of the particle deposits during a cleaning cycle as was done in our single cartridge tests. The deposits that remain on the filter cartridge after pulse cleaning is due to the lower cleaning efficiency of the air pulses in the multi cylinder unit and due to the redeposition of particles blown off one cartridge onto another cartridge. Figure 24 shows that the steel filter has a significant particle deposit that remains after this pulse cleaning. The filter cleaning system requires further development.

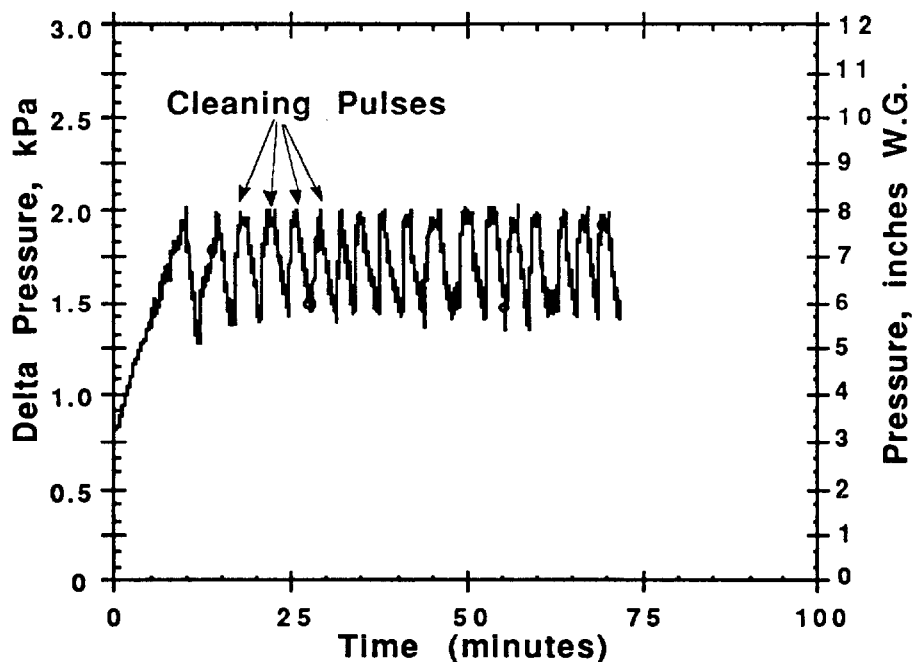


Figure 23 Filter clogging and cleaning cycles for steel filter.

After completing these clogging and cleaning tests, we ran a filter clogging test using a standard glass HEPA filter in the same filter housing. Comparing the two test results show that the 18 cleaning cycles in Figure 23 corresponded to an equivalent clogging of three glass HEPA filters. These test results gave us confidence that the steel filter could easily provide an equivalent life of 15 standard glass HEPA filters.



Figure 24 Photograph of steel filter after 18 clogging and cleaning cycles.

### VII. Y-12 Demonstration

After completing the evaluation tests at LLNL, we disassembled the filter housing and blower assembly and shipped the unit to the Y-12 plant in Oak Ridge, TN for installation in the exhaust of a uranium grit blaster. This is a facility where the surface of uranium parts are cleaned by blasting with a grit. Design and safety engineers had made extensive preparations for the installation for approximately one year prior to shipping the unit: the filtration hardware and operating system were reviewed, a concrete pad was built to support the filter housing and blower assembly, and auxiliary ducting was cut into the existing exhaust system. The existing filtration systems consisted of a bag house prefilter followed by a bank of six, single-stage HEPA filters to accommodate the 10,200 m<sup>3</sup>/hr (6,000 cfm) exhaust. A 1,700 m<sup>3</sup>/hr (1,000 cfm) slip stream is extracted from the exhaust of the grit blaster, routed through the cleanable steel filter housing and exhausted back into the bag house filter.

Measurements of the particle emissions show that the average size of the uranium oxide particles is approximately 50  $\mu\text{m}$ . This is much larger than our AC Fine dust, which had an average size of

approximately 8  $\mu\text{m}$ . Given that we have already proven we can load and clean the smaller test particles, we are confident that we will be able to load and clean the much larger particles at the Y-12 Plant. We currently have tests under way to determine the performance of the cleanable steel filter in this application.

### VIII. Conclusion

We have developed a cleanable steel filter that has 0.01% DOP penetration and a pressure drop of 0.72-0.80 kPa (2.9 - 3.2 inches w.g.) at 1,700  $\text{m}^3/\text{hr}$  (1,000 cfm). Although the steel filter cannot meet the pressure requirement for a HEPA filter specified in MIL-F-51068, it can be used in place of HEPA filters for applications not sensitive to the higher pressure drop. Further research and development is needed to reduce the pressure drop and optimize the filter design and the cleaning system. The fact the filter can be repeatedly cleaned and reused will result in significant cost savings.

### IX Acknowledgement

This work was supported by DOE's Office of Technology Development, EM-50.

### X References

- (1) U.S. Military Standard MIL-STD-282, Filter Units Protective Clothing, Gas-Mask Components and Related Products: Performance Test Methods.
- (2) U.S. Military Standard MIL-F-51068, Filters, Particulate (High-Efficiency Fire Resistant)
- (3) Bergman, W., Conner, J. Larsen, G., Lopez R., Turner, C., Valha, G., Violet, C., and Williams, K. "High efficiency steel filters for nuclear air cleaning" Proceeding of the 21st DOE/NRC Nuclear Air Cleaning Conference NUREG/CP-01116, CONF-900813, Superintendent of Documents, U.S. Govt. Printing Office, Washington, D.C., pp 733-761, 1991.
- (4) Dillmann, H.G., and Pasler, H. "Experimental investigation of aerosol filtration with deep bed fiber filters" in Proceedings of the 17th DOE Nuclear Air Cleaning Conference, CONF-820833, NTIS, Springfield, VA, pp 1160-1174, 1983.

## 22nd DOE/NRC NUCLEAR AIR CLEANING AND TREATMENT CONFERENCE

- (5) Dillman, H.G., and Pasler, H. "A filter concept to control airborne particulate releases due to severe reactor accidents and implementation using stainless-steel fiber filters" in Proceedings of the 18th DOE Nuclear Airborne Waste Management and Air Cleaning Conference, NTIS, Springfield, VA, CONF-840806, pp 1417-1428, 1985.
- (6) Dillmann, H.G., Bier, W., Linder, G., and Schubert, K., "Measurements of removal efficiencies performed on powder metal and fiber metal cartridges to be used in uranium enrichment facilities and glovebox exhaust ducts" in Proceedings of the 19th DOE/NRC Nuclear Air Cleaning Conference, NTIS, Springfield, VA, CONF-860820, NUREG/CP-0086, pp 392-407, 1987.
- (7) Klein, M. and Goossens, W.R. A. "Aerosol filtration with metallic fibrous filters" in Proceedings of the 17th DOE Nuclear Air Cleaning Conference, NTIS, Springfield, VA, CONF-820833, pp 504-522, 1983.
- (8) Randhahn, H., Gotlinsky, B., and Tousi, S., "The development of all metal filters for use in the nuclear industry" in Proceedings of the 20th DOE/NRC Nuclear Air Cleaning Conference, NTIS, Springfield, VA, CONF-880822, NUREG/CP-0098, pp 726-748, 1989.
- (9) Moore, P., Bergman, W., and Gilbert, H., "Survey of life cycle costs of glass paper HEPA filters" in Proceedings of the 22nd DOE/NRC Nuclear Air Cleaning Conference, Denver, CO, Aug. 24-27, 1992.
- (10) Schurr, G.A. "Cleanable sintered metal filters in hot off-gas systems" in Proceedings of the 16th DOE Nuclear Air Cleaning Conference, NTIS, Springfield, VA, CONF-801038. pp 708-718, 1981.
- (11) Kirstein, B.E., Paplawsky, W.J., Pence, D.T., and Hedahl, T.G., "High efficiency particulate removal with sintered metal filters" in Proceedings of the 17th DOE Nuclear Air Cleaning Conference, , NTIS, Springfield, VA, CONF-801038, pp 719-744, 1981.
- (12) Flanders Filters Catalog showing separatorless filters like the Dimple Pleat™ and Super-Flow™ HEPA filters. Bulletins 812 and 871.

DISCUSSION

**DILLMANN:** Do you find any effect on the loading capacity and recleanability as a function of the aerosol concentration? High aerosol concentrations can quickly build up a filter cake. Do you have experience in this matter?

**BERGMAN:** If the high concentration does not result in particle coagulation, I would not expect to see a concentration effect on filter cake removal. However, if the particle concentration is so high that you have particle coagulation, the resulting particle size would increase and deposit more on the surface, which is easier to clean. Unfortunately, I have not conducted any experiments to verify those comments.

**PORCO:** Do you have a concern about reentrainment of submicrometer particles after you pulse them off? Would they stay in the air stream and then redeposit on the filter?

**BERGMAN:** The amount of redistribution of reentrained particles depends on the design of the system. The blowback system we used causes large chunks of the particle deposit to fall off while the small particles become suspended in the airstream and redeposit on a neighboring filter element. A blowback cleaning system having reversed air flow through the entire filter does not have the reentrainment problem, but requires off-line cleaning.

**MYERS:** I know these filters are to be used for HEPA applications in offgas systems and the like. Has there been any work to study or investigate their capabilities to withstand hydrogen explosions or detonations?

**BERGMAN:** The pleated cylindrical filter cartridges in our paper may possibly survive a hydrogen gas explosion, but we do not know since no high pressure tests have been conducted. The media, with no additional structural support, would collapse under high pressures. However, there is an interior steel core that would prevent total collapse if the thickness of the core is sufficient. Depending on the resulting pressure, the pleats may also collapse. I am not aware of any applications like that. At the 21st Nuclear Air Cleaning Conference, I presented results for the same medium in a different filter configuration for use as a vent for applications having potential pressure surges. We exposed the filter to a differential pressure of 1,000 PSI and then measured the filter efficiency. We saw no loss of efficiency at a penetration of  $15^{-8}$ . When the medium has a strong structural support, all of the forces are put on the support and not the medium. The flat, unpleated, filter medium in our previous study was supported by a very strong inner cylinder that provided this support. I doubt that the multiple cylinder filter presented today could survive anything close to that.

**GREENE:** In addition to the reverse pressure pulse to clean the fibers, have you considered alternative techniques such as ultrasonic vibrations that might be more effective for reverse pulsing?

**BERGMAN:** Ultrasonic cleaning in air would probably not be very effective, but if the filter is immersed in liquid, ultrasonics could prove beneficial. There is a large variety of liquid cleaning techniques that could be used, such as reverse sprays, reverse liquid flow with and without detergents. However, a careful analysis has to be made for each application so that you don't generate excessive radioactive waste that reduces the cost savings from reusing the filter.

**MCGALLIAN:** I see that there was a cost analysis done; did it include handling equipment, since these units weight 200 lbs apiece?

## 22nd DOE/NRC NUCLEAR AIR CLEANING AND TREATMENT CONFERENCE

**BERGMAN:** Our cost analysis did not include special handling equipment for the 200 pound steel filter that is described in our report. The data in the cost analysis applies to a steel HEPA filter after several more years of development effort. I have assumed that the final steel HEPA filter will weight less than 90 pounds, not 200 pounds, and therefore assumed that no special handling equipment would be needed. The steel HEPA filter will, presumably, be in the facility for the life of the facility, which we assumed is equivalent to about 15 HEPA filters. The current filter design does not involve the filter being removed from the housing during this period. If you have to remove the filter from the housing each time you clean it, that dramatically changes the cost analysis. We have not done that kind of analysis. Every new application requires its own experimental verification and demonstration for any new technology.

**MCGALLIAN:** Has an evaluation of critically problems been approached?

**BERGMAN:** Our preliminary study shows that we cannot put any more than 500 grams of PU in the filter without having it go critical. The present filter cannot be used in applications where this critical mass can accumulate. You will have to do something to both the filter design and the material to avoid this critically potential.

**MCGALLIAN:** Basically, this application is for new applications instead of those replacing existing filtration systems.

**BERGMAN:** No, that is not our intent. Our intent is to use the steel filter for both new applications and for existing facilities. If the filters are retrofitted into existing facilities, there will have to be some modifications, depending on what kind of cleaning is envisioned. If you want in-situ cleaning, you will have to modify the ducting and housing to provide a means for filter cleaning and removal of deposits. For new facilities, you could provide for these needs from the start. Moreover, for a new facility, you are not locked into a 2' x 2' x 1' frame, as pointed out by the previous speaker. You can use an optimum design. I don't believe the standard filter frame will be the most optimum design.

**LEIBOLD:** You optimized the filter pleats for initial pressure drop and efficiency. I think it would be much better to optimize pleats for the condition of recleaning. I expect that the narrow pleats will clog irreversibly.

**BERGMAN:** I believe you are correct; optimization should be done with respect to filter cleaning. We have not completed this study. Although the theoretical optimization was done for the initial efficiency and pressure drop, as shown in Figures 4 and 5, we did conduct three experiments on optimizing the filter design for filter cleaning. We built three different filter cartridges having different pleat widths and different pleat heights, and the results are shown in Figures 5 and 6 as A, B, and C. We found that filter C with the most narrow pleats had the worst cleaning performance. This poor performance is likely due to the closely spaced pleats that are in contact. But you are absolutely right; if we had a mathematical understanding of filter cleaning, it would be far better to optimize for cleaning than to optimize for efficiency and pressure drop.

**KAHN:** It appears that there should be a life cycle energy cost in your Table I cost estimates. You are talking about a 3.5 in. w. clean resistance vs 1 in. w. for the standard HEPA filter. This is a penalty. Is that right?

## 22nd DOE/NRC NUCLEAR AIR CLEANING AND TREATMENT CONFERENCE

**BERGMAN:** That is correct. At the present time there will be an energy penalty. As I said, this study is a preliminary effort. Table I represents the estimated cost comparisons for a stainless steel HEPA filter that has the same pressure drop as a standard glass paper filter. There would, therefore, be no cost penalty relative to the glass HEPA. The steel filter presented in our paper has a much higher pressure drop and would therefore, have a significant energy penalty. Table I does not refer to the present filter but rather to the filter after several years of further development. The prototype that we presented today is only in the early development stage.

DEVELOPMENT AND EVALUATION OF A HEPA FILTER FOR INCREASED STRENGTH AND RESISTANCE TO ELEVATED TEMPERATURE\*

Humphrey Gilbert,<sup>1</sup> Werner Bergman, and Jan K. Fretthold<sup>2</sup>

Lawrence Livermore National Laboratory  
P. O. Box 5505  
Livermore, CA 94550

Abstract

We have completed a preliminary study of an improved HEPA filter for increased strength and resistance to elevated temperature to improve the reliability of the standard deep pleated HEPA filter under accident conditions. The improvements to the HEPA filter consist of a silicone rubber sealant and a new HEPA medium reinforced with a glass cloth. Three prototype filters were built and evaluated for temperature and pressure resistance and resistance to rough handling. The temperature resistance test consisted of exposing the HEPA filter to 1,000 scfm (1,700 m<sup>3</sup>/hr) at 700°F (371°C) for five minutes. The pressure resistance test consisted of exposing the HEPA filter to a differential pressure of 10 in. w.g. (2.5 kPa) using a water saturated air flow at 95°F (35°C). For the rough handling test, we used a vibrating machine designated the Q110. DOP filter efficiency tests were performed before and after each of the environmental tests. In addition to following the standard practice of using a separate new filter for each environmental test, we also subjected the same filter to the elevated temperature test followed by the pressure resistance test. The efficiency test results show that the improved HEPA filter is significantly better than the standard HEPA filter. Further studies are recommended to evaluate the improved HEPA filter and to assess its performance under more severe accident conditions.

I Introduction

Previous studies have shown that the standard glass fiber HEPA filter may be structurally damaged under accident conditions that may occur in nuclear facilities<sup>(1-10)</sup>. These studies have shown that the HEPA filter may be damaged when it is exposed to high values of

<sup>1</sup>Consultant, McLean, VA 22101.

<sup>2</sup>EG&G Rocky Flats, Inc., Golden, CO 80402.

---

\*This work was performed under the auspices of the U. S. Department of Energy by the Lawrence Livermore National Laboratory under Contract No. W-7405-ENG. 48.

temperature, moisture, smoke loadings, air flows, and pressure drops. The moisture weakens the strength of the filter medium and also restricts the air flow which causes an increased pressure drop. The smoke loadings from fires also restricts the air flow. due to the deposits. If the blower in the ventilation system has sufficient power to overcome the increased filter air resistance, then it is possible to structurally damage the filter medium and even blow out the entire medium from the HEPA frame.

The earliest environmental tests on HEPA filters were developed by the U.S. Army and specified in MIL-F-51068<sup>(11)</sup>. This standard describes a heated air test in which HEPA filters are exposed to an air flow at 700°F (371°C) for five minutes. It also describes a pressure resistance test in which a filter is exposed to a sufficient flow of humid air to produce a pressure drop of 10 in. w.g. for one hour. Another test method in the standard is the rough handling test in which the HEPA filter is vibrated. These tests comprise a portion of the tests that are required for HEPA filters to be used in U.S. Department of Energy facilities. Although these tests were adequate to address many environmental challenges for U.S. Army applications, they were not sufficient to evaluate the variety and severity of accident conditions postulated in nuclear accidents.

To investigate the performance of HEPA filters under simulated accident conditions, special test facilities were built in the U.S. and Europe. Los Alamos National Laboratory built a test facility at the New Mexico State University to study the effects of pressure shocks and tornados on HEPA filters. <sup>(1)</sup> A fire test facility was built at Lawrence Livermore National Laboratory to study the effects of fire and smoke on the ventilation system and HEPA filters.<sup>(2)</sup> The KFK institute in Germany built separate test facilities for high humidity and for high air flow studies.<sup>(3,4,9,10)</sup> The Atomic Energy Authority in England built a high temperature filter facility to measure filter efficiency under hot dynamic conditions.<sup>(5,6)</sup> The French CEA also built a similar high temperature facility for studying HEPA filters.<sup>(7)</sup> Except for the high temperature facilities, the other test facilities cannot measure the filter efficiency under the test conditions. The practice is to expose the filter to the desired environmental condition and then measure the filter efficiency in a separate test.

Previous researchers have shown that the reliability of the HEPA filter can be significantly improved by replacing components of the filter with stronger and/or more temperature resistant materials. Pratt <sup>(6)</sup> described a HEPA filter using a glass cloth reinforced filter medium from Lydall Inc. along with an unspecified high temperature sealant to

seal the medium into the filter case. The filter was able to survive an exposure to 932°F (500°C) air flow with no observable damage. No efficiency measurements were reported. Ruedinger et al (9,10) also described high strength HEPA filters made with the reinforced HEPA paper from Lydall Inc.. They also described pleat separators made with inclined corrugations, that also improved the filter strength. They did not report any efficiency measurements. Ruedinger et al(10) reported that the German nuclear power plants are now using the higher strength HEPA filters.

The present study represents a preliminary effort to develop a HEPA filter with improved reliability to withstand accident conditions in U.S. nuclear facilities. This work represents a continuation of the previous work by Ruedinger(9-10) and Pratt(6) in developing a more robust HEPA filter. Like these previous researchers, we also used the glass cloth reinforced HEPA media from Lydall Inc. to make our prototype HEPA filter. In addition we used RTV silicone rubber for the sealant to seal the HEPA media into the frame for greater temperature resistance.

We had several prototype filters built and evaluated them against standard HEPA filters at the Rocky Flats Plant Filter Test Laboratory. This laboratory has existing test facilities for conducting heated air tests, pressure resistance tests and rough handling tests as specified in MIL-F-0051068(11). Although more severe tests would be a better representation of potential accident conditions, there are no U.S. facilities comparable to those in Europe for high temperature and moisture exposure. Nevertheless, we felt that the available test facilities at Rocky Flats would still provide a relative comparison of the performance between the prototype and standard HEPA filter.

## II Prototype HEPA Specification

The specifications for the prototype HEPA filter are given in Table 1. The elements of the specification affecting frame, gasket, separators, and test performance are not unique. The requirements conform to Military Specification MIL-F-51068.(11) The variation by which temperature resistance and strength were sought was centered on the filter medium and the sealant. The filter medium was a water-repellent treated medium of glass fibers, corresponding to the Military Specification MIL-F-51079(12), but supplemented with a single scrim of glass monofilament. The monofilament measured 6.5 um in diameter and had a mesh size of 42 by 31 filaments to the inch. The filter was positioned for test with the scrim on the downstream face.

## 22nd DOE/NRC NUCLEAR AIR CLEANING AND TREATMENT CONFERENCE

The conventional media to frame sealant for HEPA filters that is currently marketed is a polyurethane material containing a fire retardant. A room-temperature vulcanizing silicone rubber was chosen instead for this design. Although RTV silicone rubber is a more expensive material, its selection to provide additional temperature resistance for a specialized application was a logical choice.

Table 1. Specification of Prototype Filter

Dimensions	24 x 24 x 11.5 inches, excluding gasket.
Frame	304 or 409 Stainless Steel. Four frame members to be preformed with double flanges, joints coated with sealant identified below before closing and closed with four bolts, nuts, and cut lock washers.
Medium	Lydair 3255-LW1.
Separators alloy	3003-H19, 1145-H19, or 5052-H39 Aluminum alloy of 0.0015 inch minimum thickness.
Sealant	Room Temperature Vulcanizing Silicone Rubber, Dow Corning 116.
Gasket	Oil-Resistant Expanded Cellular Rubber, ASTM D1056 SCE-43 or -44, 3/4 inch of width and 1/4 inch of thickness.
Test Performance	Penetration not to exceed 0.03% when tested at air flows of 1,000 and 200 SCFM with a Q107 DOP Penetrometer. Resistance to air flow of 1,000 SCFM not to exceed 1.0 inch, water gauge.

Filters were fabricated to the design specified. Each was visually examined and tested for dioctyl phthalate (DOP) penetration at the DOE Filter Test Facility, Rocky Flats Plant, Golden, Colorado, and each conformed to the specification imposed on the manufacturer. These figures were maintained as a base so that penetration of a filter after testing could be used to assess degradation of the unit.

### III Filter Evaluation

The test filters were subjected to one or two of three different tests: heated air test, pressure resistance test, and rough handling test.

#### Heated Air Test

Apparatus for the heated air test is shown in the sketch of Figure 1. It consists of a duct containing a blower, a natural gas manifold, adjustable vanes, and a movable exhaust duct that serves as a chuck to hold the filter in the path of the heated air. The Rocky Flats heated air apparatus generates an air flow of 1,000 standard cubic feet of air per minute (SCFM) ( $1,700 \text{ m}^3/\text{hr}$ ) which is heated to  $700^\circ\text{F}$  ( $371^\circ\text{C}$ ). The rig incorporates a number of improvements in design from the original model at the Edgewood Area of Aberdeen Proving Ground, Maryland, and the Underwriters Laboratories apparatus located at Northbrook, Illinois. The test method is described in Underwriters Laboratories Standard UL 586.<sup>(3)</sup>

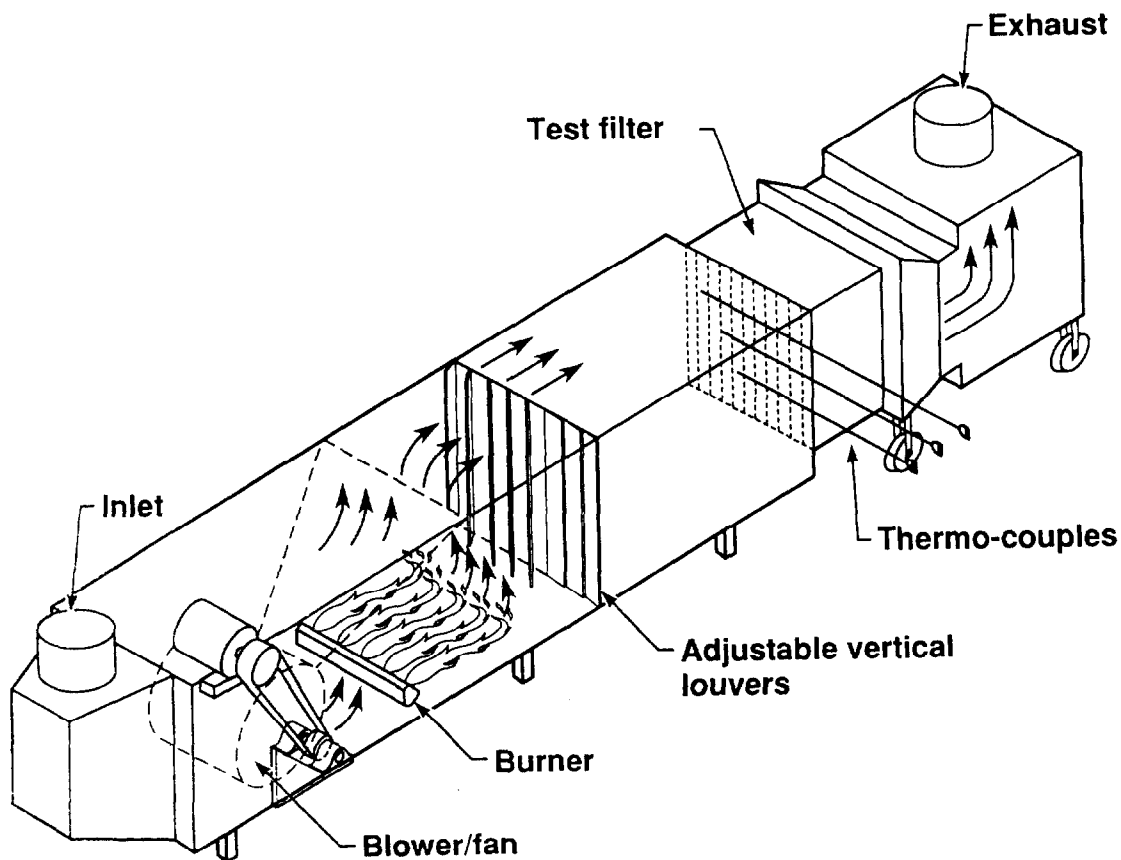


Figure 1 Heated Air Test Apparatus

One of the prototype filters was placed in the holding chuck of the heated air rig, shown in Figure 2. The blower was started and the air temperature was brought to  $700 \pm 50^\circ\text{F}$  ( $371 \pm 28^\circ\text{C}$ ), at which point the five-minute test began. Following this period of exposure, the gas flame was discontinued, and continued air flow cooled the apparatus to 80-100 degrees to permit removal of the filter.

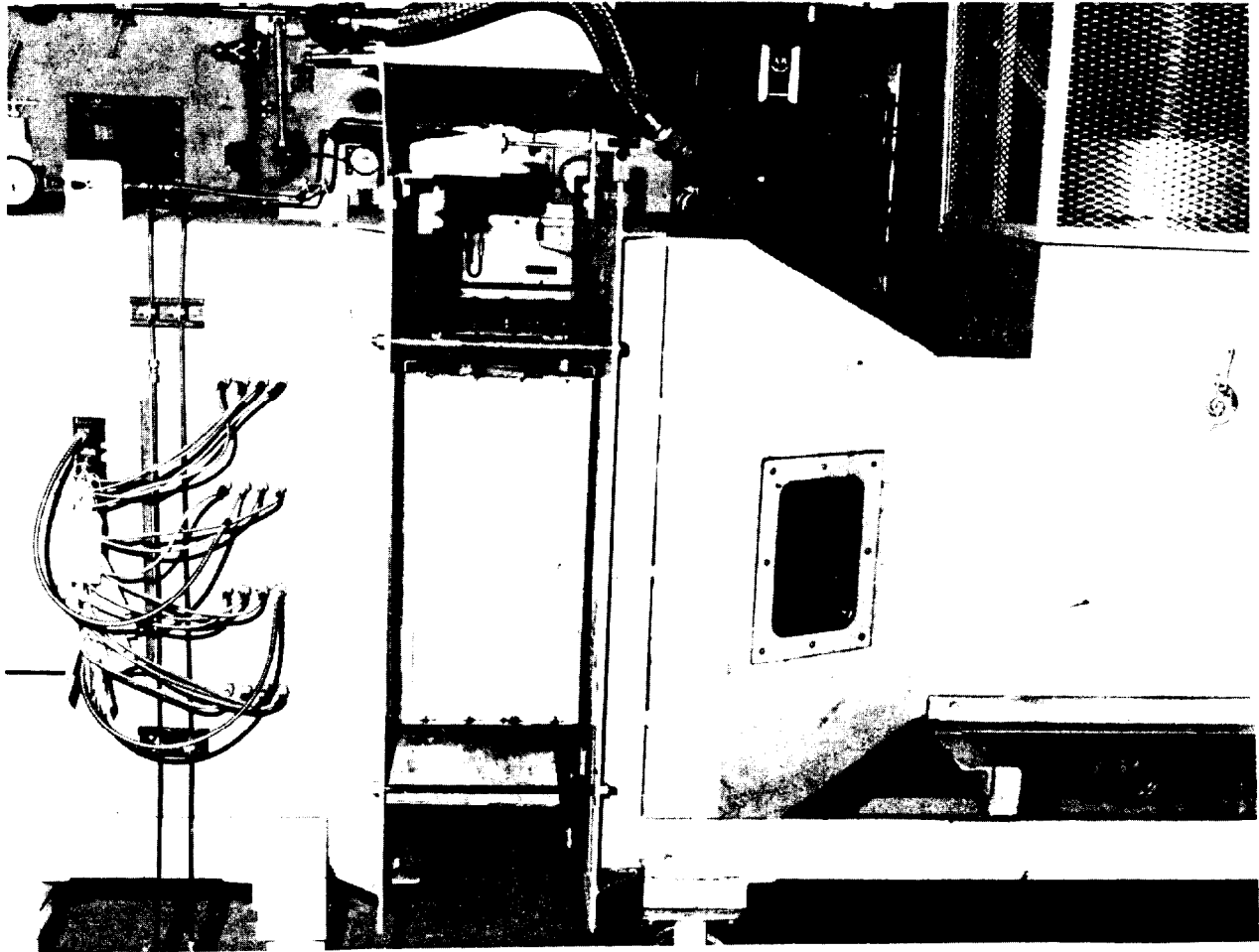


Figure 2 Filter Holding Chuck

Inspection of the prototype unit following the heated air test identified only one change. A few pleats of medium and separators deflected in the center of the pack and near the lower edge of the frame. This is shown in Figure 3. The change is attributed to expansion

of the metal frame under the heat of the test and subsequent contraction after cooling. Pratt and Green<sup>(5)</sup> observed tears along the pleats when a high temperature sealant was used to join the filter pack to a metal frame. Ensinger et al<sup>(15)</sup> had observed similar kinking of the filter pleats, but no tears, when the conventional HEPA media was glued to a steel frame with silicone adhesive.

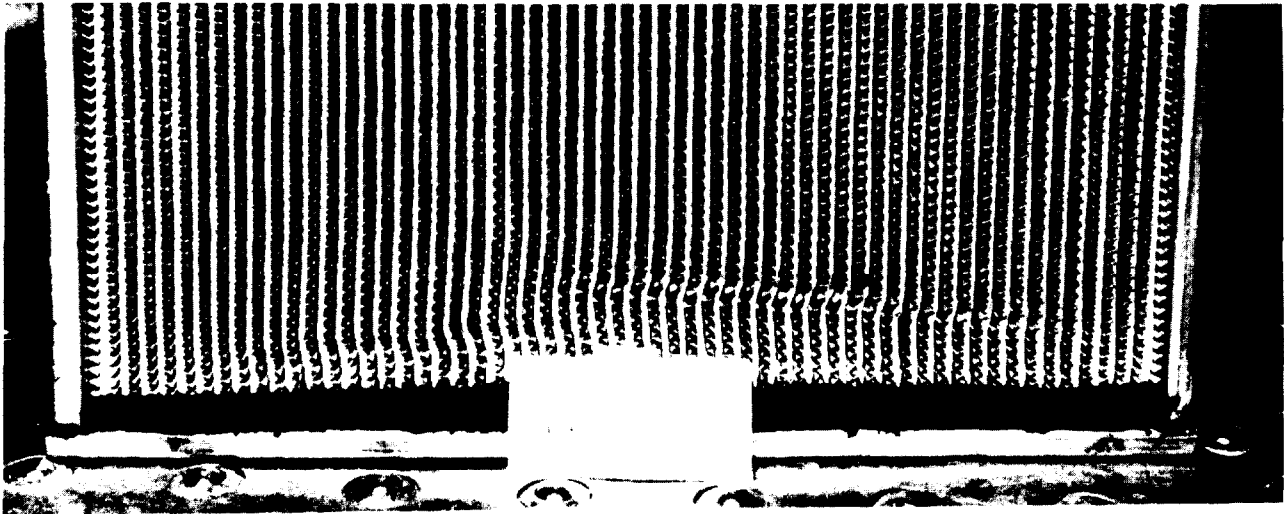


Figure 3 Deflected Medium and Separators

A standard HEPA filter fabricated with a wood frame and polyurethane as the sealant was designated as a control and subjected to the same test procedure. Following the testing, both units were measured for penetration with the Q107 DOP Penetrometer. Results of this stage of testing are given in Table 2.

Table 2 Results of Heated Air Test

	<u>Percent Penetration</u>	
	<u>Before</u>	<u>After</u>
Filter Unit A	0.010	0.070
Control	0.016	0.500

These two filters together with another of the prototype units were placed in an environmental chamber for 24 hours, Figure 4, where the relative humidity was controlled at 95%,  $\pm 5\%$ , and the temperature was held at  $95 \pm 5^\circ\text{F}$  ( $35 \pm 3^\circ\text{C}$ ). Test filters are preconditioned in preparation for the pressure resistance test.



Figure 4 Environmental Chamber

### Pressure Resistance Test

The pressure resistance test apparatus is an elongated elliptical chamber through which air and moisture are recirculated to a test filter. An overhead view of the Q160 pressure resistance apparatus at Rocky Flats Plant is shown in Figure 5. A filter that is positioned for testing as viewed through the access door opening is shown in Figure 6. Refer to the the simplified sketch shown in Figure 7 to better understand the test procedure. The blower is started together with the introduction of steam, condensing to water droplets, and the volume of air is increased to maintain a resistance of 10 inches water gauge (2.5 kPa) across the filter. Water droplets are generated at a rate of one pound  $\pm$  1/4 pound (114 g) per 1,000 cubic feet (1,700 m<sup>3</sup>) of air. At 10 inches (2.5 kPa) of pressure drop the air flow, combined with the moisture, measures between 7,000 to 8,000 cfm (11,900 - 13,600 m<sup>3</sup>/hr) . This pressure is maintained on the filter for a minimum of one hour.

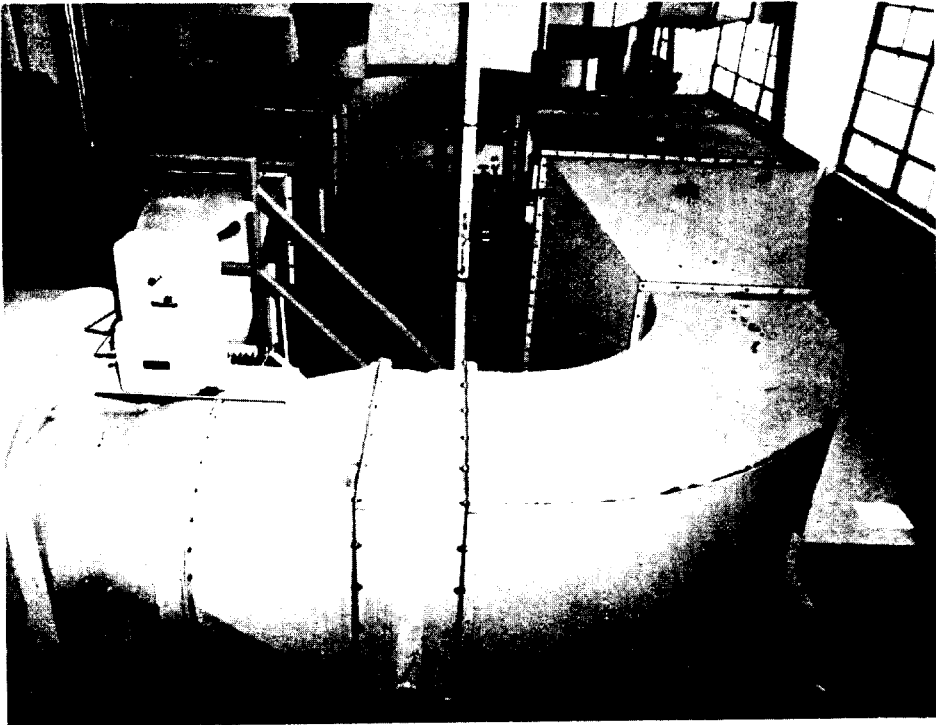


Figure 5 Pressure Resistance Apparatus

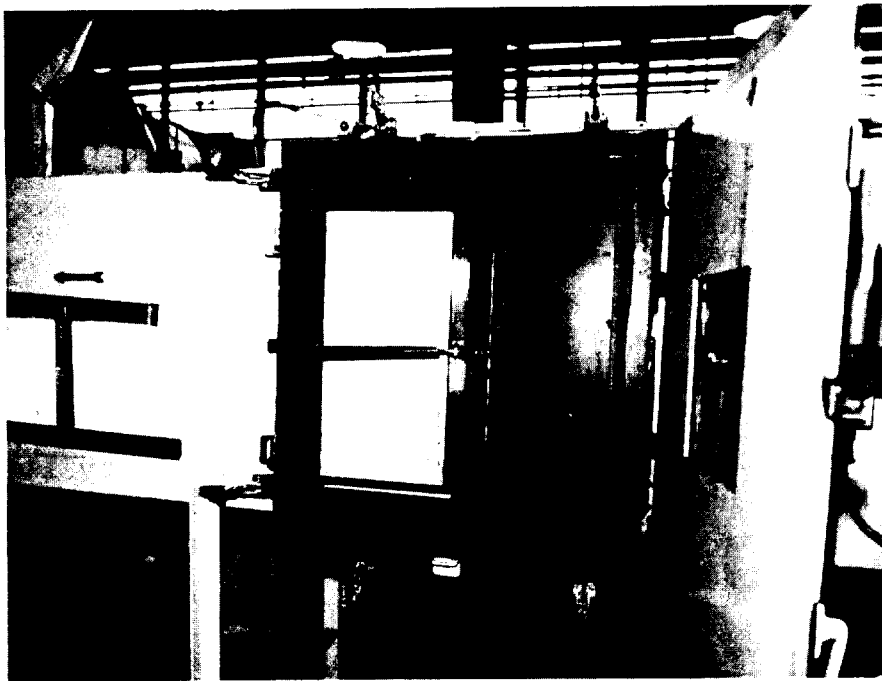


Figure 6 Test Filter with Access Door Open

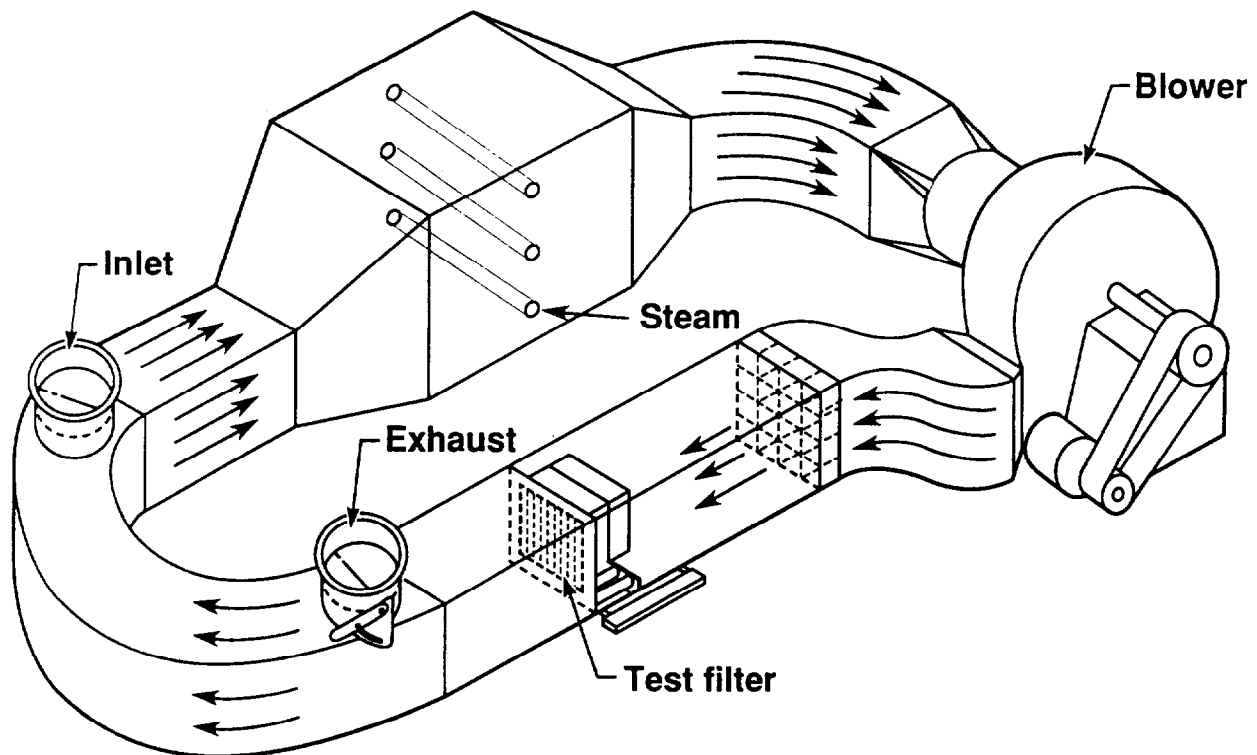


Figure 7 Diagram of the Pressure Resistance Apparatus

Although the practice at the Edgewood Area of Aberdeen Proving Ground is to measure penetration of the filter promptly after its test, the procedure at Rocky Flats is to terminate water droplets and continue the air briefly to remove detectable water and let the filter stand over night before measuring its penetration. The Rocky Flats modification assumes that any perforations of the filter from the pressure resistance test will be detected where otherwise they might be bridged and occluded by residual moisture.

The three filters which had been preconditioned for 24 hours were tested with the Q160 pressure resistance equipment. Results are shown in Table 3.

Table 3 Results of Heated Air and Pressure Resistance Tests

	<u>Percent Penetration</u>		
	<u>Before Testing</u>	<u>After Heated Air</u>	<u>After Pressure Resistance</u>
Filter Unit A	0.010	0.070	0.070
Control Filter	0.016	0.500	1.000
Filter Unit B	0.005	---	0.006

Filter Unit A changed from an initial penetration of 0.01% to 0.07% after the heated air test, which is better than expected, and showed no additional increase after exposure to a 10-inch (2.5 kPa) pressure drop of air and water for an hour. In contrast, the control filter increased from 0.016 to 0.5% after the heated air test and additionally to 1.0% after the pressure test. Figure 8 shows the severe charring of the urathane sealant on the upstream side of the filter. The charring was equally severe on the the downstream side. Two vertical linear cracks in one pleat are visible in the center of the downstream face, Figure 9. These cracks appeared after the combined exposure of heated air and pressure resistance. A second prototype filter, unit B, was subjected to a one hour pressure resistance test and showed only a slight increase in penetration from 0.005% to 0.006%. Comparing the penetration of filter unit B to unit A shows that the heated air test is more damaging to the HEPA filter than the pressure resistance test.

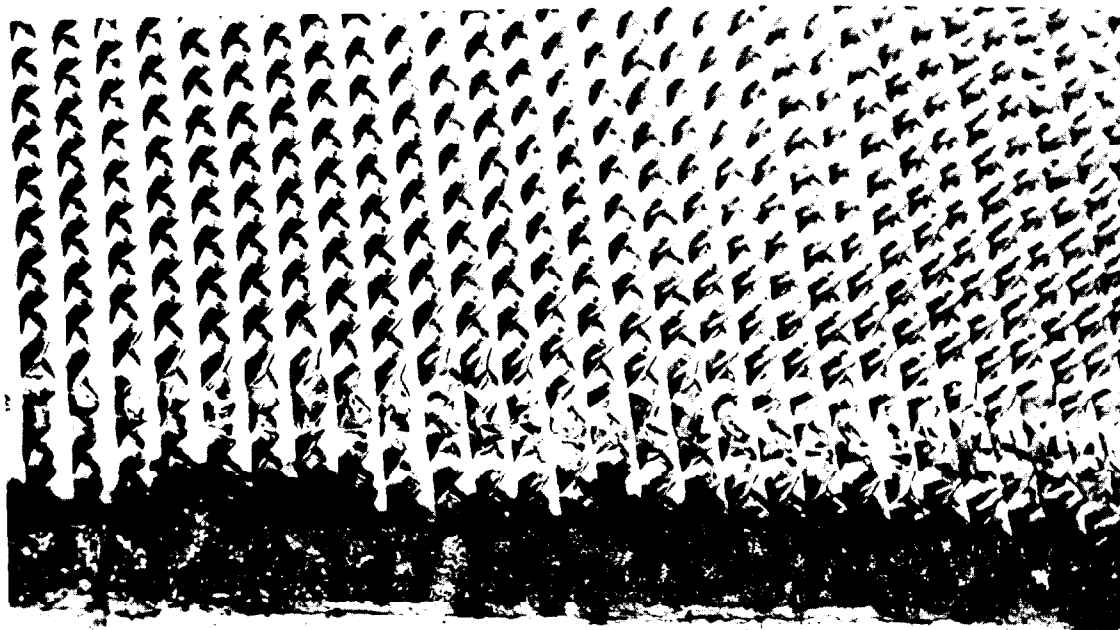


Figure 8 Upstream Face of Control Filter

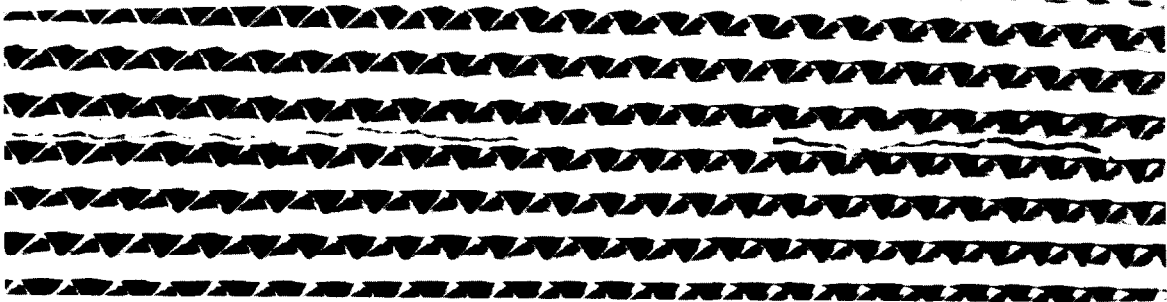


Figure 9 Cracked Pleats on Downstream Face

The maximum allowed penetration of a filter after exposure to heated air is 3.0% according to MIL-F-51068 although any excess beyond 1.0% after this test is a rare occurrence. The performance of the control filter therefore was within the allowable increase of penetration. The ruptured pleat following the pressure resistance test was not expected, however. All of the filters met the current test requirements.

#### Rough Handling Test

The rough handling test has been used for many years and the test procedure is described in the 1956 issue of MIL-STD-282.<sup>(4)</sup> The equipment in essence is a vibrating machine designated the Q110 and is designed to simulate transportation vibrations. It provides a platform, to which the filter is attached, and it mechanically moves the bed 200 cycles per minute at an amplitude of 3/4 inch. A view of one of the two cams that lifts and drops the platform is shown in Figure 10.

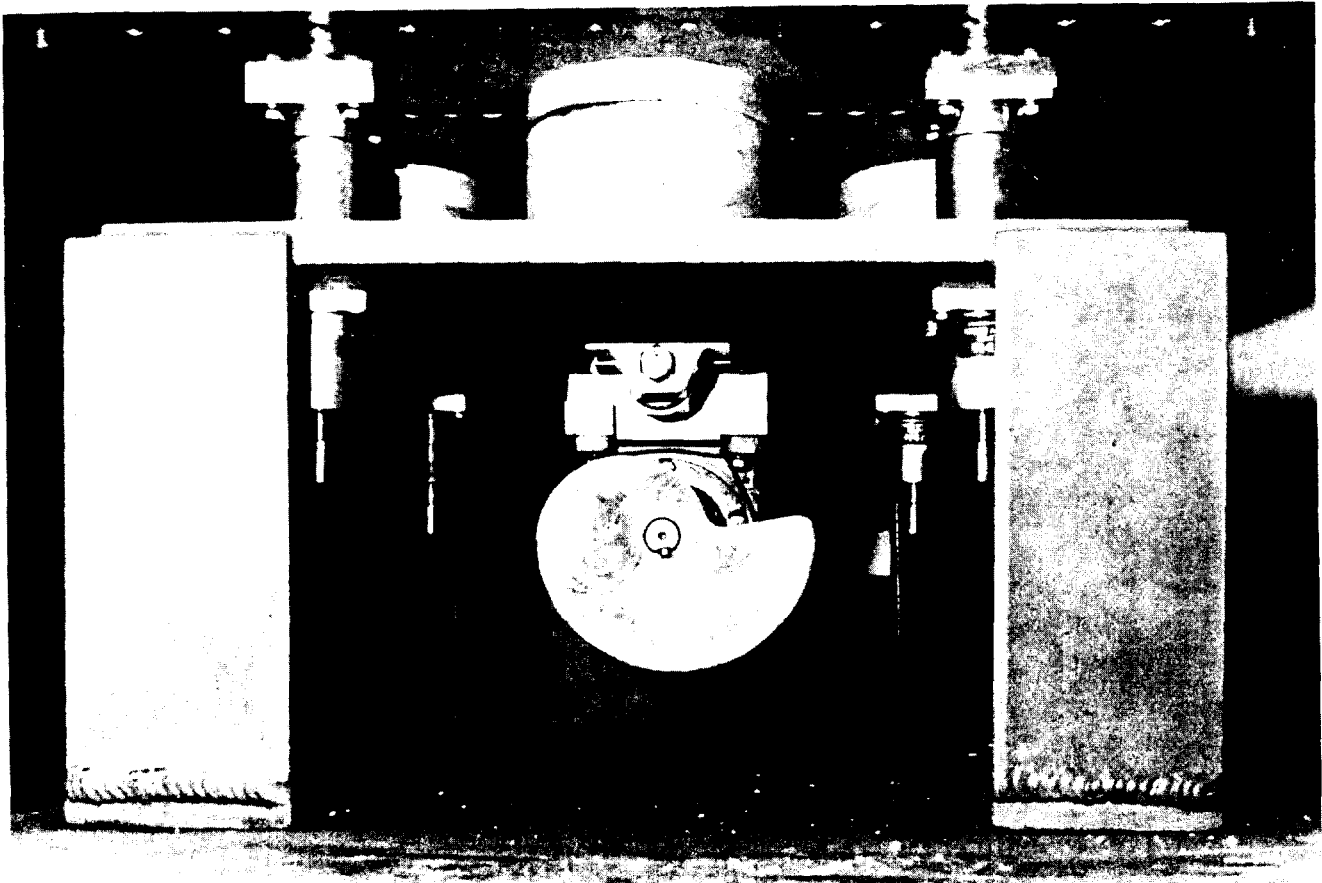


Figure 10 Cam for Lift/Drop Platform on Rough Handling Apparatus

The normal test procedure is to remove the filter from its shipping carton and strap it to the Q110 Vibrating Machine for test. Sixteen years of quality assurance testing at Rocky Flats dictated that transportation of the filter induced more mechanical damage than any other cause. Therefore the test procedure for rough handling was modified to test the filter within its shipping carton. Frequency of 200 cycles per minute and amplitude of 3/4 inch were unchanged. Damage is determined by any increase of DOP penetration above the penetration recorded upon initial test following receipt of the filter. The original procedure to test the uncartoned filter element removed from its shipping carton required two long threaded studs to which a bar was bolted across the filter. The modified test procedure employs four such studs positioned on four sides of the filter packaged in its shipping carton. A plate is bolted to the four studs to hold the filter enclosed in its shipping carton to the platform. The studs and plate are shown in Figure 11. Figure 12 depicts the enclosed filter ready for testing.

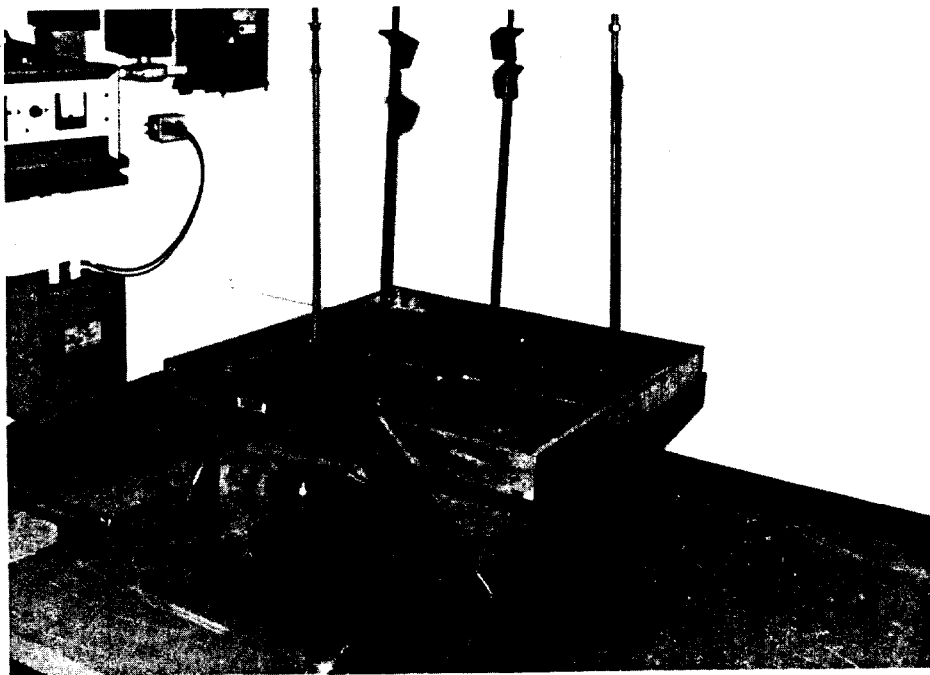


Figure 11 Rough Handling Test Apparatus

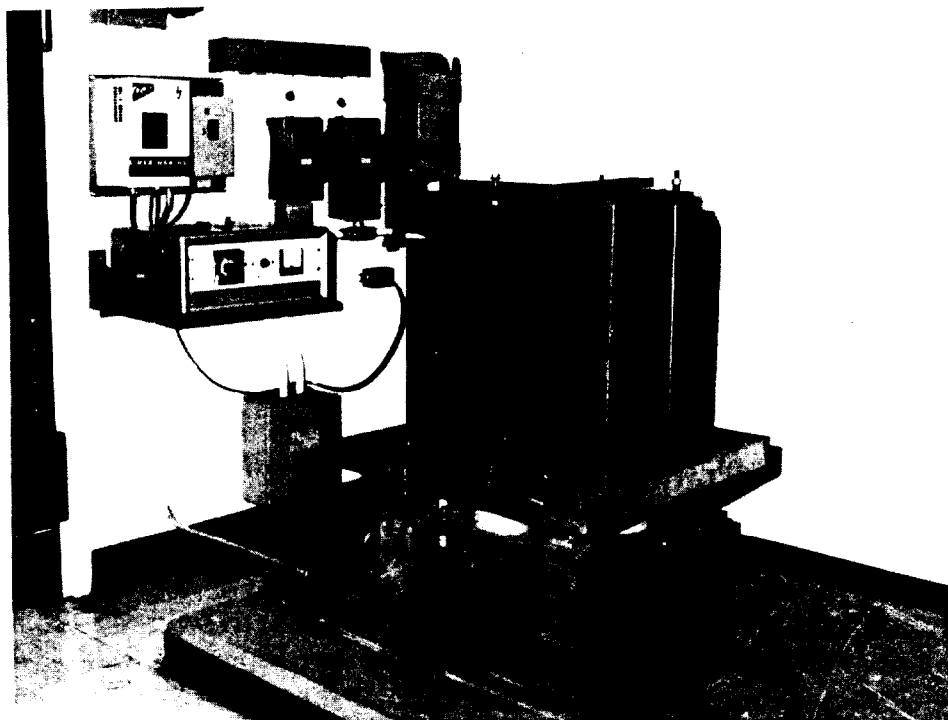


Figure 12 Enclosed Filter Ready for Testing

One of the prototype filters, enclosed in its carton, was bolted to the platform of the Q110 Vibrating Machine, and the test apparatus was operated for the 15 minutes stipulated for the test. Penetration of the filter before and after testing is given in Table 4.

Table 4 Results of Rough Handling Test

	<u>Percent Penetration</u>	
	<u>Before</u>	<u>After</u>
Filter Unit C	0.006	0.006

Penetration through Filter Unit C was unchanged after the rough handling test.

#### IV. Conclusion

All of the tests described above are termed destructive tests. They are intended to evaluate the fire resistance, strength, and reliability of the design of a HEPA filter. Many HEPA filters, of both conventional and novel design, have withstood these tests at the Edgewood Area of Aberdeen Proving Ground. This is required for identification on the Qualified Products List (QPL) of the Department of Defense. In addition, many models of HEPA filters have successfully undergone the heated air test of UL 586 in order to bear the "UL" label. Although these tests were adequate to address many environmental challenges for Army applications, they are not sufficient to evaluate the variety and severity of accident conditions postulated in nuclear accidents. We have nevertheless used these tests because of their availability and the fact that they can provide a relative comparison between prototype and standard HEPA filters.

This study differs from most previous investigations of HEPA filters under accident conditions in that the same test filter was subjected to more than one environmental test. The previous practice was to subject a filter to only one destructive test. In our study, we evaluated the prototype and standard HEPA filters in a test sequence consisting of a heated air test followed by a pressure resistance test.

Ruedinger et al<sup>(10)</sup> had previously reported that they used a test sequence consisting of elevated temperature in still air, pressure resistance in high air flow, and humid air resistance to qualify filters for use in nuclear reactors.

The results from our preliminary study show that the prototype filter can withstand exposures to heated air and higher pressure significantly better than the standard HEPA filter. The scrim backed

medium and the silicone rubber seals are considered the most significant contributors to the improved performance of the prototype, and the design might be given serious consideration for use in applications subjected to a harsh environment and to design basis accidents in nuclear facilities. We recommend that further studies be conducted to assess the filter's performance under more severe accident conditions.

#### V. Acknowledgment

The authors acknowledge the cooperation of the Technical Papers Division of Lydall, Inc., in this project.

#### **References**

1. Gregory, W.S., Andrae, R.W., Duerre, D.H., Horak, H.L., Smith, P.R., Ricketts, C.I., and Gill, W. "Air cleaning systems analysis and HEPA filter response to simulated tornado loadings" Proceedings of the 15th DOE Nuclear Air Cleaning Conference, CONF-780819, NTIS, Springfield, VA, pp. 694-706 (1979).
2. Alvared, N., Beason, D., Bergman, W., Ford, H., and Lipska, A. "Fire protection countermeasures for containment ventilation systems", Proceedings of the 16th DOE Nuclear Air Cleaning Conference, NTIS, Springfield, VA, pp.1213-1276 (1981).
3. Ruedinger, V., Ricketts, C.I., Wilhelm, J.G. "Limits of HEPA filter application under high humidity conditions" Proceedings of the 18th DOE Nuclear Airborne Waste Management and Air Cleaning Conference, CONF -840806, NTIS, Springfield, VA, pp. 1058-1084 (1985).
4. Ricketts, C.I., Ruedinger, V., Wilhelm, J.G., "HEPA filter behavior under high humidity airflows" Proceedings of the 19th DOE/NRC Nuclear Air Cleaning Conference, NUREG/CP-0086, CONF-860820, Superintendent of Documents, U.S. Govt. Printing Office, Washington, DC, pp. 319-352 (1987).
5. Pratt, R.P., and Green, B.L., "Performance testing of HEPA filters under hot dynamic conditions" Proceedings of the 18th DOE Nuclear Airborne Waste Management and Air Cleaning Conference, CONF - 840806, NTIS, Springfield, VA, pp. 1107-1127 (1985).
6. Pratt, R.P. "The performance of filters under hot dynamic conditions" Gaseous Effluent Treatment in Nuclear Installations, G.

Fraser and F. Luykx, editors, Graham & Trotman, Luxembourg, pp. 824-836 (1986).

7. Briand, A., Laborde, J.C., and Mulcey, P., "Limits of HEPA filters operation under high temperature conditions" Proceedings of the 19th DOE/NRC Nuclear Air Cleaning Conference, NUREG/CP-0086, CONF-860820, Superintendent of Documents, U.S. Govt. Printing Office, Washington, DC, pp. 890-904 (1987).
8. Johnson, J.S., Beason, D.G., Smith, P.R., and Gregory, W.S., "The effect of age on the structural integrity of HEPA filters" Proceedings of the 20th DOE/NRC Nuclear Air Cleaning Conference, NUREG/CP-0098, CONF-880822, Superintendent of Documents, U. S. Government Printing Office, Washington, DC, pp. 366-381 (1989).
9. Ruedinger, V., Ricketts, C.I., Wilhelm, J.G., and Alken, W. "Development of glass-fiber HEPA filters of high structural strength on the basis of the establishment of the failure mechanisms", Proceedings of the 19th DOE/NRC Nuclear Air Cleaning Conference, NUREG/CP-0086, CONF-860820, Superintendent of Documents, U.S. Govt. Printing Office, Washington, DC, pp. 947-966 (1987).
10. Ruedinger, V., Ricketts, C. I., and Wilhelm, J. G., "The realization of commercial high strength HEPA filters," Proceedings of the 20th DOE/NRC Nuclear Air Cleaning Conference, NUREG/CP-0098, CONF-880822, Superintendent of Documents, U. S. Government Printing Office, Washington, pp 917-942 (1989).
11. Filter, Particulate, High-Efficiency, Fire Resistant, Military Specification MIL-F-0051068, Commander, U. S. Army Armament, Munitions and Chemical Command, ATTN: DRSMC-CLW-E/A, Aberdeen Proving Ground, MD 21010-5423.
12. Filter Medium, Fire-Resistant, High-Efficiency, Military Specification MIL-F-0051079, Commander, U.S. Army Armament, Munitions and Chemical Command, supra.
13. High Efficiency Particulate Air Filter Units, Standard for Safety UL 586, Underwriters Laboratories Inc., 333 Pfingsten Road, Northbrook, IL 60062. Also identified as ANSI B132.1, American National Standards Institute, 1430 Broadway, New York, NY 10018.
14. Filter Units, Protective Clothing, Gas-Mask Components and Related Products Performance-Test Methods, Method 105.9, Military

22nd DOE/NRC NUCLEAR AIR CLEANING AND TREATMENT CONFERENCE

Standard MIL-STD-282, Commanding Officer, Frankford Arsenal, Navy Department, ATTN: SMUFA-N1100, Philadelphia, PA 19137.

15. Ensinger, U., Ruedinger, U., and Wilhelm, J."Efficiency of HEPA filters at elevated temperatures: Investigations with the TiO<sub>2</sub> test method" Proceedings of the 20th DOE/NRC Nuclear Air Cleaning Conference, p334 (1989).

## 22nd DOE/NRC NUCLEAR AIR CLEANING AND TREATMENT CONFERENCE

### CLOSING COMMENTS OF SESSION CO-CHAIRMAN ANDERSON

This session has concentrated on filter unit design and evaluation with several papers exploring advanced filtration devices for special requirements.

Dr. Wilhelm from Karlsruhe addressed the problem of the effects and challenges within ventilation systems during accident conditions and presented current status of potential solutions. Two papers addressed the need for devices that could be used for specific operating conditions. Mr. Davis, from Flanders Filters, proposed the use of radial flow units in a variety of system configurations to facilitate handling, changing, and disposal of filters used by the nuclear industry. Mr. Gilbert presented a Livermore development of an improved HEPA filter of increased strength and resistance to elevated temperatures. Confirmation of enhanced performance was achieved experimentally and unit reliability under accident conditions is to be expected.

Two papers explored the behavior of filter units during unusual off-gas conditions. Mr. Jannakos, from Karlsruhe, studied the effect of water droplets on filter performance while Mr. Leibold reported high dust concentrations on the life and performance of HEPA systems.

Two papers provided an update on the use of metal fibers as an alternative for nuclear air filtration technologies. Mr. Milatovic, from Fluor Daniel, described a 1,000 cfm unit currently involved in demonstration testing at Oak Ridge. Dr. Bergman, from Livermore, outlined a similar unit that has been system tested in his laboratory. Although filtration efficiencies equal to current requirements can be achieved, excessive pressure drop, cost, and weight will prevent these units from being a drop-in replacement.

Mr. Klassen, from Argonne, described a computer-directed program for prediction of filter mass loading as a function of pressure drop across a prefilter/HEPA system. Preliminary verification data were included in the presentation.

This concludes this mornings session. We thank the authors for their interesting presentations and you, the audience, for participating.